



저작자표시-비영리-변경금지 2.0 대한민국

이용자는 아래의 조건을 따르는 경우에 한하여 자유롭게

- 이 저작물을 복제, 배포, 전송, 전시, 공연 및 방송할 수 있습니다.

다음과 같은 조건을 따라야 합니다:



저작자표시. 귀하는 원저작자를 표시하여야 합니다.



비영리. 귀하는 이 저작물을 영리 목적으로 이용할 수 없습니다.



변경금지. 귀하는 이 저작물을 개작, 변형 또는 가공할 수 없습니다.

- 귀하는, 이 저작물의 재이용이나 배포의 경우, 이 저작물에 적용된 이용허락조건을 명확하게 나타내어야 합니다.
- 저작권자로부터 별도의 허가를 받으면 이러한 조건들은 적용되지 않습니다.

저작권법에 따른 이용자의 권리는 위의 내용에 의하여 영향을 받지 않습니다.

이것은 [이용허락규약\(Legal Code\)](#)을 이해하기 쉽게 요약한 것입니다.

[Disclaimer](#)

이학박사 학위논문

Transition Metal Catalyzed Eco-friendly
Reaction Development Using Sustainable
C1 Source

전이금속을 촉매로 이용한 친환경
반응법 개발

2017 년 2 월

서울대학교 대학원

화학과 유기화학전공

김 승 효

전이금속을 촉매로 이용한 친환경 반응법 개발

지도교수 Soon Hyeok Hong

이 논문을 이학박사 학위논문으로 제출함

2016 년 12 월

서울대학교 대학원
화학과 유기화학전공
김 승 효

김승효의 이학박사 학위논문을 인준함

2016 년 12 월

위 원 장	<u>최태림</u>	(인)
부 위 원 장	<u>홍 순 핵</u>	(인)
위 원	<u>정 영 근</u>	(인)
위 원	<u>김정근</u>	(인)
위 원	<u>이철범</u>	(인)

Abstract

Transition Metal Catalyzed Eco-friendly Reaction Development Using Sustainable C1 Source

Seung Hyo Kim

Departments of Chemistry

The Graduate School

Seoul National University

This study presents an investigation of transition metal-mediated catalysis utilizing abundant C1 carbon sources such as carbon dioxide and methanol, with the corresponding state-of-the-art reactions explained in Chapter 1. The employed carbon capture and utilization (CCU) strategy (Chapter 2) involves the direct capture of carbon dioxide from exhaust gas and its subsequent use in organic transformations, achieving efficiencies similar to those observed for hyper-pure CO₂ from a commercial source, even for highly air- and

moisture-sensitive reactions. The CO₂-capturing aqueous ethanolamine solution can be continuously recycled without decreasing the reaction efficiency. Transfer hydrogenation of organic formates and cyclic carbonates was achieved for the first time using a readily available ruthenium catalyst (Chapter 3). Nontoxic and low-cost 2-propanol was employed both as a solvent and hydrogen source, circumventing the use of flammable H₂ gas under high pressure. This method provides an indirect way of producing methanol from carbon dioxide under mild conditions, also presenting an operationally simple and environmentally benign reduction of formates and carbonates. An unprecedented urea synthesis was accomplished directly from methanol and amines (Chapter 4), being highly atom economical and producing hydrogen as the sole byproduct. Commercially available ruthenium pincer complexes were used as catalysts. In addition, no additives such as bases, oxidants, or hydrogen acceptors were required. Furthermore, unsymmetrical urea derivatives were successfully obtained via a one-pot two-step reaction. Two abnormal N-heterocyclic carbene (aNHC) gold(I) complexes, [(aNHC)AuCl], were prepared from C2-protected imidazolium salts (Chapter 5). These air-stable compounds were synthesized by transmetalation, using (Me₂S)AuCl and the

corresponding silver salt, and were fully characterized by NMR, mass spectrometry, and X-ray crystallography. The catalytic activities of these NHC-based Au complexes were also compared in the hydration of alkynes, with traditional NHC-based Au complexes exhibiting higher efficiency.

Keywords: green chemistry, methanol, carbon dioxide, transition metal catalyst, C1 carbon source

Student Number: 2012-20268

Table of Contents

Abstract.....	1
Table of Contents	4
List of Tables	9
List of Schemes.....	11
List of Figures.....	14
Appendix	175
Abstract in Koreans	211

Chapter 1. Catalysis Utilizing Renewable C1 Sources, Carbon Dioxide and Methanol

1.1 Introduction.....	16
1.2 Homogeneous catalysis utilizing carbon dioxide	16
1.2.1 Methanol production from carbon dioxide	17
1.2.2 Carboxylation.....	25
1.3 Homogeneous catalytic reaction with methanol	31
1.3.1 Methylation source.....	31
1.3.2 Hydrogen generation (methanol reforming)	36
1.4 Reference	38

Chapter 2. Carbon Dioxide Capture and Use: Organic Synthesis

Using Carbon Dioxide from Exhaust Gas

2.1 Introduction.....	43
2.2 Results and discussion.....	45
2.2.1 Efficiency test of CO ₂ capturing solutions.....	45
2.2.2 Alkyne carboxylation using CO ₂ from combustion.....	49
2.2.3 Cyclic carbonate synthesis using CO ₂ from combustion	52
2.2.4 Grignard reaction with CO ₂ from combustion.....	55
2.3 Conclusion	56
2.4 Experimental section.....	57
2.4.1 General information	57
2.4.2 General procedure of CO ₂ capture and utilization from exhaust gas.....	58
2.4.3 General procedure of carboxylation of terminal alkynes with CO ₂	60
2.4.4 Characterization data for carboxylic acids	61
2.4.5 General procedure for cycloaddition reaction of epoxides with CO ₂	64
2.4.6 Characterization data for cyclic carbonates.....	65
2.4.7 General procedure for Grignard reaction with CO ₂	66
2.4.8 Characterization data for carboxylic acids.....	67
2.5 Reference	68

Chapter 3. Transfer Hydrogenation of Organic Formates and Cyclic Carbonates: An Alternative Route to Methanol from Carbon Dioxide

3.1 Introduction.....	72
3.2 Results and discussion.....	74
3.2.1 Optimization for transfer hydrogenation of methyl formate.....	74
3.2.2 Substrate scope.....	76
3.2.3 Optimization for transfer hydrogenation of cyclic carbonate.....	78
3.2.4 Substrate scope.....	79
3.2.5 Mechanistic studies.....	81
3.3 Conclusion.....	87
3.4 Experimental section.....	88
3.4.1 General information.....	88
3.4.2 General procedure for transfer hydrogenation of organic formates.....	89
3.4.3 General procedure for transfer hydrogenation of cyclic carbonates.....	89
3.4.4 Deuterium incorporation study for TH reaction of 1,3-dioxolan-2-one.....	90
3.4.5 Deuteration of 1,2-ethanediol and methanol with 2-propanol-d ₈	92

3.5 Reference	94
---------------------	----

Chapter 4. Ruthenium–Catalyzed Urea Synthesis Using Methanol as the C1 Source

4.1 Introduction.....	99
4.2 Results and discussion.....	102
4.2.1 Symmetrical urea synthesis.....	102
4.2.2 Asymmetrical urea synthesis.....	107
4.2.3 Possible mechanism.....	111
4.3 Conclusion.....	113
4.4 Experimental section.....	113
4.4.1 General information.....	113
4.4.2 General procedure for symmetrical urea synthesis.....	114
4.4.3 General procedure for unsymmetrical urea synthesis.....	115
4.4.4 Characterization data of urea	116
4.4.5 Complementary reaction optimization data.....	131
4.5 Reference	135

Chapter 5. Abnormal N–Heterocyclic Carbene Gold(I) Complexes: Synthesis, Structure, and Catalysis in Hydration of Alkynes

5.1 Introduction.....	141
5.2 Results and discussion.....	143

5.2.1 Synthesis of abnormal NHC based Au complexes	143
5.2.2 Structure analysis.....	145
5.2.3 Computational analysis.....	149
5.2.4 Hydration of alkyne	157
5.3 Conclusion	161
5.4 Experimental section.....	162
5.4.1 General information	162
5.4.2 Synthetic method of abnormal NHC based Au complexes	163
5.4.3 Computational investigation of the nature of the Au-C bond.....	168
5.5 Reference.....	169

Appendix

NMR spectra

Chapter 2.....	175
Chapter 3.....	184
Chapter 4.....	186
Chapter 5.....	207

List of Tables

Chapter 2

Table 2.1 Alkyne carboxylation reaction to test efficiencies of CO ₂ capturing solutions	46
Table 2.2 Alkyne carboxylation utilizing CO ₂ from combustion.....	49
Table 2.3 Cyclic carbonate synthesis utilizing CO ₂ from combustion	52
Table 2.4 Grignard reaction with CO ₂ from combustion.....	55

Chapter 3

Table 3.1 Transfer hydrogenation of methyl formate	75
Table 3.2 Transfer hydrogenation of organic formates.....	77
Table 3.3 Transfer hydrogenation of 4-methyl-1,3-dioxolan-2-one (8a) with various catalysts.....	78
Table 3.4 Transfer hydrogenation of organic carbonates.....	80
Table 3.5 Degree of deuterium incorporation in reduction of ethylene carbonate.....	83

Chapter 4

Table 4.1 Urea synthesis from methanol and benzylamine using various catalysts.....	102
Table 4.2 Symmetrical urea synthesis from methanol and amine.	105

Table 4.3 Unsymmetrical urea synthesis from methanol and amine	110
Table 4.4 Screening experiment for symmetrical urea synthesis.	131
Table 4.5 Turnover numbers and turnover frequencies	132
Table 4.6 Screening experiment for unsymmetrical urea synthesis	133

Chapter 5

Table 5.1 Summary of computationally and experimentally obtained values of selected bond lengths (Å) and bond angles (deg) for complexes 5–8 , 10 , and 11	149
Table 5.2 HOMO energy of free carbene, Mulliken atomic charge of C_{carbene} ($q(C_{\text{carbene}})$), and binding energy (BE) for 10 and 11 , as obtained with DFT1/DFT2.....	150
Table 5.3 Hydration of phenylacetylene with different Ag (I) –salt using (aNHC) AuCl.....	159
Table 5.4 Hydration of phenylacetylene.....	160

List of Schemes

Chapter 1

Scheme 1.1 Cascade strategy to produce methanol from CO ₂	18
Scheme 1.2 Ru and amine catalyzed hydrogenation of CO ₂ to methanol.....	20
Scheme 1.3 Conversion of CO ₂ from air into methanol using polyamine	21
Scheme 1.4 CO ₂ capture and hydrogenation to form methanol.....	22
Scheme 1.5 Indirect routes for methanol synthesis from CO ₂	23
Scheme 1.6 Catalytic hydrogenation of cyclic carbonates.....	24
Scheme 1.7 Grignard reaction to prepare carboxylic acid	25
Scheme 1.8 Pd catalyzed reductive carboxylation of aryl bromides	26
Scheme 1.9 Ni catalyzed reductive carboxylation of aryl chlorides	27
Scheme 1.10 Cu catalyzed reductive carboxylation of aryl iodides ..	27
Scheme 1.11 Carboxylation of terminal alkynes with CO ₂	28
Scheme 1.12 Direct sp ² C–H carboxylation with CO ₂	29
Scheme 1.13 The methanol utilization mechanism.....	31
Scheme 1.14 Rh catalyzed α –methylation of ketone using methanol	32
Scheme 1.15 Ir catalyzed α –methylation of ketone using methanol	33

Scheme 1.16 Ir catalyzed α – methylation of nitrile using methanol	33
Scheme 1.17 Ir catalyzed N – methylation of amines using methanol	34
Scheme 1.18 Ru catalyzed N – methylation of amines using methanol	35
Scheme 1.19 Dehydrogenation of methanol.....	36

Chapter 3

Scheme 3.1 Generation of Ru – hydrides from complex 1	82
Scheme 3.2 Deuteration of 1,2 – ethanediol and methanol.....	84
Scheme 3.3 Proposed mechanism.....	87
Scheme 3.4 Transfer hydrogenation of intermediates.....	87

Chapter 4

Scheme 4.1 Synthesis of urea derivatives.....	100
Scheme 4.2 Attempts to synthesize unsymmetrical urea derivatives	108
Scheme 4.3 Control experiments.....	111
Scheme 4.4 Proposed mechanism.....	112
Scheme 4.5 Screening experiment for unsymmetrical urea.....	134

Chapter 5

Scheme 5.1 Synthesis of aNHC–Au complexes 5 and 6	144
Scheme 5.2 Synthesis of (NHC) –Au complexes 7 and 9	145
Scheme 5.3 (a) Coordinate system for population analysis, and (b) schematic illustration of orbital interactions between carbene and AuCl.....	155

List of Figures

Chapter 2

Figure 2.1 Carbon dioxide capture and utilization	44
Figure 2.2 CO ₂ capture process using an amine solution	59
Figure 2.3 Reaction set up utilizing the captured CO ₂ solution	60

Chapter 3

Figure 3.1 Reaction profile for transfer hydrogenation of ethylene carbonate	85
Figure 3.2 Reaction profile for transfer hydrogenation of 2-hydroxyethyl isopropyl carbonate	85
Figure 3.3 NMR spectra for deuterium incorporation study (entries 1, 2, and 6, Table 3.5)	91
Figure 3.4 NMR spectra for deuterium incorporation study (entries 3, 5, and 7, Table 3.5)	91
Figure 3.5 NMR spectra for deuteration of 1,2-ethanediol and methanol	93

Chapter 4

Figure 4.1 The LC chart for 1,3-bis(1-phenylethyl)urea.....	134
Figure 4.2 The LC chart for 1,3-bis((S)-1-phenylethyl)urea....	134

Chapter 5

Figure 5.1 Imidazolium salts used as traditional and mesoionic NHC precursors.....	142
Figure 5.2 Traditional and mesoionic NHC–based Au complexes	143
Figure 5.3 Molecular structure of complexes 5 and 6 showing 50% probability ellipsoids.....	147
Figure 5.4 Molecular structure of complex 7 and 8 showing 50% probability ellipsoids.....	148
Figure 5.5 Population analyses (a) with the AO basis and (b) with the FO basis. DFT1 data are presented.....	156
Figure 5.6 Comparison of reaction progress with complex 5–8 using GC	161
Figure 5.7 Molecular structure of complex 9 showing 50% probability ellipsoids. Selected bond lengths.....	168

Chapter 1. Catalysis Utilizing Renewable C1 Sources, Carbon Dioxide and Methanol

1.1 Introduction

Environmental problems caused by anthropogenic chemicals are a matter of great concern around the world. Therefore, significant efforts have been devoted to minimizing the use and generation of hazardous compounds in chemical reactions. In recent years, the utilization of carbon dioxide and methanol as coupling partners in catalysis to replace classic halogenated reagents has attracted much attention, since this approach avoids the generation of toxic waste. In this chapter, transition metal-catalyzed reactions using CO₂ or methanol as a C1 source are described.

1.2 Homogeneous catalysis utilizing carbon dioxide

Carbon dioxide is an ideal C1 feedstock for the synthesis of fine chemicals due to its abundance and low toxicity.¹ However, its exploitation in organic synthesis is challenging, since CO₂ is thermodynamically and kinetically stable. Conventionally, harsh

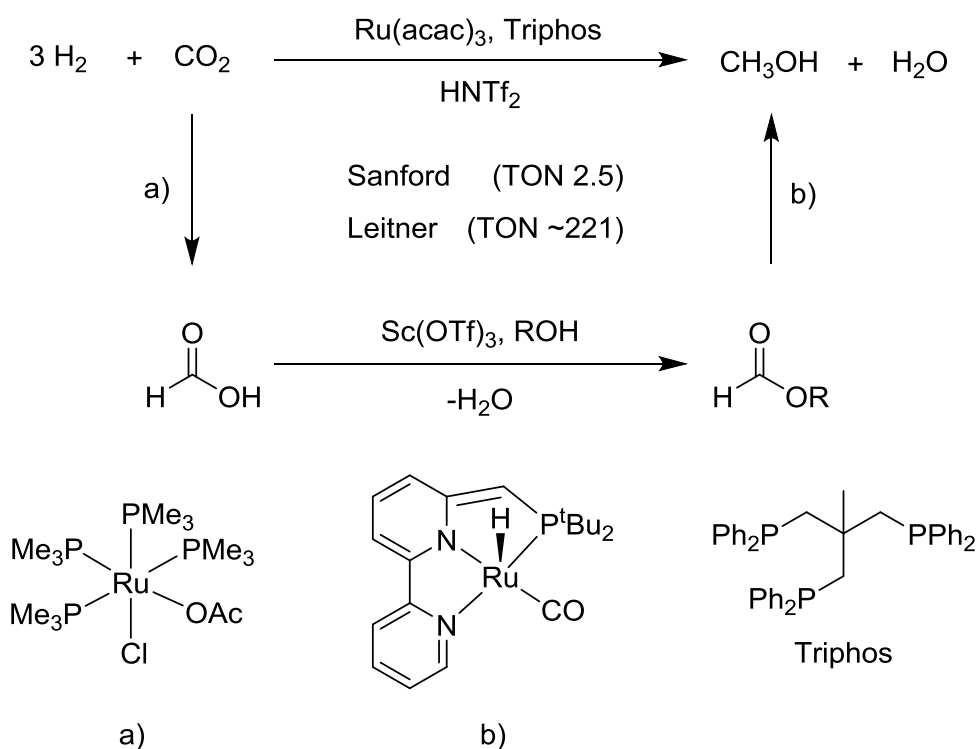
reaction conditions and strong nucleophiles such as Grignard reagents have been required to overcome the high energy barrier, resulting in toxic waste generation and large energy consumption. Hence, the development of an efficient catalytic system avoiding the use of organometallic reagents in stoichiometric amounts is a promising strategy to utilize CO₂ under mild reaction conditions.

1.2.1 Methanol production from carbon dioxide

Methanol is a versatile compound that is used in organic synthesis as a solvent and a basic building block.² In particular, the utilization of methanol in the production of olefins, methyl *t*-butyl ether (MTBE), and dimethyl ether (DME) has rapidly grown.³ Moreover, methanol is a readily biodegradable and clean-burning fuel, being an attractive alternative for powering vehicles and ships and generating electricity.⁴

Currently, methanol is industrially produced by the hydrogenation of toxic carbon monoxide. However, this process is catalyzed by copper/zinc-based heterogeneous catalysts under harsh reaction conditions (above 250 °C),⁵ which should ideally be replaced by an eco-friendly safe reaction.

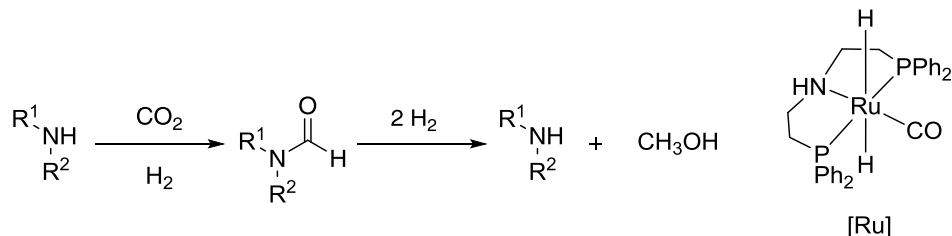
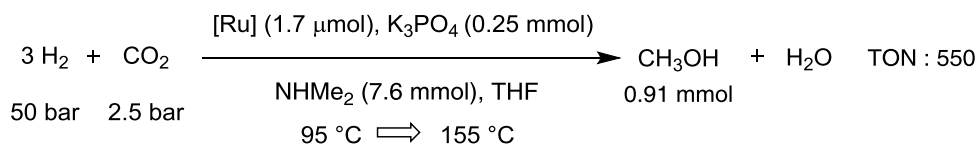
The catalytic hydrogenation of CO₂ to methanol is a promising solution to reduce the use of CO. The heterogeneous metal-catalyzed hydrogenation of CO₂ has already been reported,⁶ but the described system suffered from harsh reaction conditions and low selectivity, resulting in high energy consumption.



Scheme 1.1 Cascade strategy to produce methanol from CO₂.

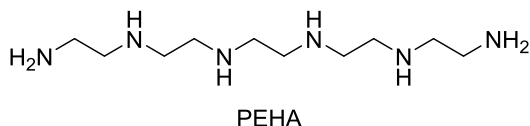
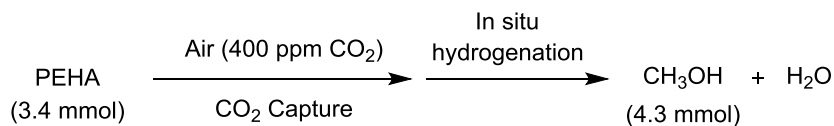
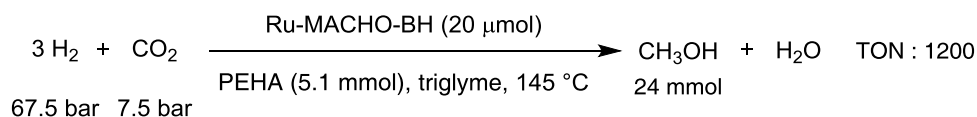
To date, significant progress has been made in the homogeneous metal-catalyzed hydrogenation of CO₂ and its derivatives to

methanol. In 2011, the Sanford group proposed the first cascade approach to produce methanol from CO₂ by using three different homogeneous catalysts in a one-pot reaction,⁷ which proceeded in three steps: 1) hydrogenation of CO₂ to formic acid, 2) esterification of formic acid to formyl esters, 3) hydrogenation of these esters to methanol, as illustrated in Scheme 1.1. The compatibility of each employed catalyst is a big hurdle to overcome. Indeed, the deactivation of the Ru-PNN complex by Sc(OTf)₃ and CO₂ was the primary factor hampering excellent turnover numbers (TONs). Shortly afterwards, the Leitner group improved the reaction efficiency by utilizing a single Ru-phosphine complex in the presence of catalytic amounts of acid.⁸ The pathway of this reaction is similar to that of Sanford's system, with the in situ generated Ru-phosphine complex responsible for both steps (a) and (b). The above catalytic reaction showed good selectivity toward methanol, with no byproducts such as CO and CH₄ formed.



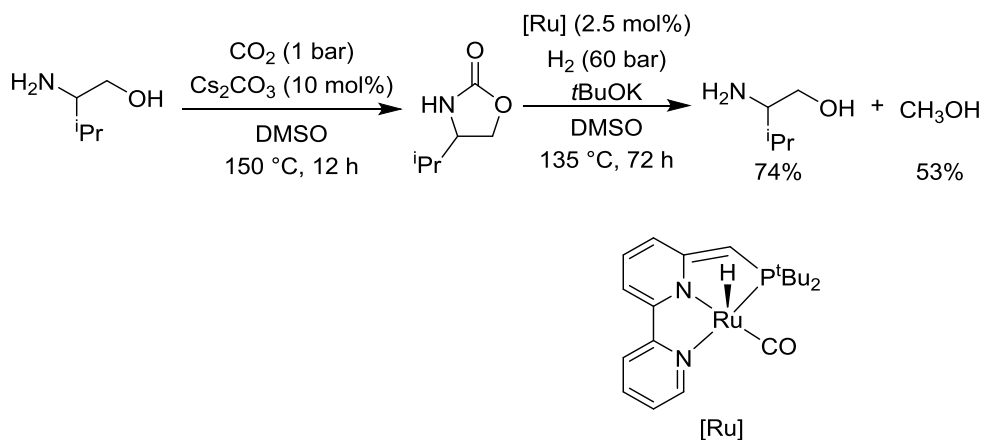
Scheme 1.2 Ru and amine catalyzed hydrogenation of CO₂ to methanol.

In 2014, the Sanford group reported another tandem process to produce methanol from CO₂ (Scheme 1.2).⁹ Hydrogenation of CO₂ in the presence of amines has been known to give formamides in high yields and selectivities, but the consecutive hydrogenation of formamides to methanol is unprecedented. The Sanford group realized formamide-mediated methanol production from CO₂ in the presence of a ruthenium catalyst and base.



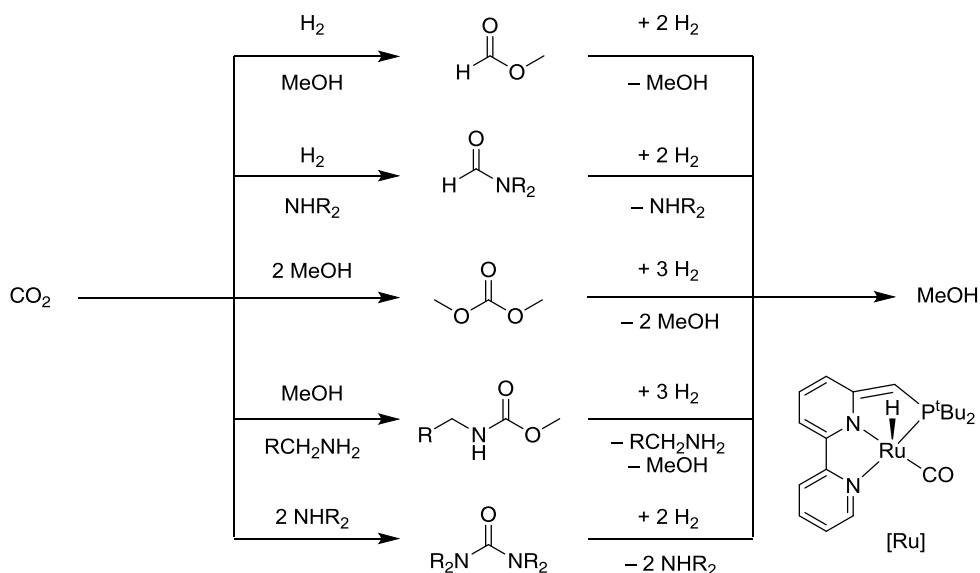
Scheme 1.3 Conversion of CO₂ from air into methanol using polyamine.

The Prakash group further improved Sanford's system by utilizing a polyamine and the same Ru–PNP pincer catalyst (Scheme 1.3).¹⁰ Compared to the previous system, the hydrogenation of CO₂ to methanol was undertaken by this group at constant temperature in the absence of additional base to achieve a higher TON. It is worth noting that CO₂ captured from air (containing less than 400 ppm of CO₂) was successfully converted to methanol in the described catalytic system.



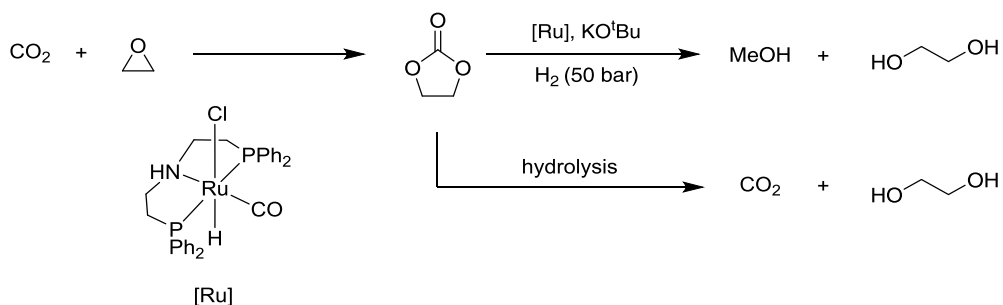
Scheme 1.4 CO_2 capture and hydrogenation to form methanol.

The Milstein group reported a similar cascade approach to produce methanol at low pressures of CO_2 (Scheme 1.4).¹¹ In this setup, CO_2 is captured by an amino alcohol in the presence of base, which generates the corresponding oxazolidone that is further hydrogenated without purification after addition of the Ru–PNN pincer catalyst, furnishing methanol and the amino alcohol as products.



Scheme 1.5 Indirect routes for methanol synthesis from CO₂.

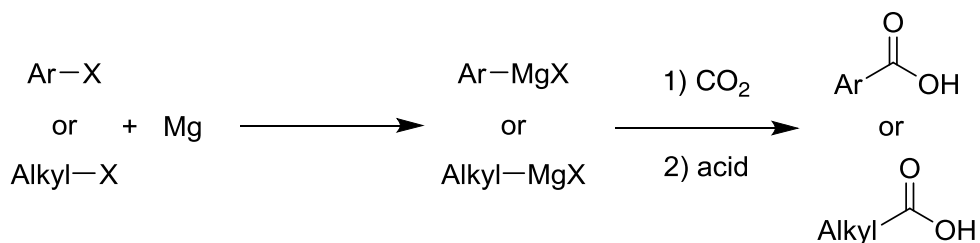
The hydrogenation of CO₂-derived molecules such as alkyl formates, formamides, dimethyl carbonate, organic carbamates, and urea derivatives provides alternative routes for converting CO₂ into methanol (Scheme 1.5).¹² For a long time, the hydrogenation of these compounds was considered very difficult, because the resonance stabilization by alkoxy and amine groups adjacent to the carbonyl group make hydrogenation of these substrates more difficult compared to the case of ketones. The Milstein group developed a method for the catalytic hydrogenation of these molecules using the versatile Ru-PNN pincer complex as a catalyst.¹²



Scheme 1.6 Catalytic hydrogenation of cyclic carbonates.

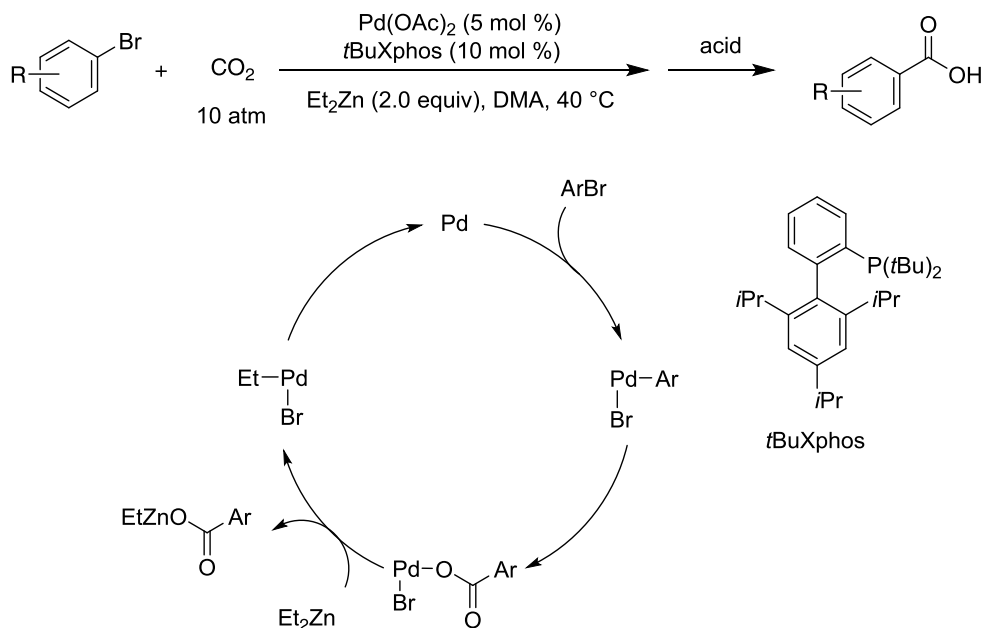
The Ding group reported another strategy, based on the indirect production of methanol via ethylene carbonate (Scheme 1.6).¹³ In the Omega industrial process, the hydrolysis of ethylene carbonate, which is easily obtained by incorporation of CO_2 into the corresponding epoxide, is currently used to produce ethylene glycol. The researchers replaced the hydrolysis step by hydrogenation on the Ru–PNP catalyst to generate methanol as a co–product.

1.2.2 Carboxylation



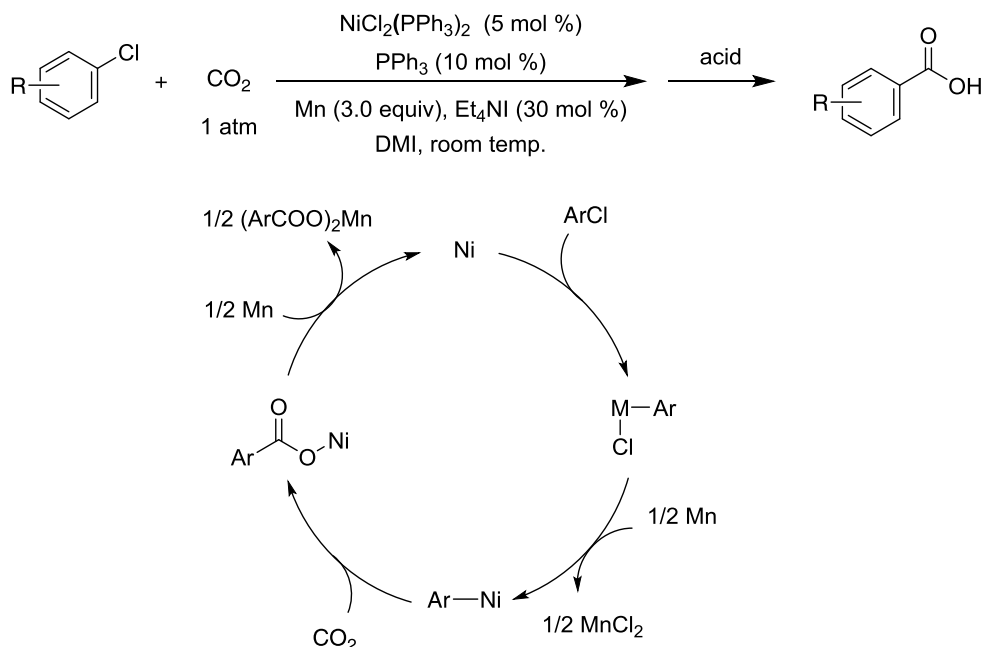
Scheme 1.7 Grignard reaction to prepare carboxylic acid.

Organic molecules containing carboxylic acid derivatives are readily found in a wide range of medically relevant compounds. Direct carboxylation of organometallic reagents (e.g., organolithium and organomagnesium compounds) with CO₂ is a powerful method to prepare carboxylic acids (Scheme 1.7).^{1a,14} However, the required stoichiometric amounts of well-defined and air-sensitive organometallic complexes limit the general use of this method. In addition, carbonyl-based functional groups are usually not tolerated by the reagents due to their high reactivity. Recently, a significant breakthrough has been achieved in transition metal-catalyzed direct carboxylation, using CO₂ as a readily available substrate.^{1a,14b,15}



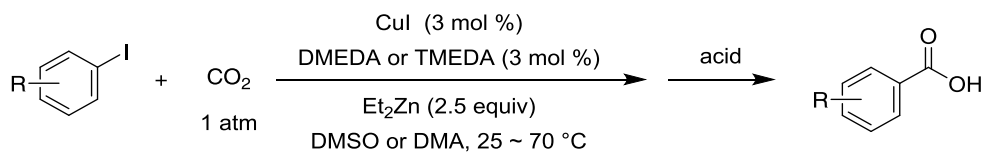
Scheme 1.8 Pd catalyzed reductive carboxylation of aryl bromides.

In 2009, the Martin group reported palladium-catalyzed reductive carboxylation of aryl bromides with CO₂ using Et₂Zn as a reducing reagent (Scheme 1.8).¹⁶ It was demonstrated that aryl halides, being common electrophiles, could be converted into nucleophilic species that further attacked carbon dioxide to form C-C bonds. A stoichiometric amount of diethylzinc was essential to operate the catalytic cycle smoothly, but the in-situ-generated organozinc nucleophiles did not directly attack CO₂. Various kinds of aryl bromides bearing sensitive functional groups such as ketones, esters, and alkenes were successfully carboxylated in good to excellent yields.



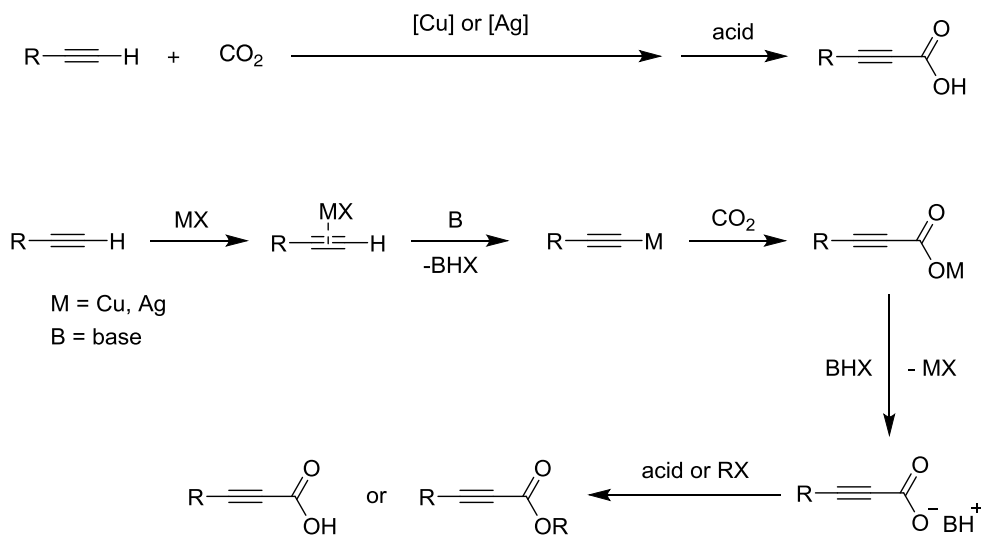
Scheme 1.9 Ni catalyzed reductive carboxylation of aryl chlorides.

In 2012, the Tsji group reported nickel-catalyzed carboxylation involving the direct use of less reactive aryl chlorides under mild conditions (Scheme 1.9).¹⁷ Stoichiometric quantities of reducing reagents were required to abstract chloride from Ni(II) species to generate Ni(I) species.



Scheme 1.10 Cu catalyzed reductive carboxylation of aryl iodides.

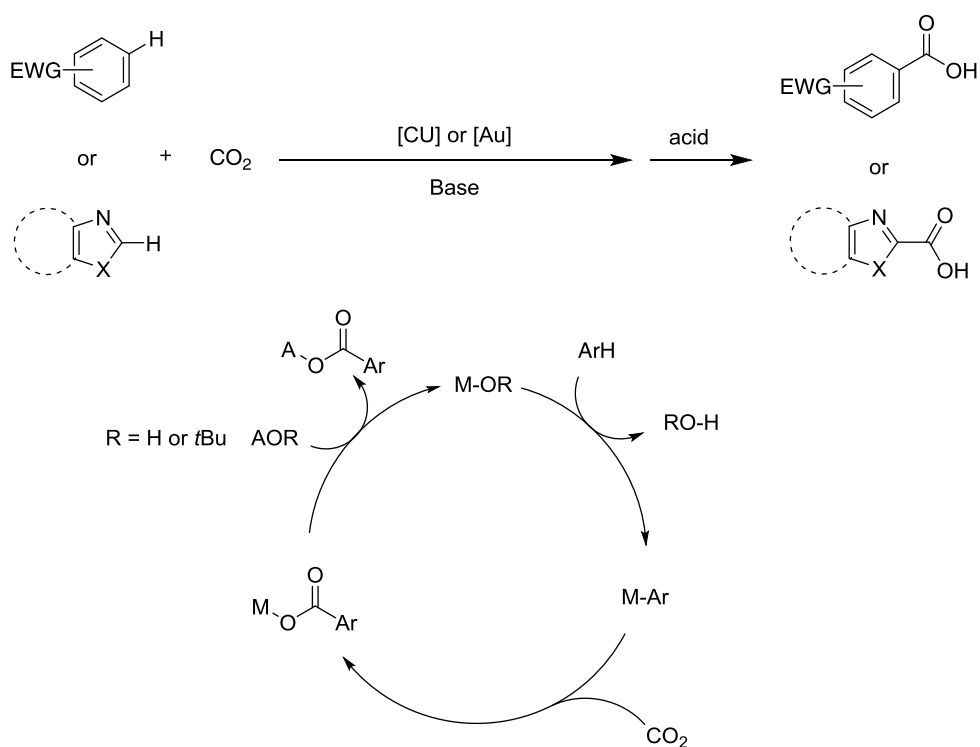
The Daugulis group found that less expensive copper catalysts are also active in the carboxylation of aryl iodides in the presence of Et_2Zn as a reducing agent (Scheme 1.10).¹⁸



Scheme 1.11 Carboxylation of terminal alkynes with CO_2 .

Direct carboxylation via C–H bond activation is also an important and challenging area. Recently, numerous studies on the carboxylation of terminal alkynes utilizing copper and silver catalysts have been reported.¹⁹ Group 11 elements are widely used as alkyne activators due to their notable affinity to sp C–H bonds, favoring alkyne deprotonation (1.11). The Inoue group was the first to apply

this concept to incorporate carbon dioxide into copper acetylides that are generated in situ by alkyne deprotonation.²⁰ Subsequently, the reaction efficiency was further improved by numerous groups using copper or silver-based catalysts, especially in the absence of ligands.¹⁹ Various propiolic acids and esters were successfully synthesized in good to excellent yields.



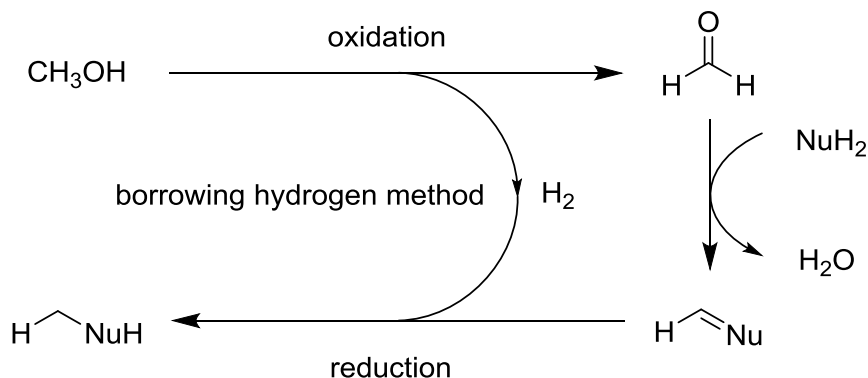
Scheme 1.12 Direct sp^2 C-H carboxylation with CO_2 .

In 2010, the Nolan group developed the catalytic carboxylation of sp^2 C-H bonds, utilizing CO_2 in the presence of an N-heterocyclic

carbene (NHC) –gold hydroxide complex and base (Scheme 1.12).²¹ Activated polyhalogenated arenes and azoles were used as substrates, undergoing highly selective carboxylation. Shortly afterwards, the Nolan²² and Hou groups²³ independently reported NHC –copper –catalyzed carboxylation. Both newly developed reactions were similar to the one observed for the NHC –gold system. The Hou group successfully isolated and structurally characterized key intermediates such as benzoxazolylcopper and carboxylate complexes, clarifying the mechanism of this reaction.

1.3 Homogeneous catalytic reaction with methanol

1.3.1 Methylation source

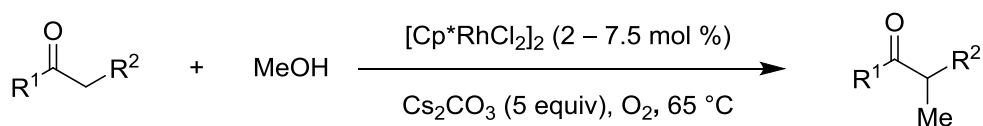


Scheme 1.13 The methanol utilization mechanism.

Carbon–carbon and carbon–nitrogen bond formation reactions are fundamentally important transformations in organic synthesis. Traditionally, the nucleophilic attack of substrates on alkyl halides/pseudohalides is mainly used to form C–C or C–N bonds, generating stoichiometric amounts of waste.

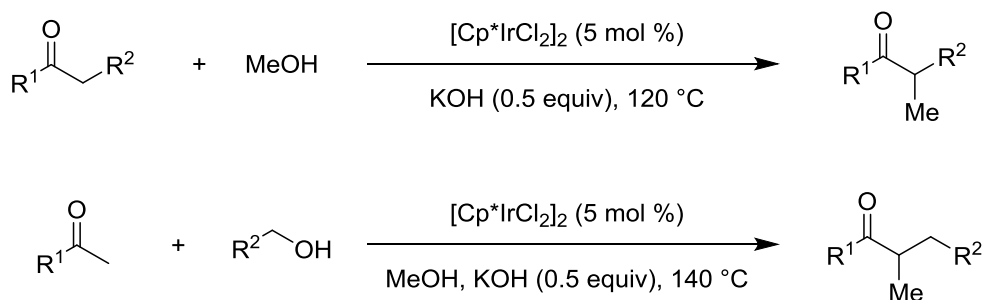
The hydrogen borrowing method (hydrogen auto–transfer), depicted in Scheme 1.13, represents a promising alternative to the formation of C–C and C–N bonds.²⁴ In this method, an alcohol is oxidized to the corresponding aldehyde, which further undergoes condensation with other nucleophiles. The hydrogen generated in situ

during oxidation is re-used to reduce olefins or imines, affording the desired products. Indeed, the use of alcohols as alkylating reagents has been extensively described.²⁵ Although numerous advances were achieved in this field, the use of methanol for methylation is still unexplored, which is related to its higher dehydrogenation activation energy in comparison with those of higher alcohols.^{2b,2c,24e,26}



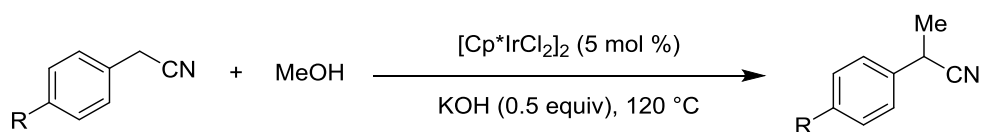
Scheme 1.14 Rh catalyzed α –methylation of ketone using methanol.

In 2013, the Donohoe group disclosed α –methylation of ketones using methanol as the methyl source in the presence of a rhodium catalyst and cesium carbonate (Scheme 1.14).²⁷ The reaction proceeded smoothly under an oxygen atmosphere (~98%). On the other hand, the efficiency of this catalytic system decreased when the reaction was carried out under argon, giving the desired product in 57% yield.



Scheme 1.15 Ir catalyzed α –methylation of ketone using methanol.

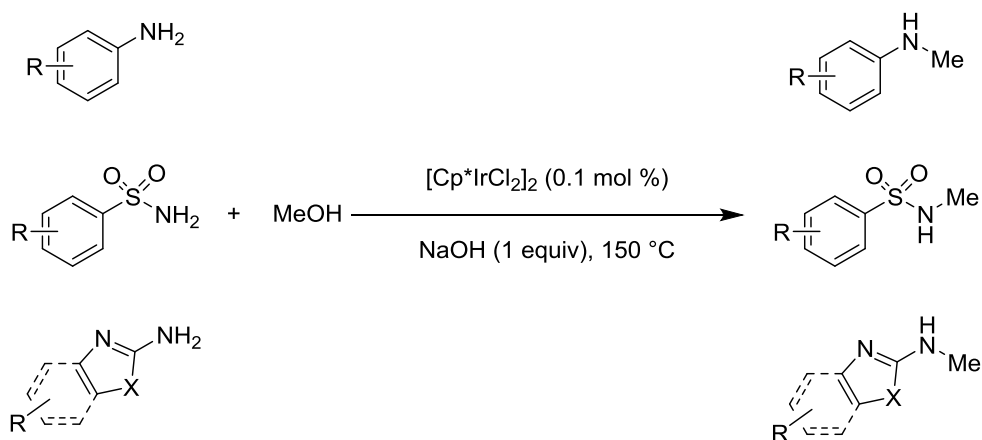
In 2014, the Obara group demonstrated that $[\text{Cp}^*\text{IrCl}_2]_2$, widely used in the reactions of alcohols, could be utilized in selective α – (di)methylation of ketones in the absence of oxygen (Scheme 1.15).²⁸ Notably, the catalytic system was successfully extended to a three – component one – pot reaction, resulting in α –methylation of methyl ketones using methanol and primary alcohols.



Scheme 1.16 Ir catalyzed α –methylation of nitrile using methanol.

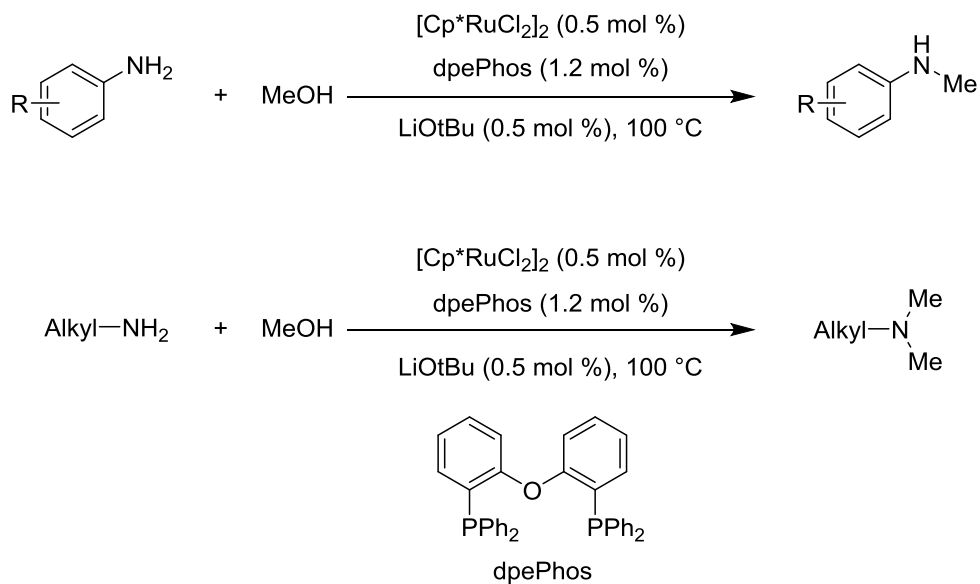
The same group further extended this catalytic system to other

compounds (Scheme 1.16).²⁸ A series of phenylacetonitriles containing electron-donating or electron-withdrawing groups afforded α -methylated products in good to excellent yields.



Scheme 1.17 Ir catalyzed N-methylation of amines using methanol.

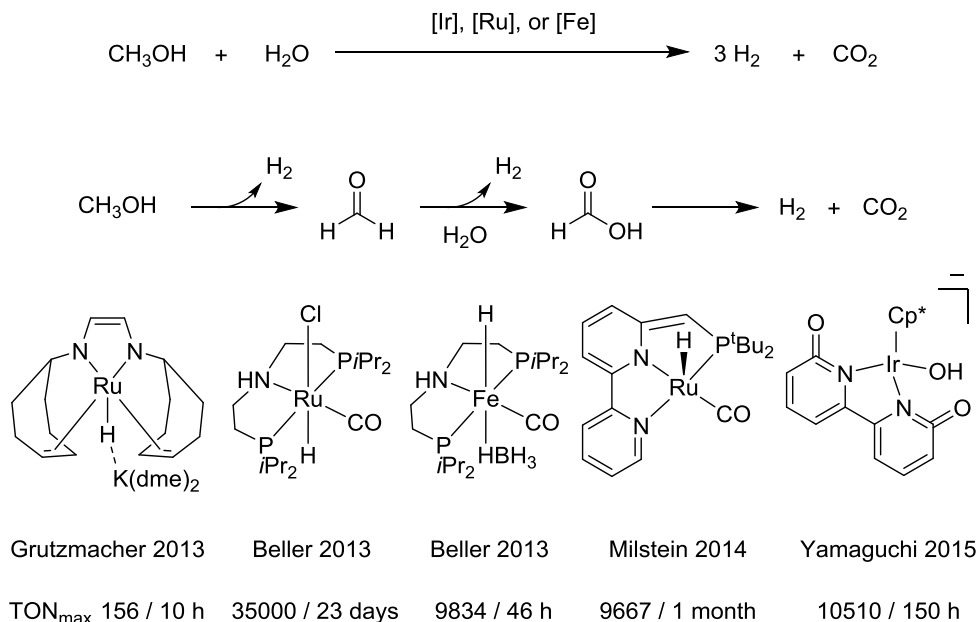
In 2012, the Feng Li group reported direct N-monomethylation of primary aromatic amines such as arylamines, arylsulfonamides, and aminoazoles in the presence of an iridium catalyst and sodium hydroxide (Scheme 1.17).^{26b} The catalytic system showed excellent selectivities toward N-monomethylation, with no N,N-dimethylated products detected.



Scheme 1.18 Ru catalyzed N–methylation of amines using methanol.

The Seayad group demonstrated that the ruthenium catalyst generated in situ from $[\text{RuCp}^*\text{Cl}_2]_2$ and the dpePhos ligand achieved N–methylation of amines under mild reaction conditions,^{2d} presenting selective N–monomethylation of primary aromatic amines and sulfonamides (Scheme 1.18). In addition, when aliphatic amines were used as substrates, N,N–dimethylated products were obtained in good to excellent yields.

1.3.2 Hydrogen generation (methanol reforming)



Scheme 1.19 Dehydrogenation of methanol.

Hydrogen is a clean-burning compound, affording water as the only combustion byproduct. Hence, it can be used as a fuel for spacecraft propulsion and as an energy source for fuel cells. Unfortunately, its low boiling point makes the transportation and handling of hydrogen difficult.

Methanol is considered a promising hydrogen carrier, because it exhibits a high hydrogen storage capacity (12.6 wt.%) and is liquid at room temperature and ambient pressure. The methanol reforming

process was first described in 1987 by the Cole–Hamilton group, who used $[\text{Rh}-(\text{bipy})_2]\text{Cl}$ as a catalyst.²⁹ In 2013, this reaction was independently reported by the Beller³⁰ and the Grützmacher groups.³¹ The Beller group demonstrated the decomposition of methanol into three equivalents of hydrogen and one equivalent of carbon dioxide in the presence of the Ru–PNP pincer catalyst and potassium hydroxide (8.0 M based on the total MeOH/H₂O volume) at 95 °C. Shortly afterwards, the same group reported catalytic methanol reforming using a well-defined iron pincer complex.³² In 2014, the Milstein group reported the generation of hydrogen from methanol using the Ru–PNN complex as a catalyst, which is also used in the hydrogenation of carbon dioxide derivatives to methanol.³³ To ensure a smooth reaction, two equivalents of sodium hydroxide with respect to methanol and an additional organic solvent such as THF or toluene were required. Nevertheless, it is worth noting that the catalyst could be easily recycled by separation of the organic and aqueous layers. In this way, a high TON value (9667) could be achieved for one month. The Yamaguchi and Fujita group has recently reported the use of anionic iridium species for the production of hydrogen from a mixture of methanol and water.³⁴ Compared to the previous system, this reaction requires a smaller amount of base (0.5 mol % relative to

MeOH).

1.3 Reference

- (1) (a) Yu, D.; Teong, S. P.; Zhang, Y. *Coord. Chem. Rev.* **2015**, *293–294*, 279. (b) MacDowell, N.; Florin, N.; Buchard, A.; Hallett, J.; Galindo, A.; Jackson, G.; Adjiman, C. S.; Williams, C. K.; Shah, N.; Fennell, P. *Energ. Environ. Sci.* **2010**, *3*, 1645. (c) Gouedard, C.; Picq, D.; Launay, F.; Carrette, P. L. *Int. J. Greenh. Gas Con.* **2012**, *10*, 244.
- (2) (a) Sun, C. L.; Zou, X. Y.; Li, F. *Chem.–Eur. J.* **2013**, *19*, 14030. (b) Ortega, N.; Richter, C.; Glorius, F. *Org. Lett.* **2013**, *15*, 1776. (c) Moran, J.; Preetz, A.; Mesch, R. A.; Krische, M. J. *Nat. Chem.* **2011**, *3*, 287. (d) Dang, T. T.; Ramalingam, B.; Seayad, A. M. *ACS Catal.* **2015**, *5*, 4082.
- (3) George A. Olah, A. G., G. K. Surya Prakash Ed. *Beyond Oil and Gas: The Methanol Economy*; Wiley–VCH: Weinheim, 2011.
- (4) Reed, T. B.; Lerner, R. M. *Science* **1973**, *182*, 1299.
- (5) Behrens, M.; Studt, F.; Kasatkin, I.; Köhl, S.; Hävecker, M.; Abild–Pedersen, F.; Zander, S.; Girsdsies, F.; Kurr, P.; Knief, B.–L.; Tovar, M.; Fischer, R. W.; Nørskov, J. K.; Schlögl, R. *Science* **2012**, *336*, 893.
- (6) Graciani, J.; Mudiyanse, K.; Xu, F.; Baber, A. E.; Evans, J.;

- Senanayake, S. D.; Stacchiola, D. J.; Liu, P.; Hrbek, J.; Sanz, J. F.; Rodriguez, J. A. *Science* **2014**, *345*, 546.
- (7) Huff, C. A.; Sanford, M. S. *J. Am. Chem. Soc.* **2011**, *133*, 18122.
- (8) Wesselbaum, S.; vom Stein, T.; Klankermayer, J.; Leitner, W. *Angew. Chem. Int. Ed.* **2012**, *51*, 7499.
- (9) Rezayee, N. M.; Huff, C. A.; Sanford, M. S. *J. Am. Chem. Soc.* **2015**, *137*, 1028.
- (10) Kothandaraman, J.; Goeppert, A.; Czaun, M.; Olah, G. A.; Prakash, G. K. S. *J. Am. Chem. Soc.* **2016**, *138*, 778.
- (11) Khusnutdinova, J. R.; Garg, J. A.; Milstein, D. *ACS Catal.* **2015**, *5*, 2416.
- (12) (a) Balaraman, E.; Gunanathan, C.; Zhang, J.; Shimon, L. J. W.; Milstein, D. *Nat. Chem.* **2011**, *3*, 609. (b) Balaraman, E.; Ben-David, Y.; Milstein, D. *Angew. Chem. Int. Ed.* **2011**, *50*, 11702. (c) Klankermayer, J.; Wesselbaum, S.; Beydoun, K.; Leitner, W. *Angew. Chem. Int. Ed.* **2016**, *55*, 7296.
- (13) Han, Z. B.; Rong, L. C.; Wu, J.; Zhang, L.; Wang, Z.; Ding, K. *Angew. Chem. Int. Ed.* **2012**, *51*, 13041.
- (14) (a) Omae, I. *Coord. Chem. Rev.* **2012**, *256*, 1384. (b) Cokoja, M.; Bruckmeier, C.; Rieger, B.; Herrmann, W. A.; Kühn, F. E. *Angew. Chem. Int. Ed.* **2011**, *50*, 8510.

- (15) (a) Börjesson, M.; Moragas, T.; Gallego, D.; Martin, R. *ACS Catal.* **2016**, *6*, 6739. (b) Maeda, C.; Miyazaki, Y.; Ema, T. *Catal. Sci. Technol.* **2014**, *4*, 1482.
- (16) Correa, A.; Martín, R. *J. Am. Chem. Soc.* **2009**, *131*, 15974.
- (17) Fujihara, T.; Nogi, K.; Xu, T.; Terao, J.; Tsuji, Y. *J. Am. Chem. Soc.* **2012**, *134*, 9106.
- (18) Tran–Vu, H.; Daugulis, O. *ACS Catal.* **2013**, *3*, 2417.
- (19) (a) Zhang, X.; Zhang, W. Z.; Ren, X.; Zhang, L. L.; Lu, X. B. *Org. Lett.* **2011**, *13*, 2402. (b) Manjolinho, F.; Arndt, M.; Gooßen, K.; Gooßen, L. J. *ACS Catal.* **2012**, *2*, 2014. (c) Gooßen, L. J.; Rodríguez, N.; Manjolinho, F.; Lange, P. P. *Adv. Synth. Catal.* **2010**, *352*, 2913. (d) Yu, D. Y.; Tan, M. X.; Zhang, Y. G. *Adv. Synth. Catal.* **2012**, *354*, 969.
- (20) Fukue, Y.; Oi, S.; Inoue, Y. *J. Chem. Soc. Chem. Comm.* **1994**, 2091.
- (21) Boogaerts, I. I. F.; Nolan, S. P. *J. Am. Chem. Soc.* **2010**, *132*, 8858.
- (22) Boogaerts, I. I. F.; Fortman, G. C.; Furst, M. R. L.; Cazin, C. S. J.; Nolan, S. P. *Angew. Chem. Int. Ed.* **2010**, *49*, 8674.
- (23) Zhang, L.; Cheng, J.; Ohishi, T.; Hou, Z. *Angew. Chem. Int. Ed.*

2010, 49, 8670.

- (24) (a) Gunanathan, C.; Milstein, D. *Chem. Rev.* **2014**, *114*, 12024.
(b) Gunanathan, C.; Milstein, D. *Science* **2013**, *341*, 6143 (c)
Gunanathan, C.; Ben-David, Y.; Milstein, D. *Science* **2007**, *317*, 790.
(d) Gnanaprakasam, B.; Zhang, J.; Milstein, D. *Angew. Chem. Int. Ed.*
2010, *49*, 1468. (e) Kang, B.; Hong, S. H. *Adv. Synth. Catal.* **2015**,
357, 834. (f) Chen, C.; Zhang, Y.; Hong, S. H. *J. Org. Chem.* **2011**, *76*,
10005. (g) Chen, C.; Hong, S. H. *Org. Biomol. Chem.* **2011**, *9*, 20.
- (25) (a) Guillena, G.; J. Ramón, D.; Yus, M. *Chem. Rev.* **2010**, *110*,
1611. (b) Yang, Q.; Wang, Q.; Yu, Z. *Chem. Soc. Rev.* **2015**, *44*, 2305.
(c) Hamid, M. H. S. A.; Slatford, P. A.; Williams, J. M. J. *Adv. Synth.*
Catal. **2007**, *349*, 1555.
- (26) (a) Ogawa, S.; Obora, Y. *Chem. Commun.* **2014**, *50*, 2491. (b)
Li, F.; Xie, J.; Shan, H.; Sun, C.; Chen, L. *RSC Adv.* **2012**, *2*, 8645.
- (27) Chan, L. K. M.; Poole, D. L.; Shen, D.; Healy, M. P. d.; Donohoe,
T. J. *Angew. Chem. Int. Ed.* **2014**, *53*, 761.
- (28) Ogawa, S.; Obora, Y. *Chem. Commun.* **2014**, *50*, 2491.
- (29) Morton, D.; Cole-hamilton, D. J. *J. Chem. Soc. Chem. Comm.*
1988, 1154.
- (30) Nielsen, M.; Alberico, E.; Baumann, W.; Drexler, H. J.; Junge,
H.; Gladiali, S.; Beller, M. *Nature* **2013**, *495*, 85.

- (31) Rodríguez-Lugo, R. E.; Trincado, M.; Vogt, M.; Tewes, F.; Santiso-Quinones, G.; Grützmacher, H. *Nat. Chem.* **2013**, *5*, 342.
- (32) Alberico, E.; Sponholz, P.; Cordes, C.; Nielsen, M.; Drexler, H.-J.; Baumann, W.; Junge, H.; Beller, M. *Angew. Chem. Int. Ed.* **2013**, *52*, 14162.
- (33) Hu, P.; Diskin-Posner, Y.; Ben-David, Y.; Milstein, D. *ACS Catal.* **2014**, *4*, 2649.
- (34) Fujita, K.-i.; Kawahara, R.; Aikawa, T.; Yamaguchi, R. *Angew. Chem. Int. Ed.* **2015**, *54*, 9057.

Chapter 2. Carbon Dioxide Capture and Use: Organic Synthesis Using Carbon Dioxide from Exhaust Gas*

2.1 Introduction

Recycling carbon dioxide (CO₂) as a renewable and environment-friendly source of carbon is one of the most attractive solutions to reduce our dependence on petrochemicals. One of the main approaches to recycle CO₂ is its capture and utilization (CCU);¹ this approach has potential to afford value-added products from the sustainable C₁ feedstock and to make large-scale cuts in atmospheric CO₂ emissions by capturing anthropogenic CO₂ without restructuring or closing the industrial plants.

Currently, amine scrubbing technology is used for capturing CO₂ in industry,² while the development of advanced CO₂ capture materials such as ionic liquids and metal-organic framework materials is underway.³ In the amine-based CO₂ capture process, alkanolamines selectively react with CO₂ in flue gas to form the corresponding carbamates (Figure 2.1).⁴ The alkanolamines can be recovered by stripping CO₂ with water vapor at 100–120 °C and

* The majority of this work has been published: Seung Hyo Kim, Kwang Hee Kim, and Soon Hyeok Hong, *Angew. Chem. Int. Ed.* **2014**, *53*, 771–774

recycled back to the beginning of the process. After the water is condensed from the stripper vapor, the CO_2 is compressed to 100–150 bar. The condensed CO_2 is then transported via pipeline or ship for geologic sequestration, and only a small portion of it is utilized as a C1 source for chemical synthesis.⁵ A high cost is paid for the transportation and sequestration.

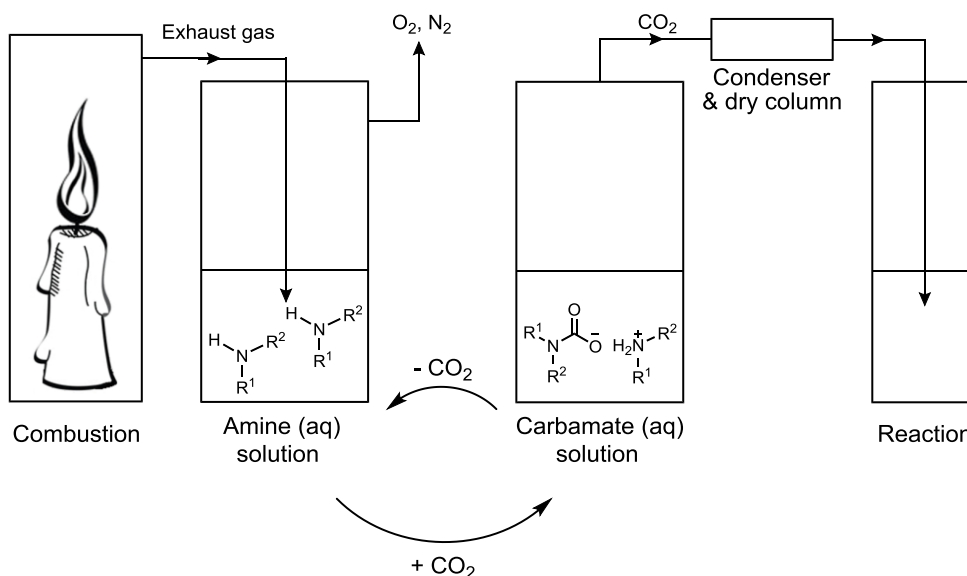


Figure 2.1 Carbon dioxide capture and utilization.

Therefore, it is highly desirable to utilize the environment –friendly raw material, CO_2 , as a C1 source for synthesizing fine chemicals. Urea has already been synthesized on an industrial scale using CO_2 .⁶ Moreover, catalytic syntheses of polycarbonates⁷ and cyclic carbonates⁸ have recently been commercially utilized. Significant

amounts of academic research have been conducted to transform CO₂ into fine chemicals.⁹ A classic example of CO₂ utilization in organic chemistry is carboxylic acid synthesis.⁹ To utilize CO₂ in organic synthesis, high purity CO₂ gas is required. In particular, the reactions mediated by transition metal complexes require hyper-pure CO₂ gas (>99.999%). Inspired by the overall CCU concept, we envisioned that the CO₂ from exhaust gas rather than commercial CO₂ gas can be utilized for usual organic syntheses. Herein, we report an unprecedented strategy for utilizing CO₂ that is captured from combustion sources for organic syntheses (Figure 2.1).

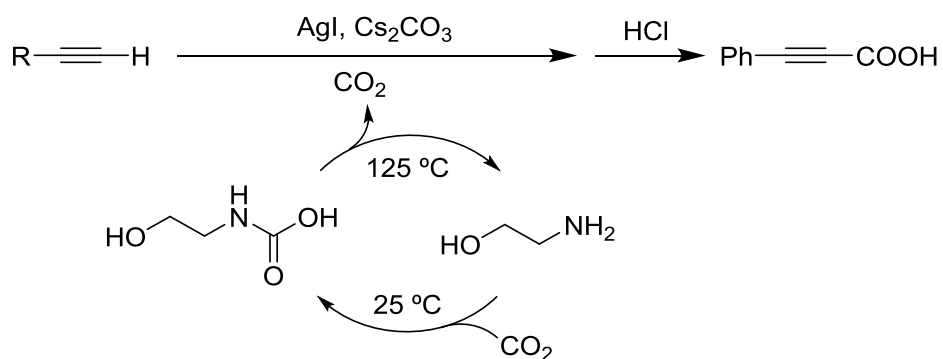
2.2 Result and discussion

2.2.1 Efficiency test of CO₂ capturing solutions

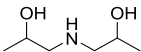
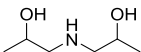
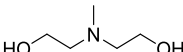
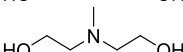
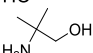
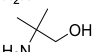
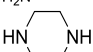
We devised our strategy as follows: 1) selective capturing of CO₂ generated from fossil fuel combustion using an alkanolamine solution¹⁰ and then 2) conduct organic reactions with CO₂ released from the captured material (Figure 2.1). The alkanolamine solution used in the process can be recycled for subsequent capture and release processes. In order to test this idea, previously reported silver-catalyzed carboxylation of alkynes¹¹ was chosen as the model reaction to confirm if the amount and purity of CO₂ released from the

captured materials are sufficient to carry out an organic reaction (Table 2.1).¹² When hyper-pure CO₂ (>99.999%) was directly applied to the reaction mixture under atmospheric pressure, the carboxylation of acetylene afforded the corresponding product in 83% yield (Table 2.1, entry 1).¹¹

Table 2.1 Alkyne carboxylation reaction to test efficiencies of CO₂ capturing solutions.^a



entry	amine ^b	solvent	volume ^c	yields
1 ^d	Pure CO ₂	—	—	83%
2	HOCH ₂ CH ₂ NH ₂	H ₂ O	25 mL	82%
3	HOCH ₂ CH ₂ NH ₂	H ₂ O	10 mL	77%
4	HOCH ₂ CH ₂ NH ₂	H ₂ O	5 mL	67%
5	HOCH ₂ CH ₂ NH ₂	H ₂ O	2.5 mL	38%
6	HOCH ₂ CH ₂ NH ₂	DMF	5 mL	73%
7	HOCH ₂ CH ₂ NHCH ₂ CH ₂ OH	H ₂ O	5 mL	73%
8	HOCH ₂ CH ₂ NHCH ₂ CH ₂ OH	DMF	5 mL	59%

9		H ₂ O	5 mL	8%
10		DMF	5 mL	67%
11		H ₂ O	5 mL	19%
12		DMF	5 mL	NR
13		H ₂ O	5 mL	69%
14		DMF	5 mL	69%
15		H ₂ O	5 mL	64%

^aReaction conditions: phenylacetylene (1.0 mmol, 1.0 equiv), AgI (2.5 mol%), Cs₂CO₃ (1.5 equiv), CO₂ (ambient pressure) from an amine solution, DMF (10 mL), 25 °C, 16 h. ^bPure CO₂ was captured by the amine solution for 25 min. ^cVolume of solvent, and molality of amine solutions: 7 m. ^dThe reaction was performed with hyper-pure CO₂ gas. NR = No reaction.

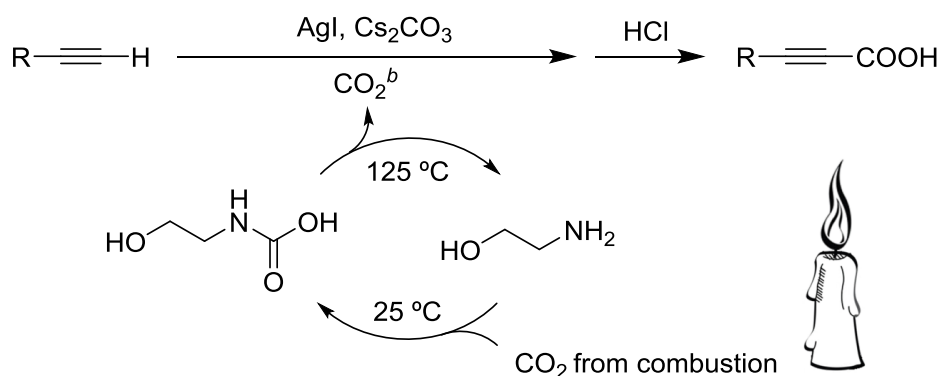
Several alkanolamine solutions either in DMF or water (e.g., 7 molality (m), ~30% ethanolamine (MEA) by weight, the most used concentration and CO₂ capture material in industry, respectively) have been tested as CO₂ capture and release materials.¹⁰ To optimize the reaction conditions, hyper-pure CO₂ gas (>99.999%) obtained from a commercial supplier was introduced into the alkanolamine solution for 15 min, and the saturated CO₂ solution was used as the CO₂ source for the model reactions. Most of the tested alkanolamine solutions were suitable to be used as CO₂ capture and release material (Table 2.1). Both DMF and water worked well as the solvent

for MEA (Table 2.1, entries 2–6).² For our reaction scale (1 mmol), about 35 mL of aqueous MEA solution (7 m, 25 mL of the solvent) was enough to show activity comparable to that obtained using commercial hyper-pure CO₂ gas (Table 2.1, entries 1 and 2). In the case of diethanolamine, a secondary amine, the reaction afforded better yield of the product in water than in DMF (Table 2.1, entries 7 and 8). The use of diisopropanolamine afforded a poor yield (8%) of the product in water; however, a moderate yield (67%) was obtained in DMF (Table 2.1, entries 9 and 10).¹³ Because tertiary *N*-methyldiethanolamine (no acidic H present) cannot react with CO₂, its solution in DMF could not be used to capture CO₂ (no reaction, Table 2.1, entry 12).¹⁴ However, its aqueous solution afforded 19% yield of the product (Table 2.1, entry 11). This is because *N*-methyldiethanolamine acts as a base and promotes CO₂ hydrolysis to afford carbonates that can produce CO₂ upon heating.¹⁴ Sterically hindered 2-amino-2-methyl-1-propanol that was used to prevent degradation at high temperature afforded the product in good yields (69%, Table 2.1, entry 13 and 14).¹⁴ An aqueous piperazine solution afforded the product in moderate yield (64%, Table 2.1, entry 15). Among the alkanolamine solutions tested, the aqueous MEA solution was chosen as the optimum CO₂ capturing solution because of

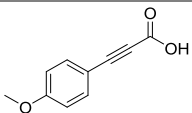
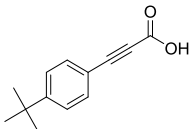
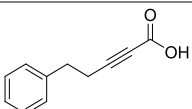
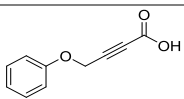
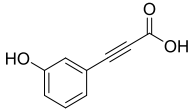
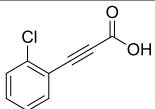
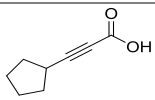
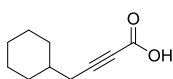
excellent CO₂ capture and release capability and low cost, which also account for it being the most popularly used in industry.

2.2.2 Alkyne carboxylation using CO₂ from combustion

Table 2.2 Alkyne carboxylation utilizing CO₂ from combustion.^a



entry	substrates	recycle times	yields
1		1	82%
2		19	82%
3		33	79%
4		55	80%
5 ^c		—	81%
6 ^d		—	NR
7 ^e		—	39%
8		2	84%
9		22	83%
10		5	75%
11		24	78%

12		7	80%
13		26	80%
14		14	88%
15		31	84%
16 ^f		23	78%
17 ^f		32	81%
18		13	81%
19		30	85%
20		17	90%
21		21	90%
22 ^f		20	89%
23 ^f		27	87%
24 ^f		18	67%
25 ^f		25	64%
26 ^f		12	65%
27 ^f		29	58%

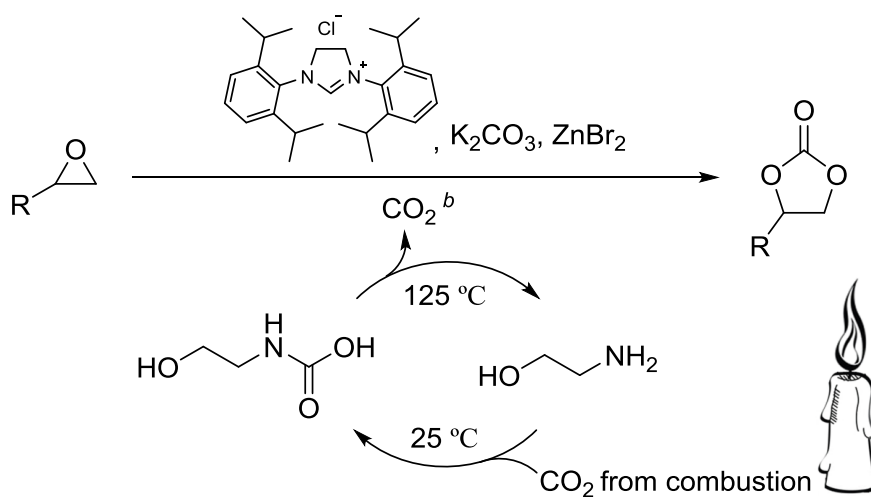
^aReaction conditions: alkynes (1.0 mmol, 1.0 equiv), AgI (2.5 mol%), Cs₂CO₃ (1.5 equiv), CO₂ (ambient pressure) from an aqueous MEA solution (7 m, 25 mL of H₂O), DMF (10 mL), 25 °C, 16 h. ^bA candle was burned for 3 h, and the CO₂ from the exhaust gas was captured in the MEA solution. ^cCO₂ was generated by methanol combustion. ^dExhaust gas was directly introduced to the reaction mixture for 7 h. ^eDry ice was directly added to the reaction mixture. ^f50 °C, 24h.

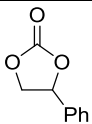
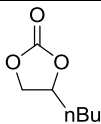
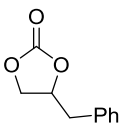
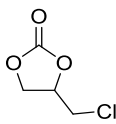
Encouraged by the initial results, the strategy to utilize CO₂ from exhaust gas was further applied to the carboxylation of various alkynes (Table 2.2).¹¹ A burning candle, generating a mixture of C₂₀–C₄₀ hydrocarbons, was selected as the combustion source. An aqueous MEA solution (7 m, 25 mL of H₂O) in a reaction tube was chosen to capture CO₂ from the combustion source and then release CO₂ for the target reaction. The recycled solution was used for the experiments listed in Tables 2.2 and 2.4. Photographs of the reaction set up following the design in Figure 2.1 are presented in the experimental section (Figures 2.2 and 2.3). Although some soot was produced due to incomplete combustion, to our delight, the carboxylation reactions with released CO₂, which was captured by the MEA solution from the combustion of the candle, were as efficient as that with hyper-pure CO₂ gas (79–82% yields, Table 2.2, entries 1–4). Furthermore, even after recycling the MEA solution 55 times, the reaction yield did not reduce significantly (80% yield, Table 2.2, entry 4). When another combustion source, methanol, was used for CO₂ generation, the reaction efficiency was not affected either (Table 2.2, entry 5). However, no reaction occurred when the exhaust gas from the combustion of candle was directly introduced into the reaction medium (Table 2.2, entry 6), which showed that it was

essential to use the MEA solution to increase the CO₂ concentration and purity of the combustion gas. Dry ice, a general source of CO₂ in organic chemistry, was directly introduced into the reaction; however, the yield (39%) was low, presumably due to the reaction being sensitive to air and water (Table 2.2, entry 7). The substrate scope was expanded using the recycled aqueous MEA solution. All of the reactions were run twice, and proceeded smoothly exhibiting comparable reaction yields with previously reported studies using hyper-pure CO₂ gas.¹¹ The reaction yields were consistent regardless of the number of times that the aqueous MEA solution was recycled (Table 2.2, entries 8–27).

2.2.3 Cyclic carbonate synthesis using CO₂ from combustion

Table 2.3 Cyclic carbonate synthesis utilizing CO₂ from combustion.^a



entry	substrate	yields ^c	entry	substrate	yields ^c
1		90%	3		93%
2		91%	4		92%

^aReaction conditions: epoxides (2.0 mmol 1.0 equiv), ZnBr₂ (2 mol%), K₂CO₃ (2 mol%), 1,3-bis-(2,6-diisopropylphenyl)imidazolinium chloride (2 mol%), CO₂ (ambient pressure) from the captured material, DMSO (1 mL), 24 h, 80 °C. ^bA candle was burned for 5 h, and the CO₂ from the exhaust gas was captured in the MEA (aq) solution (70 mL, 7 m). ^cIsolated yields.

Next, CO₂ was incorporated into epoxides to form cyclic carbonates to check for the applicability of this method to other reactions.⁸ There is an increasing demand for cyclic carbonates in both industry and academia.^{8,15} Carbonates are used as monomers to synthesize polycarbonates and polyurethanes.⁷ Furthermore, the hydrogenation of cyclic carbonates is a promising route to convert CO₂ to methanol, an excellent alternative fuel.¹⁶ Therefore, the syntheses of carbonates utilizing CO₂ gas from combustion sources are an attractive route for carbon recycling. The incorporation of CO₂

into epoxides to synthesize carbonates is usually performed at pressures higher than 1 atm.⁸ Recently, Shi and co-workers reported a carbonate synthesis under atmospheric pressure using commercially available N-heterocyclic carbene (NHC) and ZnBr₂ as the catalyst.¹⁷ We applied our strategy to evaluate this reaction. Although the reactions involving NHC are usually air and moisture sensitive, all of the products were obtained in excellent yields using the released CO₂ that was captured by the MEA solution from the combustion source (90–93%, Table 2.3). Therefore, the quality of CO₂ captured using the MEA solution was sufficient to conduct even air and moisture sensitive reactions using NHC-based transition metal catalysts.

2.2.4 Grignard reaction with CO₂ from combustion

Table 2.4 Grignard reaction with CO₂ from combustion.^a

Reaction scheme: $\text{R-MgBr} \xrightarrow[\text{CO}_2^b]{\text{THF}} \xrightarrow{\text{HCl}} \text{R-COOH}$

CO₂ cycle: $\text{HOCH}_2\text{CH}_2\text{NHCOOH} \xrightarrow{125\text{ }^\circ\text{C}} \text{CO}_2 + \text{HOCH}_2\text{CH}_2\text{NH}_2$
 $\text{HOCH}_2\text{CH}_2\text{NH}_2 + \text{CO}_2 \xrightarrow{25\text{ }^\circ\text{C}} \text{HOCH}_2\text{CH}_2\text{NHCOOH}$ (CO₂ from combustion)

entry	substrate	yields ^c	entry	substrate	yields ^c
1		98%	3	Hexyl	89%
2 ^d		96%	4		>99%

^aReaction conditions: Grignard reagents (1.0 mmol), THF (1 mL), CO₂ (ambient pressure) from the recycled captured material, 25 °C, 1 h. ^bA candle was burned for 3 h, and the CO₂ from the exhaust gas was captured in the aqueous MEA solution (7 m, 25 mL H₂O). ^cIsolated yields. ^dDry-ice was directly added into the reaction tube as the CO₂ source.

Finally, we applied our strategy to one of the most widely used organic reactions, Grignard reaction.¹⁸ The reaction of Grignard reagents with CO₂ using dry ice is a well-known synthetic route to obtain carboxylic acids. We conducted Grignard reactions to confirm the quality of CO₂ captured using the recycled aqueous MEA solution that had been used for alkyne carboxylation. Grignard reagents are very sensitive to moisture, as it causes protonation, and to O₂ in air, as it forms peroxides.¹⁸ Therefore, it would be good to verify if this strategy can be applied to highly moisture and oxygen sensitive reactions. The incorporation of CO₂ into phenyl magnesium bromide using our set-up afforded benzoic acid in excellent yield (98% yield, Table 2.4, entry 1), which was comparable to that of the reaction with dry ice (96%, Table 2.4, entry 2). The reaction could also be applied to other Grignard reagents performing carboxylations in high yields (89–99%, Table 2.4, entries 3–4). Notably, the use of 54-times-recycled MEA solution did not diminish the reaction efficiency.

2.3 Conclusion

In summary, an unprecedented organic synthesis strategy utilizing CO₂ from exhaust gas was demonstrated. We have validated that the CO₂ generated from several combustion sources could be used in

organic syntheses as efficiently as hyper-pure CO₂ gas with >99.999% purity from a commercial source. More importantly, the CO₂-capturing aqueous MEA solution could be recycled continuously without any decrease in the CO₂ capture and release efficiency. Furthermore, no difficulty was encountered in performing air and moisture sensitive reactions. Thus, in addition to demonstrating a model for CO₂ gas capture and utilization from combustion sources in fine chemical syntheses, we hope that our strategy could be used for carrying out organic reactions requiring CO₂ without using high-purity CO₂ gas and related equipment in an ordinary organic synthesis laboratory.

2.4 Experimental section

2.4.1 General information

All reactions were carried out in oven-dried glassware under an inert atmosphere of dry argon or nitrogen. All reagents were obtained from Alfa Aesar and Sigma Aldrich and used as received. DrieriteTM was used as a filling in a dry column. A candle was purchased in a local shop. The Special glass for combustion was designed by us. Analytical TLC was performed on a Merck 60 F254 silica gel plate (0.25mm thickness). Column chromatography was performed on

Merck 60 silica gel (230–400 mesh). NMR spectra were recorded on a Bruker DPX–300 (300 MHz) spectrometer. Tetramethylsilane was used as reference, and the chemical shifts were reported in ppm and the coupling constant in Hz.

2.4.2 General procedure of CO₂ capture and utilization from exhaust gas

MEA (10 mL, 7 mmol) and distilled water (25 mL) were placed in a Schlenk flask. To capture CO₂, the exhaust gas from the combustion of a candle was bubbled through the MEA solution for 3 h at room temperature. The CO₂–saturated solution could be stored at room temperature for more than a week and used when needed. The flask with the solution was connected to a reflux condenser. The top end of the reflux condenser was connected to a dry column linked to a bubbler. The MEA solution was heated to 125 °C for 10~15 min to purge the set up with CO₂. Next, the bubbler was replaced with a gas line with a needle in the end. The target organic reaction (1 mmol scale) was set up separately in a Schlenk flask under inert conditions. The line from the captured CO₂ solution and the vent line with a bubbler were introduced into the target reaction flask while CO₂ evolution continued. The reaction flask was purged with CO₂ gas from

the MEA solution for 5 min. Next, the vent line was exchanged with a balloon. CO₂ was captured in the balloon for 10–25 min until no more CO₂ evolved from the captured material. Next, the line from the CO₂ source was closed, and the reaction flask was isolated. The reaction continued under closed conditions with the equipped CO₂ balloon (Figures 2.2 and 2.3).



Figure 2.2 CO₂ capture process using an amine solution.

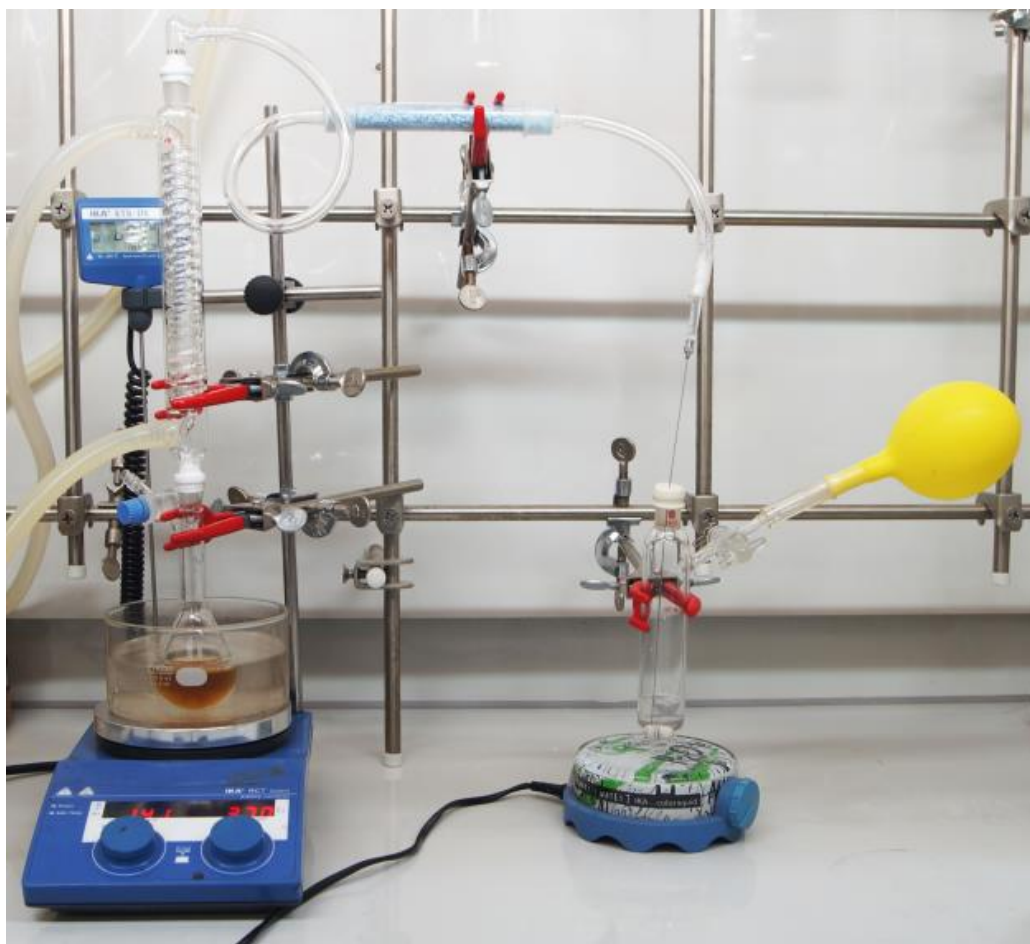


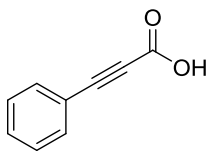
Figure 2.3 Reaction set up utilizing the captured CO₂ solution.

2.4.3 General procedure for carboxylation of terminal alkynes with CO₂

A 50 mL oven dried Schlenk tube connected with a balloon was charged with AgI (5.9 mg, 0.025 mmol), Cs₂CO₃ (487 mg, 1.5 mmol), alkyne (1.0 mmol), DMF (10 mL) under Ar atmosphere. The reaction tube was purged by CO₂ from the captured solution for 5 min. After closing the outlet, CO₂ was captured into the attached balloon for 10

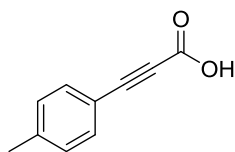
min. The reaction tube was stirred at ambient temperature ($\sim 25\text{ }^{\circ}\text{C}$) for 16 h. The reaction mixture was diluted with water (20 mL) and extracted with hexane or CH_2Cl_2 ($3 \times 20\text{ mL}$). The aqueous layer was acidified with aqueous HCl (2 N, 30 mL) at lowered temperature and then extracted with diethyl ether ($3 \times 30\text{ mL}$). The combined organic layers were washed with water and brine and dried over MgSO_4 . The solvent was removed under vacuum to afford the product.

2.4.4 Characterization data for carboxylic acids



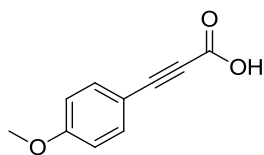
Phenylpropionic acid

^1H NMR (300 MHz, CDCl_3 , δ): 7.61–7.64 (m, 2H, Ar H), 7.52–7.55 (m, 1H, Ar H), 7.44–7.49 (m, 2H, Ar H)



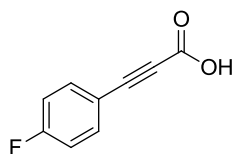
4-Methylphenylpropionic acid

^1H NMR (300 MHz, CDCl_3 , δ): 7.51 (d, $J = 8.1\text{ Hz}$, 2H Ar H), 7.20 (d, $J = 8.3\text{ Hz}$, 2H Ar H), 2.38 (s, 3H CH_3).



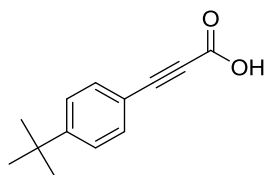
4-Methoxyphenylpropionic acid

^1H NMR (300 MHz, CDCl_3 , δ): 7.58 (d, $J = 8.3$ Hz, 2H, Ar H), 6.91 (d, $J = 8.7$ Hz, 2H, Ar H), 3.85 (s, 3H OCH_3).



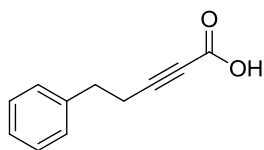
4-Fluorophenylpropionic acid

^1H NMR (300 MHz, CDCl_3 , δ): 9.39 (br s, 1H, COOH) 7.69–7.62 (m, 2H), 7.17–7.09 (m, 2H).



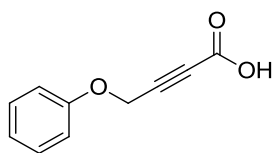
4-tert-Butylphenylpropionic acid

^1H NMR (300 MHz, CDCl_3 , δ): 7.56 (d, $J = 8.6$ Hz, 2H, Ar H), 7.41 (d, $J = 8.6$ Hz, 2H, Ar H), 1.32 (s, 9H, t -butyl H).



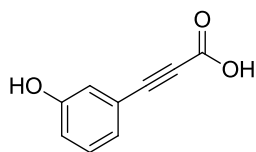
5-Phenyl-2-pentynoic acid

^1H NMR (300 MHz, CDCl_3 , δ): 11.50 (s, 1H, COOH), 7.42–7.29 (m, 5H, Ar H), 2.97 (d, $J = 7.4$ Hz, 2H, CH_2), 2.70 (d, $J = 7.4$ Hz, 2H, CH_2).



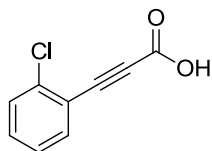
4-Phenoxy-2-butynoic acid

^1H NMR (300 MHz, CDCl_3 , δ): 7.37–7.30 (m, 2H, Ar H), 7.10–7.02 (m, 1H, Ar H), 7.01–6.90 (m, 2H, Ar H) 4.84 (s, 2H, CH_2)



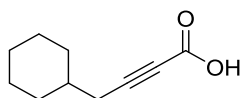
3-Hydroxyphenylpropionic acid

^1H NMR (300 MHz, CD_3OD , δ): 7.25 (t, $J = 8.0$ Hz, 1H, Ar H) 7.08–7.04 (m, 1H, Ar H), 6.99–6.90 (m, 2H, Ar H).



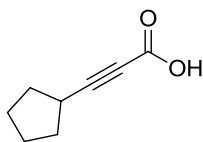
2-Chlorophenylpropionic acid

^1H NMR (300 MHz, CD_3OD , δ): 7.67–7.65 (m, 1H, Ar H), 7.57–7.46 (m, 2H, Ar H), 7.42–7.35 (m, 1H Ar H).



4-Cyclohexyl-2-butynoic acid

^1H NMR (300 MHz, CDCl_3 , δ): 10.79 (br s, 1H, COOH), 2.26 (d, J = 6.7 Hz, 2H, CH_2), 1.86–1.50 (m, 6H, Cy H), 1.3–0.94 (m, 5H, Cy H).



3-Cyclopentyl-2-propynoic acid

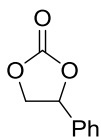
^1H NMR (300 MHz, CDCl_3 , δ): 11.18 (br s, 1H, COOH), 2.81–2.74 (m, 1H, CH), 2.00–1.59 (m, 8H).

2.4.5 General procedure for cycloaddition reaction of epoxides with CO_2

1,3-Bis-(2,6-diisopropylphenyl)imidazolinium chloride (17.6 mg, 0.04 mmol), K_2CO_3 (5.5 mg, 0.04 mmol), ZnBr (9.0 mg, 0.04 mmol), epoxide (2 mmol), and DMSO (1 mL) were added in a 10 mL oven

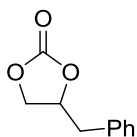
dried Schlenk tube connected with a balloon under Ar atmosphere. The reaction tube was purged by CO₂ from the captured solution for 5 min. After closing the outlet, CO₂ was captured into the attached balloon for 25 min. The reaction was heated to 80 °C for 24 h. After being cooled down, water (30 mL) was added to the reaction mixture. The organic layer was extracted with CH₂Cl₂ (3 × 10 mL), and filtered through a silica plug. All volatiles were removed under vacuum, and the product was collected without further purification.

2.4.6 Characterization data for cyclic carbonates



4-Phenyl-1,3-dioxolan-2-one

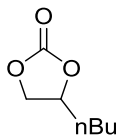
¹H NMR (300 MHz, CDCl₃, δ): 7.47–7.35 (m, 5 H, Ar H), 5.68 (t, *J* = 8.0 Hz, 1 H CH), 4.80 (t, *J* = 8.4 Hz, 1 H, CH₂), 4.35 (t, *J* = 8.2 Hz, 1 H, CH₂).



4-Benzyl-1,3-dioxolan-2-one

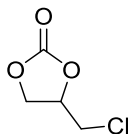
¹H NMR (300 MHz, CDCl₃, δ): 7.38–7.20 (m, 5H, Ar H), 4.98–4.88 (m, 1H, CH), 4.44 (t, *J* = 8.1 Hz, 1H, CH₂), 4.17 (t, *J* = 7.2 Hz, 1 H,

CH₂), 3.15 (dd, $J = 14.0, 6.4$ Hz, 1H, CH₂), 2.99 (dd, $J = 14.2, 6.4$ Hz, 1H, CH₂).



4-Butyl-1,3-dioxolan-2-one

¹H NMR (300 MHz, CDCl₃, δ): 4.72–4.65 (m, 1H, CH), 4.51 (t, 1H, $J = 8.0$ Hz, CH₂), 4.05 (t, $J = 8.0$, 1H, CH₂), 1.82–1.61 (m, 2H, CH₂), 1.46–1.27 (m, 4H, CH₂), 0.89 (t, $J = 7.2$ Hz, 3H CH₃)



4-(Chloromethyl)-1,3-dioxolan-2-one

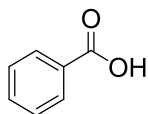
¹H NMR (300 MHz, CDCl₃, δ): 4.99–4.92 (m, 1H), 4.59 (t, $J = 8.4$ Hz, 1H), 4.41 (dd, $J = 5.7, 8.8$ Hz, 1H), 3.81–3.69 (m, 2H, CH₂Cl)

2.4.7 General procedure for Grignard reaction with CO₂

Grignard reagents (1.0 mmol) and THF (1.0 mL) were placed in a Schlenk tube connected with a balloon under Ar atmosphere. The reaction tube was purged by CO₂ from the captured solution for 5 min. After closing the outlet, CO₂ was captured into the attached balloon for 10 min. The reaction tube was stirred at ambient temperature (~25 °C) for 1 h. The reaction mixture was diluted with water (10

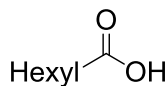
mL). Aqueous HCl solution (2 N, 10 mL) was slowly added to the reaction mixture at lowered temperature. It was extracted with CH_2Cl_2 (3×20 mL). The combined organic layers were dried over MgSO_4 . All volatiles were removed under vacuum to afford the product.

2.4.8 Characterization data for carboxylic acids



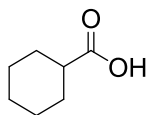
Benzoic acid

^1H NMR (300 MHz, CDCl_3 , δ): 12.62 (s, 1H, COOH), 8.15 (d, $J = 7.8$, 2H, Ar H), 7.63 (t, $J = 7.2$ Hz, 1H, Ar H), 7.49 (t, $J = 7.4$ Hz, 2H, Ar H).



Heptanoic acid

^1H NMR (300 MHz, CDCl_3 , δ): 10.29 (s, 1H, COOH), 2.34 (t, $J = 7.84$ Hz, 2H CH_2), 1.54–1.68 (m, 2H, CH_2), 1.19–1.39 (m, 6H, CH_2) 0.80–0.94 (m, 3H, CH_3)



Cyclohexanoic acid

^1H NMR (300 MHz, CDCl_3 , δ): 11.31 (br s, 1H, COOH), 2.39–2.67 (m, 1H, CH), 1.93 (d, $J = 12.9$ Hz, 2H), 1.86–1.57 (m, 3H) 1.54–1.38 (m, 2H), 1.36 – 1.18 (m, 3H)

2.5 Reference

(1) (a) Yang, Z.-Z.; He, L.-N.; Gao, J.; Liu, A.-H.; Yu, B. *Energy Environ. Sci.* **2012**, *5*, 6602. (b) Takeda, Y.; Okumura, S.; Tone, S.; Sasaki, I.; Minakata, S. *Org. Lett.* **2012**, *14*, 4874. (c) He, L. N.; Wang, J. Q.; Wang, J. L. *Pure Appl. Chem.* **2009**, *81*, 2069.

(2) Rochelle, G. T. *Science* **2009**, *325*, 1652.

(3) (a) Zhang, X.; Zhang, X.; Dong, H.; Zhao, Z.; Zhang, S.; Huang, Y. *Energy Environ. Sci.* **2012**, *5*, 6668. (b) Sumida, K.; Rogow, D. L.; Mason, J. A.; McDonald, T. M.; Bloch, E. D.; Herm, Z. R.; Bae, T. H.; Long, J. R. *Chem. Rev.* **2012**, *112*, 724. (c) MacDowell, N.; Florin, N.; Buchard, A.; Hallett, J.; Galindo, A.; Jackson, G.; Adjiman, C. S.; Williams, C. K.; Shah, N.; Fennell, P. *Energy Environ. Sci.* **2010**, *3*, 1645.

(4) (a) Goff, G. S.; Rochelle, G. T. *Ind. Eng. Chem. Res.* **2006**, *45*, 2513. (b) Danckwerts, P. V. *Chem. Eng. Sci.* **1979**, *34*, 443.

(5) Haszeldine, R. S. *Science* **2009**, *325*, 1647.

(6) (a) Shi, F.; Deng, Y.; SiMa, T.; Peng, J.; Gu, Y.; Qiao, B. *Angew. Chem. Int. Ed.* **2003**, *42*, 3257. (b) Tai, C.-C.; Huck, M. J.; McKoon, E. P.; Woo, T.; Jessop, P. G. *J. Org. Chem.* **2002**, *67*, 9070.

(7) (a) Sujith, S.; Min, J. K.; Seong, J. E.; Na, S. J.; Lee, B. Y. *Angew. Chem. Int. Ed.* **2008**, *47*, 7306. (b) Darensbourg, D. J. *Chem. Rev.*

2007, 107, 2388. (c) Nakano, K.; Kamada, T.; Nozaki, K. *Angew. Chem. Int. Ed.* **2006**, 45, 7274. (d) Coates, G. W.; Moore, D. R. *Angew. Chem. Int. Ed.* **2004**, 43, 6618. (e) Lu, X. B.; Darensbourg, D. J. *Chem. Soc. Rev.* **2012**, 41, 1462.

(8) (a) Yang, Y.; Hayashi, Y.; Fujii, Y.; Nagano, T.; Kita, Y.; Ohshima, T.; Okuda, J.; Mashima, K. *Catal. Sci. Technol.* **2012**, 2, 509. (b) Decortes, A.; Castilla, A. M.; Kleij, A. W. *Angew. Chem. Int. Ed.* **2010**, 49, 9822. (c) Whiteoak, C. J.; Kielland, N.; Laserna, V.; Escudero-Adan, E. C.; Martin, E.; Kleij, A. W. *J. Am. Chem. Soc.* **2013**, 135, 1228. (d) North, M.; Pasquale, R.; Young, C. *Green Chem.* **2010**, 12, 1514.

(9) (a) Omae, I. *Coord. Chem. Rev.* **2012**, 256, 1384. (b) Huang, K.; Sun, C. L.; Shi, Z. J. *Chem. Soc. Rev.* **2011**, 40, 2435. (c) Cokoja, M.; Bruckmeier, C.; Rieger, B.; Herrmann, W. A.; Kühn, F. E. *Angew. Chem. Int. Ed.* **2011**, 50, 8510. (d) Dorner, R. W.; Hardy, D. R.; Williams, F. W.; Willauer, H. D. *Energy Environ. Sci.* **2010**, 3, 884. (e) Riduan, S. N.; Zhang, Y. G. *Dalton Trans.* **2010**, 39, 3347. (f) Sakakura, T.; Choi, J.-C.; Yasuda, H. *Chem. Rev.* **2007**, 107, 2365.

(10) (a) Rebolledo-Morales, M. A.; Rebolledo-Libreros, M. E.; Trejo, A. *J. Chem. Thermodyn.* **2011**, 43, 690. (b) Aronu, U. E.; Svendsen, H. F.; Hoff, K. A. *Int. J. Greenh. Gas Control* **2010**, 4, 771. (c) Aronu,

- U. E.; Svendsen, H. F.; Hoff, K. A.; Juliussen, O. *Energy Procedia* **2009**, *1*, 1051. (d) Blauwhoff, P. M. M.; Versteeg, G. F.; Vanswaaij, W. P. M. *Chem. Eng. Sci.* **1984**, *39*, 207.
- (11) Zhang, X.; Zhang, W. Z.; Ren, X.; Zhang, L. L.; Lu, X. B. *Org. Lett.* **2011**, *13*, 2402.
- (12) (a) Wang, X.; Lim, Y. N.; Lee, C.; Jang, H.-Y.; Lee, B. Y. *Eur. J. Org. Chem.* **2013**, 1867. (b) Manjolinho, F.; Arndt, M.; Gooßen, K.; Gooßen, L. J. *ACS Catalysis* **2012**, *2*, 2014. (c) Yu, D. Y.; Tan, M. X.; Zhang, Y. G. *Adv. Synth. Catal.* **2012**, *354*, 969. (d) Yu, D. Y.; Zhang, Y. G. *Green Chem.* **2011**, *13*, 1275. (e) Gooßen, L. J.; Rodríguez, N.; Manjolinho, F.; Lange, P. P. *Adv. Synth. Catal.* **2010**, *352*, 2913. (f) Yu, D. Y.; Zhang, Y. G. *Proc. Natl. Acad. Sci. U. S. A.* **2010**, *107*, 20184.
- (13) Sutar, P. N.; Jha, A.; Vaidya, P. D.; Kenig, E. Y. *Chem. Eng. J.* **2012**, *207*, 718.
- (14) Guedard, C.; Picq, D.; Launay, F.; Carrette, P. L. *Int. J. Greenh. Gas Control* **2012**, *10*, 244.
- (15) Schöffner, B.; Schöffner, F.; Verevkin, S. P.; Börner, A. *Chem. Rev.* **2010**, *110*, 4554.
- (16) (a) Han, Z. B.; Rong, L. C.; Wu, J.; Zhang, L.; Wang, Z.; Ding, K. L. *Angew. Chem. Int. Ed.* **2012**, *51*, 13041. (b) Balaraman, E.;

Gunanathan, C.; Zhang, J.; Shimon, L. J. W.; Milstein, D. *Nat. Chem.* **2011**, *3*, 609.

(17) Liu, X.; Cao, C. S.; Li, Y. F.; Guan, P.; Yang, L. G.; Shi, Y. H. *Synlett* **2012**, 1343.

(18) Silverman, G. S., Rakita, P. E., Ed. *Handbook of Grignard Reagents*; Marcell Dekker, INC.: New York, 1996

Chapter 3. Transfer Hydrogenation of Organic Formates and Cyclic Carbonates: An Alternative Route to Methanol from Carbon Dioxide*

3.1 Introduction

Transfer hydrogenation (TH) is a highly advanced environmentally benign strategy used for the reduction of organic molecules, which does not require the use of strong and pyrophoric environmentally harmful reducing agents, such as LiAlH_4 .¹ Furthermore, this reaction proceeds at ambient pressure and in the absence of pressurized, flammable H_2 gas. 2-Propanol, a non-toxic and inexpensive reagent, is commonly used as the hydrogen source in a variety of TH reactions and significant advances have been achieved in the TH of aldehydes,² ketones,³ imines,⁴ and nitriles.⁵ However, to the best of our knowledge, TH of formates and carbonates has not yet been reported.

The alkoxy group adjacent to carbonyl carbon makes hydrogenation of esters more difficult than that of ketones due to resonance stabilization.⁶ Moreover, two alkoxy groups make carbonates extremely stable. Thus, only a few examples have, so far,

* The majority of this work has been published: Seung Hyo Kim and Soon Hyeok Hong *ACS Catalysis* **2014**, *4*, 3630–3636

been reported for the catalytic hydrogenation of formates and carbonates using H₂ at high pressures.⁷ The development of operationally simple and environmentally friendly reduction of formates and carbonates remains a major challenge.

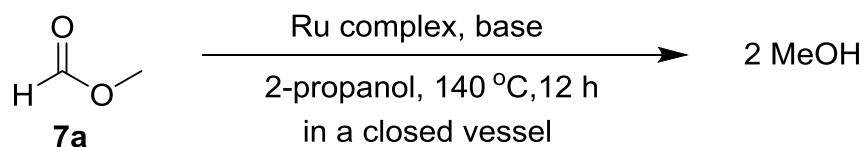
From a different perspective, hydrogenation of formates and carbonates is a highly attractive indirect route to produce methanol from CO₂, a promising solution to worldwide energy problems.⁸ Milstein and co-workers reported the generation of methanol through hydrogenation of formates, carbonates, and carbamates using PNN pincer-type Ru(II) catalysts such as complex **6**,^{7a} while Ding and co-workers recently reported hydrogenation of cyclic carbonates using complex **1** to produce methanol and diol.^{7b} Although both methods produced methanol efficiently, they required high pressures (10–50 atm) of highly flammable H₂ gas. With recently developed highly efficient catalysts for hydrogen transfer reactions,⁹ we envisioned that TH of more challenging substrates, such as formates and carbonates, could be achieved. Herein, we report, for the first time, the catalytic TH of formates and carbonates using a readily available Ru catalyst.

3.2 Results and discussion

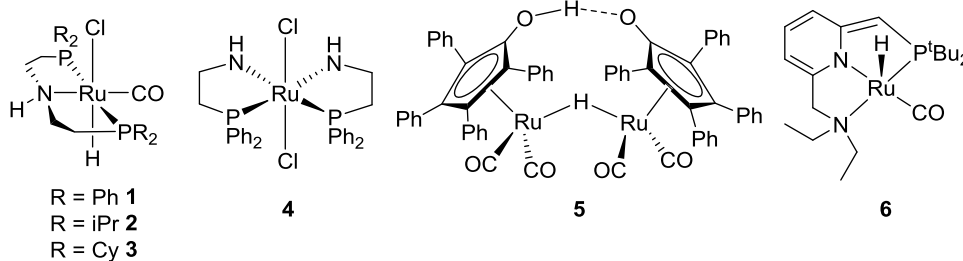
3.2.1 Optimization for transfer hydrogenation of methyl formate

To investigate the feasibility of the TH of formates, methyl formate (**7a**) was selected as a benchmark substrate. Conversion of CO₂ to formic acid or alkyl formates has been well reported.¹⁰ Various Ru complexes, known to be good catalysts for hydrogenations or TH reactions were screened (Table 3.1). Ru complex **1** was found to be the most efficient catalyst and produced MeOH quantitatively when a catalytic amount of a base such as KO^tBu (entry 1) or K₂CO₃ (entry 2) was used. No reaction took place in the absence of a base (entry 3). Analogous complexes **2–3** containing isopropyl (iPr) or cyclohexyl (Cy) groups were less effective (entries 4–5) and the rest of the ruthenium complexes screened, failed to reduce the carbonyl group (entries 6–12). Instead, a trans-esterification reaction occurred, producing methanol and isopropyl formate (**7c**).

Table 3.1 Transfer hydrogenation of methyl formate.^a



entry	[Ru] (mol %)	base	Yield (%) ^b
1	1 (0.1)	KO ^t Bu	>99
2	1 (0.1)	K ₂ CO ₃	>99
3	1 (0.1)	—	0
4	2 (0.1)	K ₂ CO ₃	97
5	3 (0.1)	K ₂ CO ₃	69
6 ^c	4 (0.5)	KO ^t Bu	50
7	5 (0.5)	—	21
8	6 (0.5)	—	10
9 ^c	RuHCl(CO) (PPh ₃) ₃ (0.5)	KO ^t Bu	50
10 ^c	RuH ₂ (CO) (PPh ₃) ₃ (0.5)	KO ^t Bu	50
11 ^c	RuCl ₂ (PPh ₃) ₃ (0.5)	KO ^t Bu	49
12 ^c	[Ru(<i>p</i> -cymene)Cl ₂] ₂ (0.5), dppb (1.0)	KO ^t Bu	50
13	—	KO ^t Bu	0



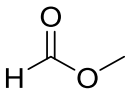
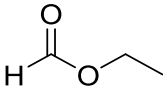
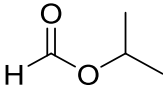
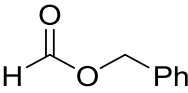
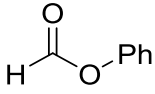
^aReaction conditions: methyl formate (2.8 mmol, 1.0 equiv), Ru complex (0.1 mol % – 0.5 mol %), base (same equiv to Ru), isopropanol (20 mL), 140 °C, 12 h in a closed vessel. ^b Determined

by GC using *p*-xylene as the internal standard. >99% of isopropyl formate was generated.

3.2.2 Substrate scope

Having identified complex **1** as the most active catalyst among those tested, we proceeded to examine the catalyst efficiency and substrate scope (Table 3.2). The reaction worked efficiently even in a gram-scale reaction (1.02 g of **7a**, 94%, entry 2). Reducing the catalyst loading to 0.02 mol % (entry 3) and 0.01 mol % (entry 4) afforded methanol in quantitative yield after 12 h and 24 h, respectively. Remarkably, excellent turnover numbers (TONs, 16600) were achieved with a 50 ppm loading of the catalyst (entry 5). In comparison, Milstein reported hydrogenation of methyl formate with a maximum TON of 4,700 with PNN pincer-type Ru(II) catalysts (0.02 mol %) using 50 atm of H₂ gas.^{7a} Other alkyl formates such as ethyl, isopropyl, and benzyl formates were also smoothly reduced producing methanol (entries 6–8). However, phenyl formate was reduced less efficiently (entry 9).

Table 3.2 Transfer hydrogenation of organic formates.^a

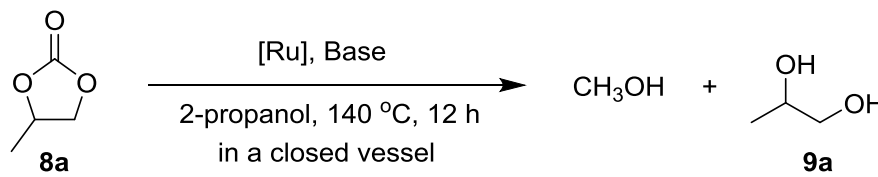
entry	substrate	1 (mol %)	Time (h)	MeOH (%) ^b	TON
1		0.05	3	>99	>1980
2 ^c		0.05	24	94	1880
3	 7a	0.02	12	>99	>4950
4		0.01	24	>99	>9900
5		0.005	48	83	16600
6	 7b	0.05	3	>99	>1980
7	 7c	0.05	5	>99	>1980
8	 7d	0.1	12	94	940
9	 7e	0.1	12	34	340

^aReaction conditions: **7** (5.6 mmol, 1.0 equiv), **1**, K₂CO₃ (same equiv to **1**), 2-propanol (20 mL), 140 °C in a closed vessel. ^bDetermined by GC using *p*-xylene as the internal standard. ^c**7a** (17.0 mmol, 1.02 g, 1.0 equiv)

3.2.3 Optimization for transfer hydrogenation of cyclic carbonate

Next, we examined the possibility of TH of cyclic carbonates to produce methanol and the corresponding diol using various ruthenium catalysts (Table 3.3). Since cyclic carbonates are easily formed by inserting CO₂ into epoxides,¹¹ TH of cyclic carbonates would be an attractive indirect strategy to produce methanol from CO₂.^{7b} Similar to the TH of methyl formate, yields of the reduced product were only moderate when ruthenium complexes **2** and **3** were used (entries 2 and 3). Only trans-esterification occurred quantitatively when other Ru-catalysts were used (entries 4–8). To our delight, 4-methyl-1,3-dioxolan-2-one (**8a**) was quantitatively converted to methanol and propylene glycol (**9a**) under our standard conditions (entry 1).

Table 3.3 Transfer hydrogenation of 4-methyl-1,3-dioxolan-2-one (**8a**) with various catalysts.^a

			
entry	[Ru] (mol %)	MeOH (%)	Diol (%) ^b
1 ^c	1 (0.1)	>99	>99

2 ^c	2 (0.1)	60	>99
3 ^c	3 (0.1)	31	>99
4	4 (0.5)	—	99
5	5 (0.5)	—	99
6	6 (0.5)	—	97
7	RuHCl(CO) (PPh ₃) ₃ (0.5)	—	98
8	RuH ₂ (CO) (PPh ₃) ₃ (0.5)	—	87
9	[Ru(cymene)Cl ₂] ₂ (0.5), dppb (1.0)	—	trace

^aReaction conditions: propylene carbonate (2.8 mmol, 1.0 equiv), Ru complex, KO^tBu (0.5 mol %), 2-propanol (20 mL), 140 °C, 12 h. ^bGC Yield using *p*-xylene as the internal standard. ^cK₂CO₃ (0.1 mol %).

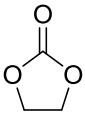
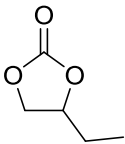
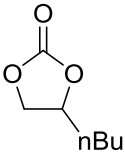
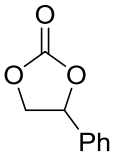
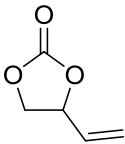
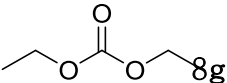
3.2.4 Substrate scope

Various cyclic carbonates were subsequently subjected to the TH conditions catalyzed by complex **1** (Table 3.4). Catalytic loadings as low as 0.025% were enough to reduce **8a** in very good yield (entry 4). A further reduction to 0.01% led to a significant decrease in the yield of methanol (51%); however, a higher amount of 1,2-propanediol (**9a**) was obtained with diisopropylcarbonate (**8h**) due to

trans-esterification with 2-propanol (entry 5). Ethylene carbonate (**8b**) was easily reduced with 0.1% of the catalyst in a short time (entry 6). Ethyl, butyl, and phenyl substituted cyclic carbonates were also efficiently reduced to afford methanol in excellent yields (entries 7–9). When 4-vinyl-1,3-dioxolan-2-one (**8f**) was subjected to the catalytic TH reaction conditions, reduction also occurred at the olefin group and 1,2-butanediol (**9c**) was obtained in excellent yields along with methanol (entry 10). Unfortunately, the scope of the reaction could not be extended to linear carbonates such as diethyl carbonate (entry 11).

Table 3.4 Transfer hydrogenation of organic carbonates.^a

entry	substrate	1 (mol %)	time (h)	MeOH (%) ^b	diol (%)
1		0.2	1	>99	>99 ^b
2		0.1	2	>99	>99 ^b
3	8a	0.05	5	>99	>99 ^b
4		0.025	48	81	>99 ^b
5		0.01	48	51	81 ^b

6		8b	0.1	3	91	91 ^c
7		8c	0.1	12	94	94 ^c
8		8d	0.1	6	>99	97 ^c
9		8e	0.1	6	93	95 ^c
10		8f	0.2	12	>99	96 ^{c,d}
11		8g	0.1	12	6	—

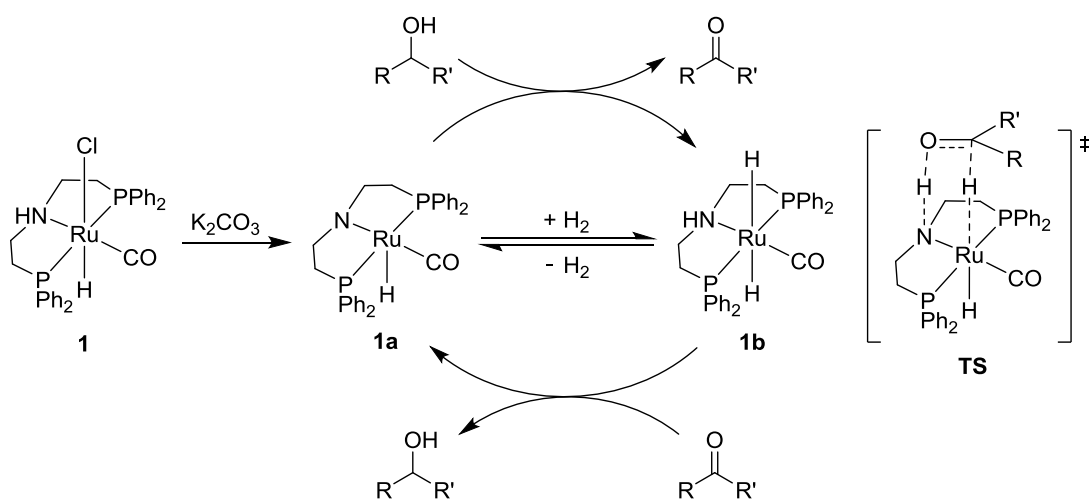
^aReaction conditions: **8** (2.8 mmol, 1.0 equiv), **1**, K₂CO₃ (same equiv to **1**), 2-propanol (20 mL), 140 °C, 12 h in a closed vessel.

^bDetermined by GC using *p*-xylene as the internal standard. ^cIsolated yield. ^d1,2-butanediol

3.2.5 Mechanistic studies

The mechanism for the complex **1** catalyzed hydrogenation and dehydrogenation reactions has been well studied (Scheme 3.1).^{7b,9a}

The 16 e⁻ amido Ru complex (**1a**), generated from the base-assisted elimination of HCl from complex **1**, is easily transformed to the 18 e⁻ Ru-dihydride complex (**1b**) either using H₂ at high pressure or a non-tertiary alcohol. Complex (**1b**) can then reversibly liberate H₂ or add to the carbonyl group of carbonates or esters (**TS**).¹²



Scheme 3.1 Generation of Ru-hydrides from complex **1**.

Using excess amount of 2-propanol as solvent, an increase of pressure in the reaction tube was observed (~ 3 bar), due to the generation of H_2 gas.^{9g,13} When carbonates were reduced in an open vessel, only small amounts of methanol were obtained ($\sim 25\%$); this indicates that existence of in situ generated H_2 gas is critical for the

efficient reduction of carbonates. This observation led us to question whether the catalytically active species **1b** was continuously generated with the evolved H₂ gas through an outer sphere-type mechanism. To address the question, deuterium-labeled 2-propanol (CD₃)₂CDOD was used as the solvent in the presence of external H₂ gas (Table 3.5).¹⁴ When the reaction was carried out without external H₂ gas (entry 1), the reduction of ethylene carbonate yielded 89% of methanol with hydrogen exchange (H/D 2:98).

Table 3.5 Degree of deuterium incorporation in reduction of ethylene carbonate.^a

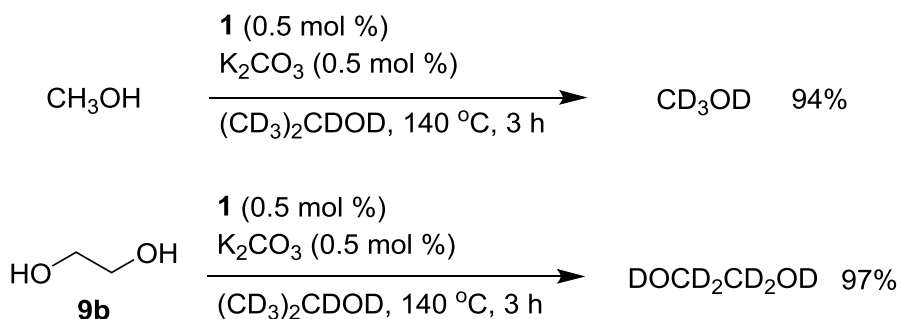
entry	H ₂ (bar)	H ₂ / propanol-d ₈ ^b	MeOH (%, H/D)	diol (%, H/D)
1	0	—	89 (2:98)	>99 (2:98)
2	3	10:90	90 (8:92)	>99 (7:93)
3 ^c	3	19:81	80 (21:79)	91 (28:72)
4	9	25:75	93 (21:79)	>99 (23:77)
5 ^c	9	41:59	89 (37:63)	>99 (47:53)

6	35	56:44	98 (54:46)	>99 (62:48)
7 ^c	35	73:27	91 (64:36)	>99 (72:28)

^aReaction conditions: **8b** (0.7 mmol, 1.0 equiv), **1** (0.5 mol %), K₂CO₃ (0.5 mol %), 2-propanol-d₈ (5 mL), 140 °C, 3 h in a closed vessel.

^bmolar ratio. ^c**8b** (0.14 mmol), 2-propanol-d₈ (1 mL).

Furthermore, when non-deuterated methanol and ethylene glycol were submitted to the reaction conditions in 2-propanol-d₈, most of the protons were substituted with deuterium (Scheme 3.2), which suggested that a reversible hydrogenation/dehydrogenation occurred. We next examined the reaction under different pressures and amounts of external H₂ gas (entries 2–7). It was found that the incorporation of deuterium decreased as the ratios of H₂ to 2-propanol-d₈ increased (entries 2–7). These results suggest that the catalytic cycle via **1b** operates reversibly with both evolved H₂ gas and 2-propanol.



Scheme 3.2. Deuteration of 1,2-ethanediol and methanol.

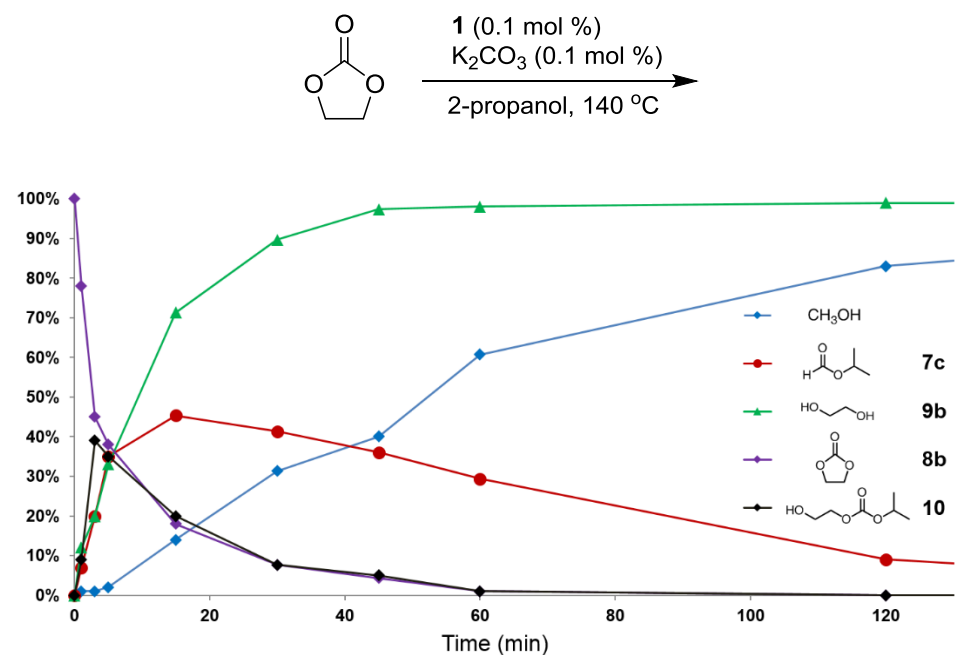


Figure 3.1 Reaction profile for transfer hydrogenation of ethylene carbonate.

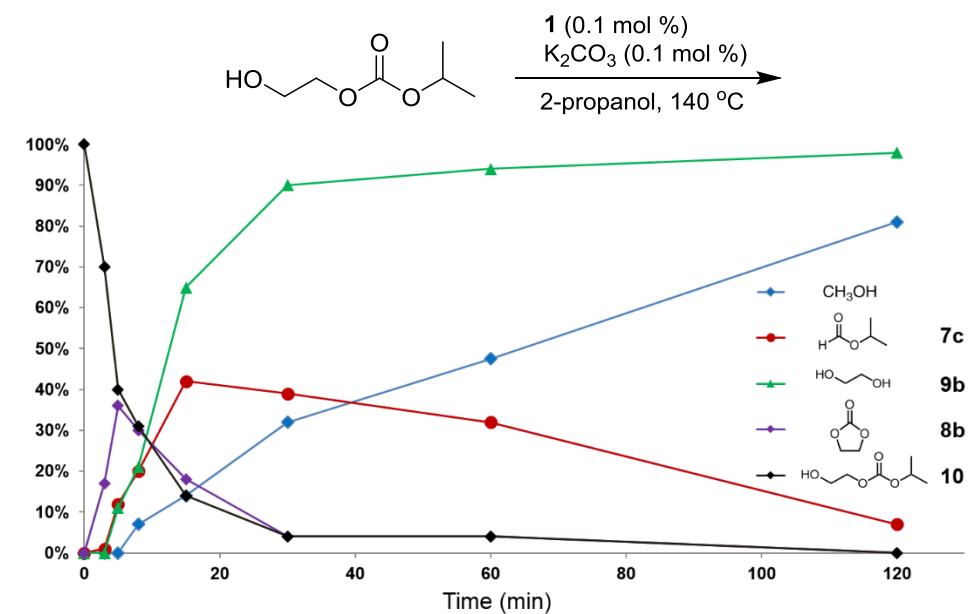
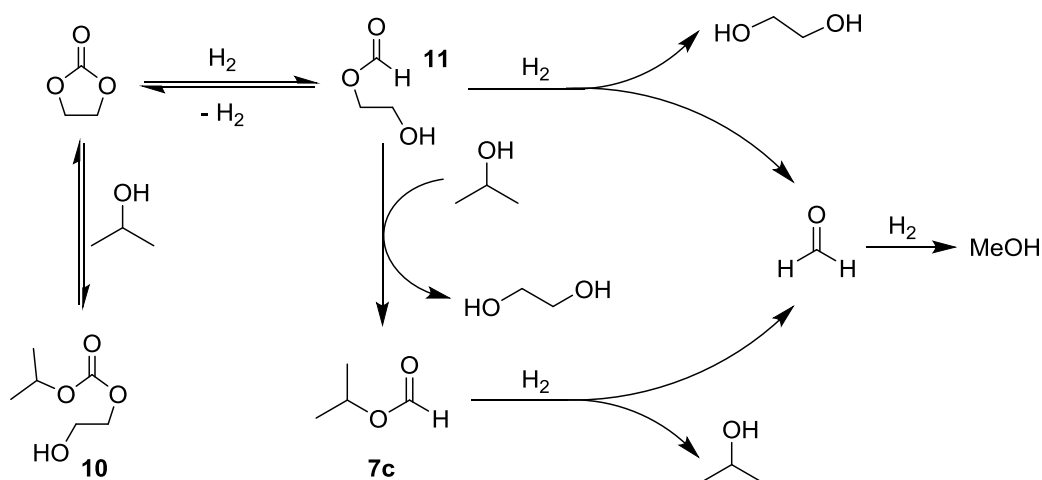


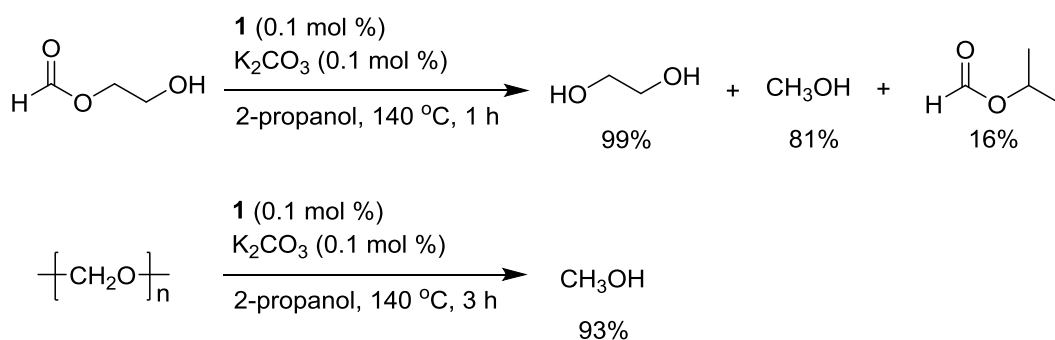
Figure 3.2 Reaction profile for transfer hydrogenation of 2-

hydroxyethyl isopropyl carbonate.

To gain insight into the possible reaction pathways, we monitored the reaction intermediates generated in the TH of ethylene carbonate (**8b**) (Figure 3.1). Initially, a rapid consumption of **8b** along with the formation of 2-hydroxyethyl isopropyl carbonate (**10**) was observed. As time progressed, the concentration of isopropyl formate (**7c**) increased and those of **8b** and **10** decreased. A similar trend was observed when **10** was submitted to the same reaction conditions (Figure 3.2). Based on these results, we propose possible reaction pathways (Scheme 3.3). The ring opening of **8b** with 2-propanol is reversible and, because the reduction of linear carbonates is not facile under our reaction conditions (entry 11, Table 3.4), we believe that the direct hydrogenation of **10** is not a plausible pathway. Thus, we propose the first step to be the hydrogenation of **8b** to form 2-hydroxyethyl formate (**11**). To support it, **11** was submitted to the reaction conditions and methanol (81%) and **7c** (16%) were formed within 1 h (Scheme 3.4). Formaldehyde, a proposed intermediate in our reaction mechanism, was also successfully reduced to methanol under our TH conditions (Scheme 3.4).



Scheme 3.3 Proposed mechanism.



Scheme 3.4 Transfer hydrogenation of intermediates.

3.3 Conclusion

The TH of formyl esters and cyclic carbonates was achieved for the first time in excellent yields using commercially available Ru catalyst and non-toxic and inexpensive 2-propanol, used both as solvent and hydrogen source. This strategy is an attractive way to produce

methanol from CO₂ indirectly, because formyl esters and cyclic carbonates are easily obtained from CO₂. Our methodology is operationally simple and replaces the use of highly flammable H₂ gas under high pressure.

3.4 Experimental section

3.4.1 General information

Unless otherwise noted, all reactions were carried out using standard Schlenk techniques or in an argon-filled glove box. All transfer hydrogenation reactions were carried out in an oven-dried pressure tolerating vessel under argon atmosphere. Ru complexes **2** and **3**,^{7b} 4-butyl-1,3-dioxolan-2-one (**8d**),¹⁵ 4-phenyl-1,3-dioxolan-2-one (**8e**),¹⁵ and 2-hydroxyethyl isopropyl carbonate (**10**)¹⁶ were prepared according to the literature procedures. Unless otherwise noted, all reagents were obtained from commercial suppliers and used as received. Analytical TLC was performed on a Merck 60 F254 silica gel plate (0.25mm thickness). Column chromatography was performed on Merck 60 silica gel (230–400 mesh). NMR spectra were recorded on a Bruker DPX-300 (300 MHz) spectrometer. Tetramethylsilane was used as reference, and the chemical shifts were reported in ppm and the coupling constant in Hz. GC analyses

were carried out on an Agilent 7890A gas chromatograph using DB-624 UI column (60 m \times 0.32 mm \times 1.80 μ m).

3.4.2 General procedure for transfer hydrogenation of organic formates

A pressure tolerating reaction vessel was charged with complex **1** (0.0056 mmol, 3.4 mg), K₂CO₃ or KO^tBu (0.0056 mmol), 2-propanol (20 mL), and methyl formate (**7a**) (5.6 mmol, 336 mg) in an argon-filled glove box. The vessel was heated to 140 °C (bath temperature), and after the reaction, it was cooled down to 0 °C for 1.5 h. The generated H₂ was released carefully in a hood. Yield of methanol was analyzed by GC using *p*-xylene as the internal standard.

3.4.3 General procedure for transfer hydrogenation of cyclic carbonates

A pressure tolerating reaction vessel was charged with complex **1** (0.0028 mmol, 1.7 mg), K₂CO₃ (0.0028 mmol, 0.39 mg), 2-propanol (20 mL), and cyclic carbonates (2.8 mmol) in a glove box. The vessel was heated to 140 °C (bath temperature), and after the reaction, it was cooled down to 0 °C for 1.5 h. The generated H₂ was released carefully in a hood. Yield of methanol was analyzed by GC using *p*-

xylene as the internal standard. Corresponding diol were purified by flash column chromatography using CH₂Cl₂ / MeOH as eluent. The products were identified by ¹H NMR spectral comparison with literature data.

3.4.4 Deuterium incorporation study for TH reaction of 1,3-dioxolan-2-one

A stainless steel autoclave was charged with complex **1** (0.5 mol %), K₂CO₃ (0.5 mol %), 2-propanol-d₈ (5 mL or 1 mL), and 1,3-dioxolan-2-one (**8b**) (0.7 or 0.14 mmol) in a glove box. The reaction vessel was purged three times with H₂ and finally pressurized with H₂ to 3 bar, 9 bar, or 35 bar. The vessel was heated to 140 °C (bath temperature) for 3 hours, and after the reaction, it was cooled down to 0 °C for 1.5 h. The residual H₂ was released carefully in a hood. Overall yields of methanol and 1,2-ethanediol were analyzed by GC using *p*-xylene as the internal standard and yields of non-deuterated methanol and 1,2-ethanediol were measured by NMR.

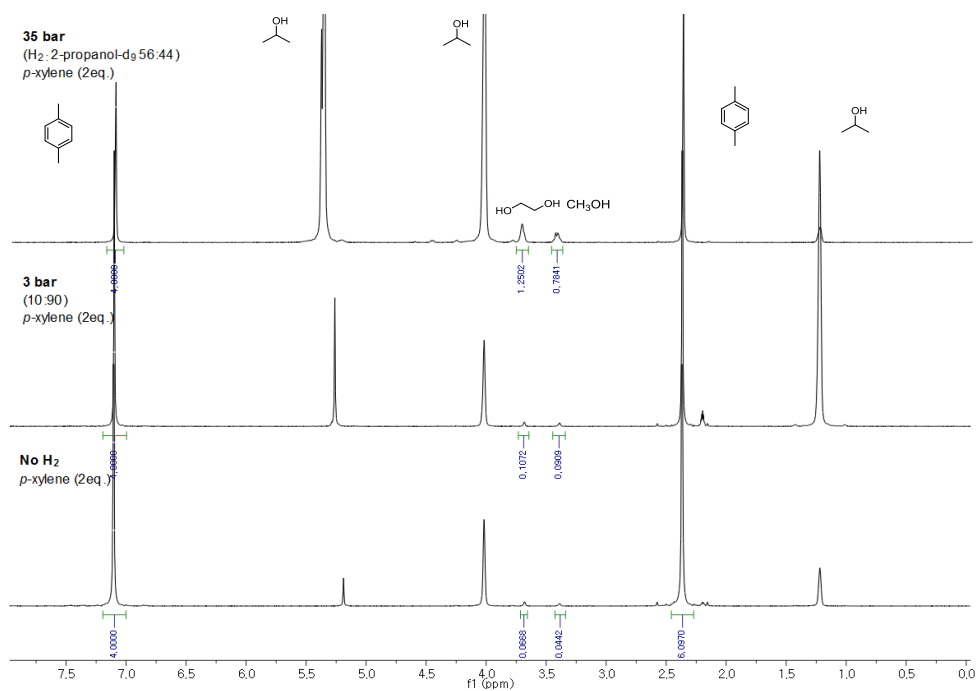


Figure 3.3 NMR spectra for deuterium incorporation study (entries 1, 2, and 6, Table 3.5).

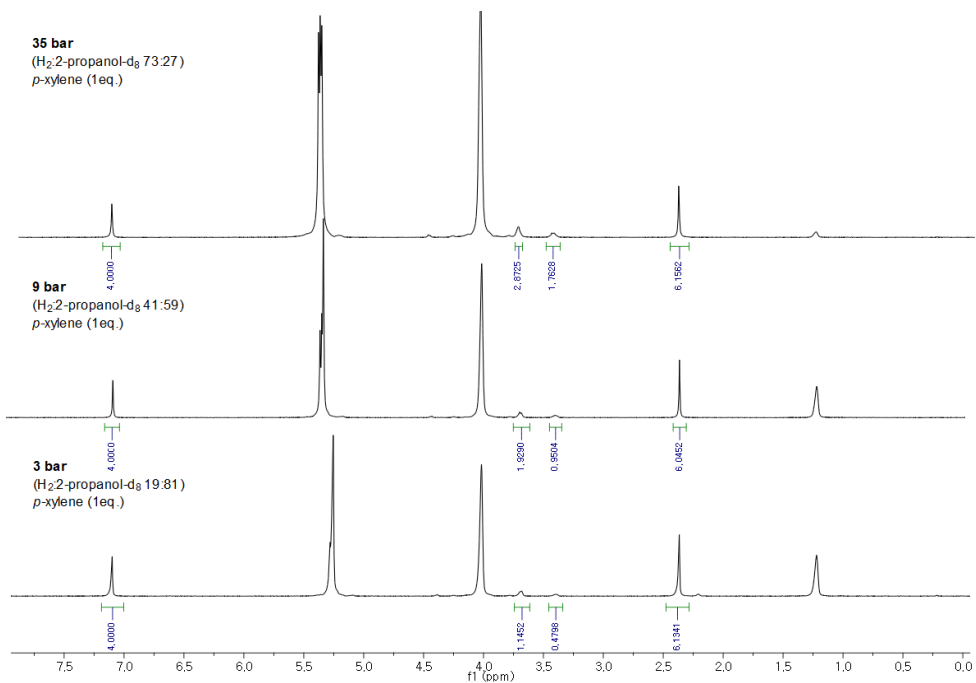


Figure 3.4 NMR spectra for deuterium incorporation study (entries 3, 4, and 5, Table 3.5).

5, and 7, Table 3.5).

3.4.5 Deuteration of 1,2-ethanediol and methanol with 2-propanol- d_8

A pressure tolerating reaction vessel was charged with complex **1** (0.5 mol %), K_2CO_3 (0.5 mol %), 2-propanol- d_8 (5 mL), and 1,2-ethanediol (**9b**) or methanol (0.7 mmol) in a glove box. The vessel was heated to 140 °C (bath temperature) for 3 h, and after the reaction, it was cooled down to 0 °C for 1.5 h. The residual H_2 was released carefully in a hood. Overall yields of methanol and 1,2-ethanediol were analyzed by GC using *p*-xylene (1.4 mmol) as the internal standard and yields of non-deuterated methanol and 1,2-ethanediol were measured by ^1H NMR spectroscopy.

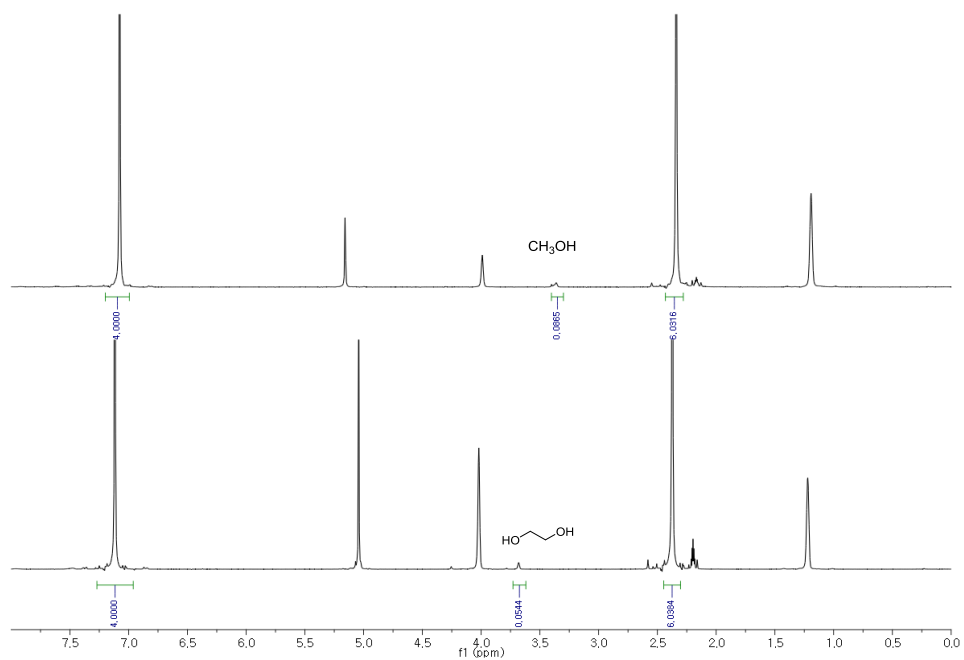


Figure 3.5 NMR spectra for deuteration of 1,2-ethanediol and methanol.

3.5 References

- (1) (a) Ikariya, T.; Blacker, A. J. *Acc. Chem. Res.* **2007**, *40*, 1300–1308. (b) Noyori, R.; Hashiguchi, S. *Acc. Chem. Res.* **1997**, *30*, 97–102.
- (2) Maytum, H. C.; Tavassoli, B.; Williams, J. M. J. *Org. Lett.* **2007**, *9*, 4387–4389.
- (3) (a) Zuo, W.; Lough, A. J.; Li, Y. F.; Morris, R. H. *Science* **2013**, *342*, 1080–1083. (b) Du, W. M.; Wang, L. D.; Wu, P.; Yu, Z. K. *Chem.–Eur. J.* **2012**, *18*, 11550–11554. (c) Zhang, Y.; Li, X. W.; Hong, S. H. *Adv. Synth. Catal.* **2010**, *352*, 1779–1783. (d) Baratta, W.; Ballico, M.; Chelucci, G.; Siega, K.; Rigo, P. *Angew. Chem., Int. Ed.* **2008**, *47*, 4362–4365. (e) Ikariya, T.; Blacker, A. J. *Acc. Chem. Res.* **2007**, *40*, 1300–1308. (f) Baratta, W.; Da Ros, P.; Del Zotto, A.; Sechi, A.; Zangrando, E.; Rigo, P. *Angew. Chem., Int. Ed.* **2004**, *43*, 3584–3588. (g) Fujii, A.; Hashiguchi, S.; Uematsu, N.; Ikariya, T.; Noyori, R. *J. Am. Chem. Soc.* **1996**, *118*, 2521–2522. (h) Hashiguchi, S.; Fujii, A.; Takehara, J.; Ikariya, T.; Noyori, R. *J. Am. Chem. Soc.* **1995**, *117*, 7562–7563.
- (4) (a) Wang, C.; Pettman, A.; Basca, J.; Xiao, J. *Angew. Chem., Int. Ed.* **2010**, *49*, 7548–7552. (b) Guijarro, D.; Pablo, Ó.; Yus, M. *Tetrahedron Lett.* **2009**, *50*, 5386–5388. (c) Samec, J. S. M.;

- Bäckvall, J.-E. *Chem.-Eur. J.* **2002**, *8*, 2955–2961. (d) Wang, G. Z.; Backväll, J. E. *J. Chem. Soc., Chem. Commun.* **1992**, 980–982.
- (5) (a) Werkmeister, S.; Bornschein, C.; Junge, K.; Beller, M. *Eur. J. Org. Chem.* **2013**, *2013*, 3671–3674. (b) Werkmeister, S.; Bornschein, C.; Junge, K.; Beller, M. *Chem.-Eur. J.* **2013**, *19*, 4437–4440.
- (6) (a) Dub, P. A.; Ikariya, T. *ACS Catal.* **2012**, *2*, 1718–1741. (b) Ito, M.; Ootsuka, T.; Watari, R.; Shiibashi, A.; Himizu, A.; Ikariya, T. *J. Am. Chem. Soc.* **2011**, *133*, 4240–4242.
- (7) (a) Balaraman, E.; Gunanathan, C.; Zhang, J.; Shimon, L. J. W.; Milstein, D. *Nat. Chem.* **2011**, *3*, 609–614. (b) Han, Z.; Rong, L.; Wu, J.; Zhang, L.; Wang, Z.; Ding, K. *Angew. Chem., Int. Ed.* **2012**, *51*, 13041–13045. (c) Spasyuk, D.; Smith, S.; Gusev, D. G. *Angew. Chem., Int. Ed.* **2012**, *51*, 2772–2775.
- (8) (a) Wesselbaum, S.; vom Stein, T.; Klankermayer, J.; Leitner, W. *Angew. Chem., Int. Ed.* **2012**, *51*, 7499–7502. (b) Huff, C. A.; Sanford, M. S. *J. Am. Chem. Soc.* **2011**, *133*, 18122–18125.
- (9) (a) Nielsen, M.; Alberico, E.; Baumann, W.; Drexler, H. J.; Junge, H.; Gladiali, S.; Beller, M. *Nature* **2013**, *495*, 85–89. (b) Ziebart, C.; Jackstell, R.; Beller, M. *ChemCatChem* **2013**, *5*, 3228–3231. (c) Otsuka, T.; Ishii, A.; Dub, P. A.; Ikariya, T. *J. Am. Chem. Soc.* **2013**,

135, 9600–9603. (d) Lazzari, D.; Cassani, M. C.; Bertola, M.; Moreno, F. C.; Torrente, D. *RSC Advances* **2013**, *3*, 15582–15584. (e) Kuriyama, W.; Matsumoto, T.; Ogata, O.; Ino, Y.; Aoki, K.; Tanaka, S.; Ishida, K.; Kobayashi, T.; Sayo, N.; Saito, T. *Org. Process Res. Dev.* **2012**, *16*, 166–171. (f) Nielsen, M.; Junge, H.; Kammer, A.; Beller, M. *Angew. Chem., Int. Ed.* **2012**, *51*, 5711–5713. (g) Nielsen, M.; Kammer, A.; Cozzula, D.; Junge, H.; Gladiali, S.; Beller, M. *Angew. Chem., Int. Ed.* **2011**, *50*, 9593–9597.

(10) (a) Hull, J. F.; Himeda, Y.; Wang, W.-H.; Hashiguchi, B.; Periana, R.; Szalda, D. J.; Muckerman, J. T.; Fujita, E. *Nat. Chem.* **2012**, *4*, 383–388. (b) Ziebart, C.; Federsel, C.; Anbarasan, P.; Jackstell, R.; Baumann, W.; Spannenberg, A.; Beller, M. *J. Am. Chem. Soc.* **2012**, *134*, 20701–20704. (c) Schmeier, T. J.; Dobereiner, G. E.; Crabtree, R. H.; Hazari, N. *J. Am. Chem. Soc.* **2011**, *133*, 9274–9277. (d) Langer, R.; Diskin-Posner, Y.; Leitun, G.; Shimon, L. J. W.; Ben-David, Y.; Milstein, D. *Angew. Chem., Int. Ed.* **2011**, *50*, 9948–9952. (e) Federsel, C.; Jackstell, R.; Beller, M. *Angew. Chem., Int. Ed.* **2010**, *49*, 6254–6257. (f) Federsel, C.; Boddien, A.; Jackstell, R.; Jennerjahn, R.; Dyson, P. J.; Scopelliti, R.; Laurenczy, G.; Beller, M. *Angew. Chem., Int. Ed.* **2010**, *49*, 9777–9780. (g) Tanaka, R.;

- Yamashita, M.; Nozaki, K. *J. Am. Chem. Soc.* **2009**, *131*, 14168. (h)
- Jessop, P. G.; Ikariya, T.; Noyori, R. *Nature* **1994**, *368*, 231–233.
- (11) (a) Kim, S. H.; Kim, K. H.; Hong, S. H. *Angew. Chem., Int. Ed.* **2014**, *53*, 771–774. (b) Lu, X.-B.; Darensbourg, D. J. *Chem. Soc. Rev.* **2012**, *41*, 1462–1484. (c) Decortes, A.; Castilla, A. M.; Kleij, A. W. *Angew. Chem., Int. Ed.* **2010**, *49*, 9822–9837. (d) Kayaki, Y.; Yamamoto, M.; Ikariya, T. *Angew. Chem., Int. Ed.* **2009**, *48*, 4194–4197.
- (12) (a) Zhao, B.; Han, Z.; Ding, K. *Angew. Chem., Int. Ed.* **2013**, *52*, 4744–4788. (b) Yamakawa, M.; Ito, H.; Noyori, R. *J. Am. Chem. Soc.* **2000**, *122*, 1466–1478.
- (13) (a) Kawahara, R.; Fujita, K.-i.; Yamaguchi, R. *J. Am. Chem. Soc.* **2012**, *134*, 3643–3646. (b) Kawahara, R.; Fujita, K.-i.; Yamaguchi, R. *Angew. Chem., Int. Ed.* **2012**, *51*, 12790–12794. (c) Fujita, K.-i.; Yoshida, T.; Imori, Y.; Yamaguchi, R. *Org. Lett.* **2011**, *13*, 2278–2281. (d) Fujita, K.-i.; Tanino, N.; Yamaguchi, R. *Org. Lett.* **2007**, *9*, 109–111.
- (14) Sandoval, C. A.; Li, Y.; Ding, K.; Noyori, R. *Chem.-Asian. J.* **2008**, *3*, 1801–1810.
- (15) Xie, H. B.; Li, S. H.; Zhang, S. B. *J. Mol. Catal. A: Chem.* **2006**, *250*, 30–34.

(16) Bhat, L.; Adiey, K.; PCT Int. Appl. WO/2012/003501 A2, 2012.

Chapter 4. Ruthenium–Catalyzed Urea Synthesis Using Methanol as the C1 Source*

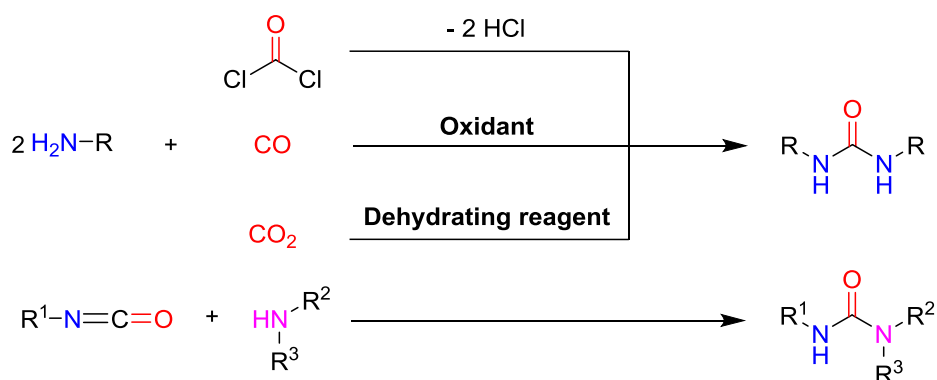
4.1. Introduction

Urea derivatives are commonly found in widespread applications, such as biologically active compounds, pharmaceuticals, agricultural pesticides, dyes for cellulose fibers, and antioxidants in gasoline.¹ Many classical protocols and catalytic transformations have been developed for urea synthesis. Traditional syntheses of urea derivatives use phosgene and isocyanates, which cause tremendous toxicological and environmental problems.² Alternative routes using carbon monoxide (CO) as the source of the carbonyl moiety have been developed;³ these carbonylation reactions are generally carried out at high temperatures under high CO pressure with oxidants. In recent years, the utilization of CO₂ has attracted significant attention because it is a renewable carbon resource.⁴ However, the required stoichiometric use of expensive and waste-producing dehydrating reagents, such as di-tert-butyl azodicarboxylate (DBAD), to

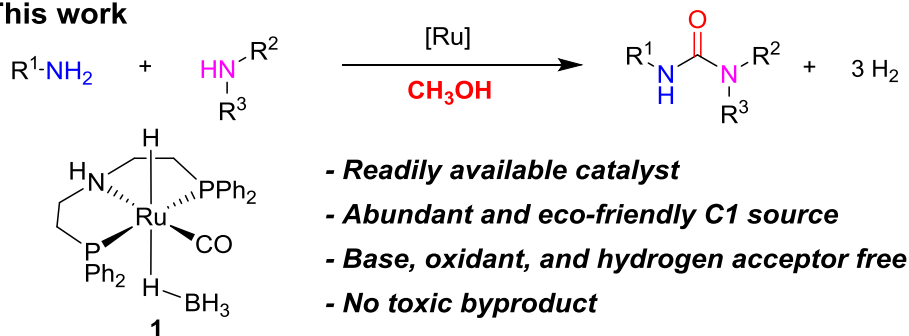
* The majority of this work has been published: Seung Hyo Kim and Soon Hyeok Hong *Org. Lett.* **2016**, *18*, 212–215

generate the isocyanate intermediates still limits the utility of the reaction.⁴ Therefore, versatile urea synthesis under mild conditions that avoids environmentally harmful reagents remains a major challenge.

Previous urea synthesis



This work



Scheme 4.1. Synthesis of urea derivatives.

Recently, environmentally benign and atom-economical C–N and C–C bond formation reactions utilizing alcohols, generating water⁵ or hydrogen^{6, 7} as byproduct, have attracted much attention. By applying

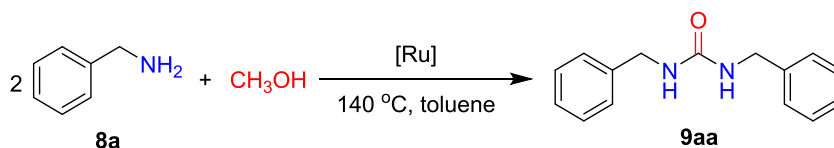
the concept of acceptorless dehydrogenative activation of alcohols,⁷ and based on the thermodynamic feasibility for the formation of 1,3-dimethyl urea from methylamine and methanol ($\Delta H_{298}^{\circ} = -66.2$ kJ/mol, $\Delta G_{298}^{\circ} = -268.8$ kJ/mol),⁸ we envisioned an unprecedented strategy to synthesize urea derivatives directly from amines utilizing methanol as the C1 source.

Utilization of methanol as the C1 feedstock could be an ideal solution to reduce the predominant dependence on conventional toxic C1 sources, such as phosgene and isocyanates, for urea synthesis.⁹ For intermolecular coupling of alcohols and amines, three pathways, i.e., imination,¹⁰ alkylation,^{7e} and amidation,¹¹ have been well reported. Recently, formylation of amines using methanol as the C1 source has been developed.¹² Inspired by previous works, we devised a possible strategy to synthesize urea utilizing methanol as follows: 1) Generation of formamide in situ and 2) coupling of the formamide with amine using an active catalyst that can mediate activation of formamide followed by dehydrogenation of the resultant hemiaminal intermediate.

4.2 Results and discussion

4.2.1 Symmetrical urea synthesis

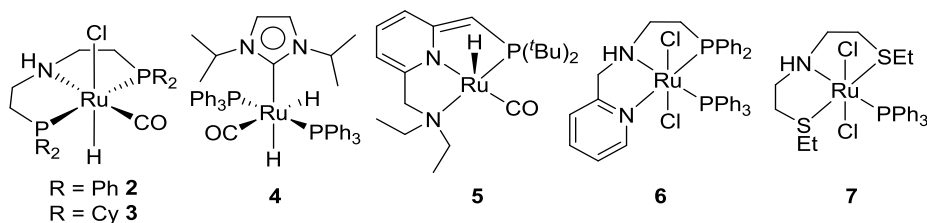
Table 4.1 Urea synthesis from methanol and benzylamine using various catalysts.^a



entry	Ru complex (0.5 mol %)	solvent	yield (%)
1	1	toluene	97
2 ^b	2	toluene	93
3 ^b	3	toluene	88
4 ^c	$[\text{Ru}(\text{cod})(2\text{-methylallyl})_2]$	toluene	0
5	4	toluene	5
6	5	toluene	0
7 ^b	6	toluene	0
8 ^b	7	toluene	0
9	1	hexane	81
10	1	THF	80
11	1	dioxane	60
12	1	<i>p</i> -xylene	87

^aReaction conditions: benzylamine (2 mmol, 1.0 equiv), $[\text{Ru}]$ (0.5 mol %), methanol (2 mmol), toluene (1.5 mL), $140\text{ }^\circ\text{C}$, 24 h in a closed vessel, NMR yield, *p*-xylene was used as a standard. ^b K_2CO_3

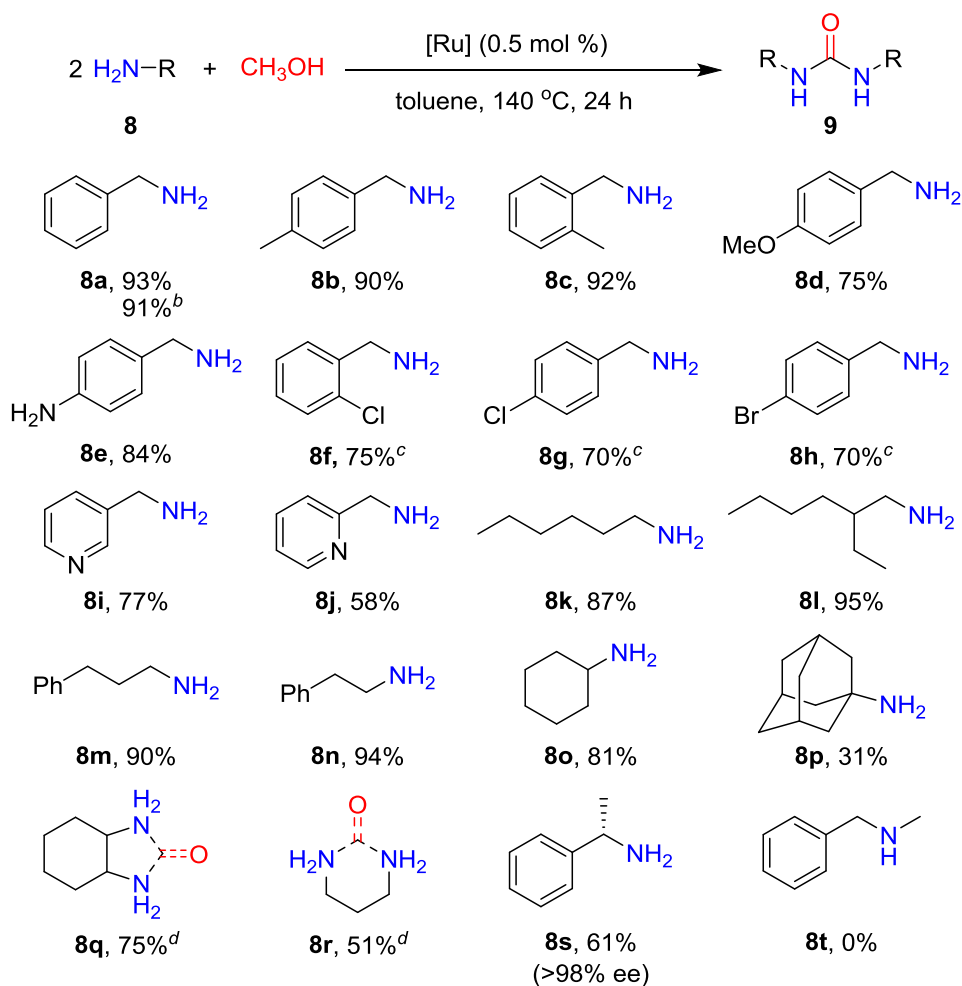
(0.5 mol %). $^{\circ}\text{[Ru(cod)(2-methylallyl)}_2\text{]}$ (0.5 mol %), KO^tBu (1.5 mol %), and dicyclohexylimidazolium chloride (ICy-HCl , 1 mol %).



To identify an active catalyst for the proposed urea synthesis, we investigated complex **4**, which was recently used for the formylation of amine and nitrile with excess methanol.^{12a} The reaction of benzylamine (**8a**) and methanol under modified conditions with less methanol (1.0 equiv. vs. amine) generated a trace amount of 1,3-dibenzyl urea (**9aa**, 5%) (Table 4.1, entry 5). Inspired by this result, other Ru-based complexes that had been reported to catalyze acceptorless dehydrogenative coupling reactions were screened to improve the reaction efficiency. The N-formylation catalytic system developed by the Glorius group was not active for urea synthesis (entry 4).^{12b} Milstein catalyst (**5**)^{11d} also did not produce any urea under the reaction conditions (entry 6). Complexes **6** and **7**, which showed excellent performance for hydrogenation of esters,¹³ were not active for this reaction (entries 7 and 8). To our delight, Ru complex **2**, which is known as the Ru-MACHO catalyst,^{6b,14} afforded

desired product **9aa** in an excellent yield (93%) in the presence of a catalytic amount of K_2CO_3 (entry 2). Analogous complex **3** containing cyclohexyl groups on the phosphine moiety gave a slightly lower yield (88%, entry 3). Finally, when complex **1** (Ru–MACHO–BH) was used as a precatalyst, a quantitative amount of **9aa** was obtained under base–free conditions (entry 1). The reaction was optimized in a closed reaction vessel due to the low boiling point of methanol. Toluene was the best solvent among those tested (entries 9–12). Notably, the developed reaction is highly atom–economical, produces hydrogen gas as the sole byproduct, and is catalyzed by a low loading of Ru catalyst (0.1 mol %, TONs ~295, Table 4.5) without any additive such as base, oxidant, or hydrogen acceptor.

Table 4.2. Symmetrical urea synthesis from methanol and amine.^a



^aReaction conditions: amine (2 mmol, 1.0 equiv), **1** (0.5 mol %), methanol (2 mmol), toluene (1.5 mL), 140 °C, 24 h in a closed vessel, isolated yield. ^bamine (10 mmol, 1.0 equiv). **1** (0.5 mol %), ^c**1** (2 mol %), methanol (4 mmol), KOH (15 mol %). ^damine (1 mmol, 1.0 equiv), **1** (1 mol %), methanol (2 mmol).

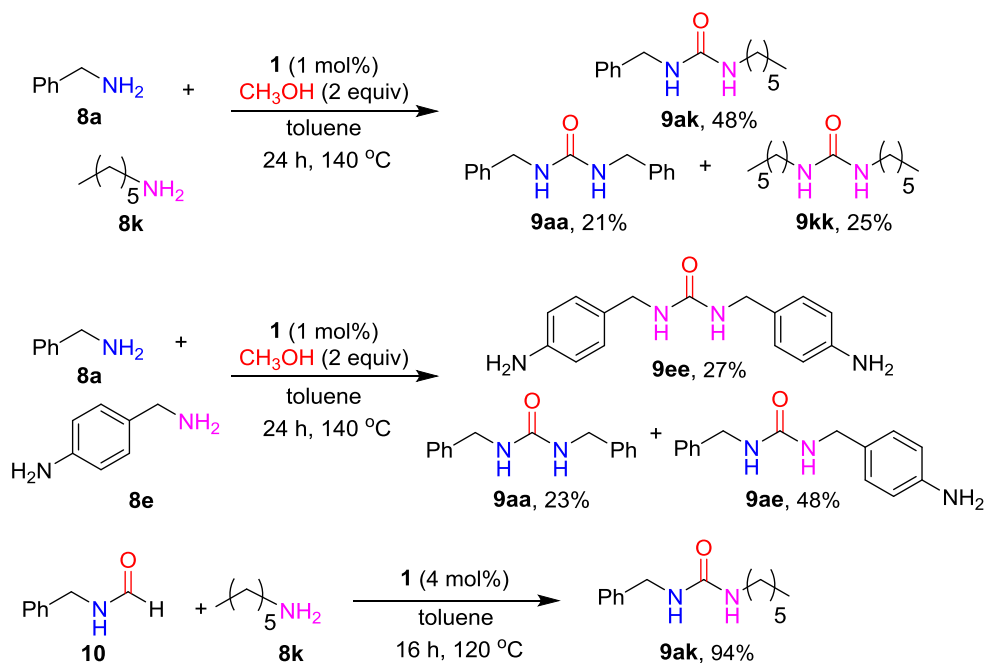
Using the optimized conditions, the scope of the reaction was examined (Table 4.2). Various amines smoothly provided the

corresponding symmetrical urea products in good to excellent yields. Electron-rich benzylamines (**8a–e**) produced the corresponding ureas smoothly. The reaction worked efficiently even in a gram-scale reaction (1.07 g of **8a**, 91%). The use of chloride- and bromide-substituted benzylamines (**8f–8h**) required higher catalyst loading (1, 2 mol %) and a base additive (KOH, 15 mol %) to obtain the products in good yields. Pyridine functional groups (**8i** and **8j**) were tolerated under the reaction conditions. Various kinds of aliphatic amines afforded the desired urea products in very good to excellent yields (**8k–8o**). In the case of 2-adamantyl amine (**8p**), a poor yield of **9pp** (31%) was observed and most of the **8p** remained; this was presumably due to high steric hindrance. Furthermore, the use of diamines **8q** and **8r** in the reaction resulted in the production of cyclic ureas. The yield of the product was relatively decreased probably due to coordination effect of diamine. To our delight, subjection of chiral amine **8s** to the reaction generated urea product **9ss** with no epimerization. However, secondary amines, such as **8t**, and electron-deficient aryl amines, such as aniline, were not applicable under the developed reaction conditions. In the case of **8t**, the corresponding formamide was formed as the major product, which implies that the second nucleophilic addition of the secondary

amine to formamide could be the limiting step for the urea synthesis. Aniline did not react at all under the reaction conditions. Therefore, in the case of 4-aminobenzyl amine (**8e**), selective urea formation on the aliphatic amine group was achieved in an 84% yield

4.2.2 Asymmetrical urea synthesis

Next, we turned our attention to the synthesis of unsymmetrical urea derivatives. Traditionally, unsymmetrical ureas are synthesized via nucleophilic attack of amines on isocyanates. Recently, Buchwald and coworkers reported an unsymmetrical urea synthesis using an arylisocyanate intermediate synthesized by Pd-catalyzed cross coupling of aryl chlorides and triflates with sodium cyanate.¹⁵ Other efforts have been devoted to achieve in situ generation of isocyanates from different precursors, such as carboxylic acids, carbamic acids,^{4c} carbamates,¹⁶ acyl azides,¹⁷ hydroxamic acids,¹⁸ or acetoacetanilide.¹⁹ They have also been prepared by functionalization of mother ureas via N-alkylation²⁰ or N-arylation.²¹ Despite the significant advances in this field, many procedures still suffer from a limited availability of starting materials and restricted substrate scope.



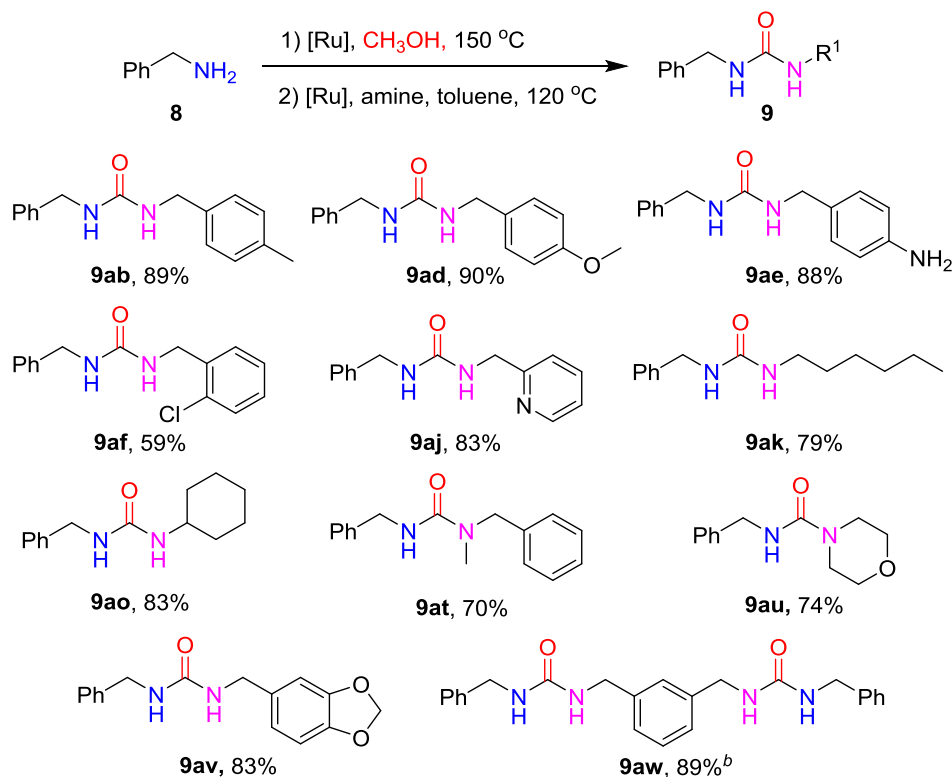
Scheme 4.2 Attempts to synthesize unsymmetrical urea derivatives.

To elucidate the viability of the optimized reaction conditions for the synthesis of unsymmetrical urea, two different aliphatic amines, i.e., **8a** and **8k**, were reacted in a reaction vessel (Scheme 4.2). This reaction produced three of the corresponding urea derivatives with a statistical distribution: Symmetrical **9aa** (21%) and **9kk** (25%), and unsymmetrical **9ak** (48%). The reaction of 4-aminobenzylamine (**8e**) with benzylamine resulted in a similar distribution of products. To improve the selectivity toward the unsymmetrical ureas, we devised a strategy comprising a sequential two-step reaction in one-pot by first generating formamide from an amine and methanol, and then

reacting the formamide with the second amine. This reaction strategy was proven to be viable by the reaction of **10** and **8k** to produce **9ak** in an excellent yield (94%) under the catalytic conditions of **1**. Recently, Reddy and co-workers reported Cu-catalyzed unsymmetrical urea synthesis from formamide and amines using tert-butylhydroperoxide (TBHP) as a stoichiometric oxidant at a relatively low efficiency (mostly <50% yields).²² Here, an unsymmetrical urea synthesis from formamide and amine was achieved under oxidant-free conditions with high efficiency.

Combining the current strategy and the previous report of formamide synthesis using methanol,¹² we attempted selective unsymmetrical urea synthesis in one-pot. After first generating benzyl formamide from **8** using methanol as the solvent, the methanol was removed in vacuum. Then, n-hexyl amine and toluene were added to the reaction tube with an additional loading of Ru complex **1** under inert conditions. After further reaction for 16 h at 120 °C, desired 1-benzyl-3-hexyl urea **9ak** was obtained in a good yield (79%).

Table 4.3 Unsymmetrical urea synthesis from methanol and amine.^a

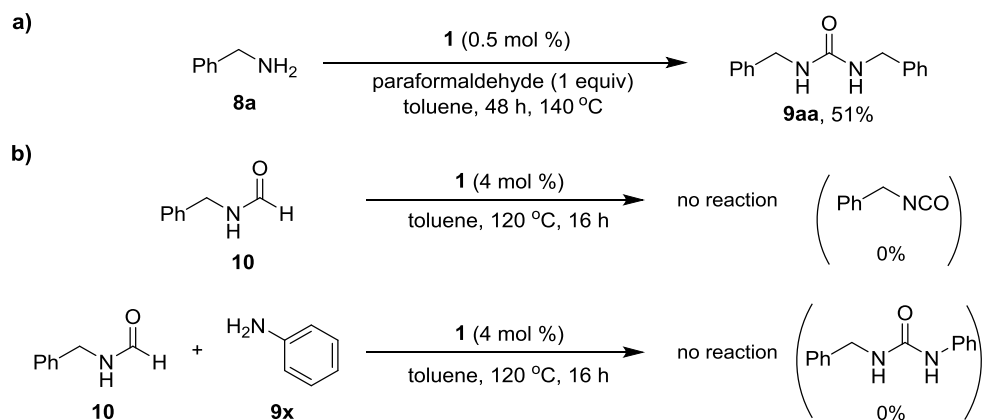


^aReaction conditions: 1) amine (0.5 mmol, 1.2 equiv), **1** (2 mol %), methanol (2 mL), 150 °C, 12 h in a closed vessel; 2) amine (0.42 mmol, 1 equiv), toluene (1.5 mL), **1** (4 mol %), 120 °C, 16 h in a closed vessel, isolated yield. ^b*m*-xylylenediamine (0.21 mmol) in the second step.

The scope of the reaction was expanded to include a variety of coupling partners and various unsymmetrical ureas were synthesized in good to excellent yields (Table 4.3). Reactions with amines containing heterocycles provided the corresponding ureas, i.e., **9aj**

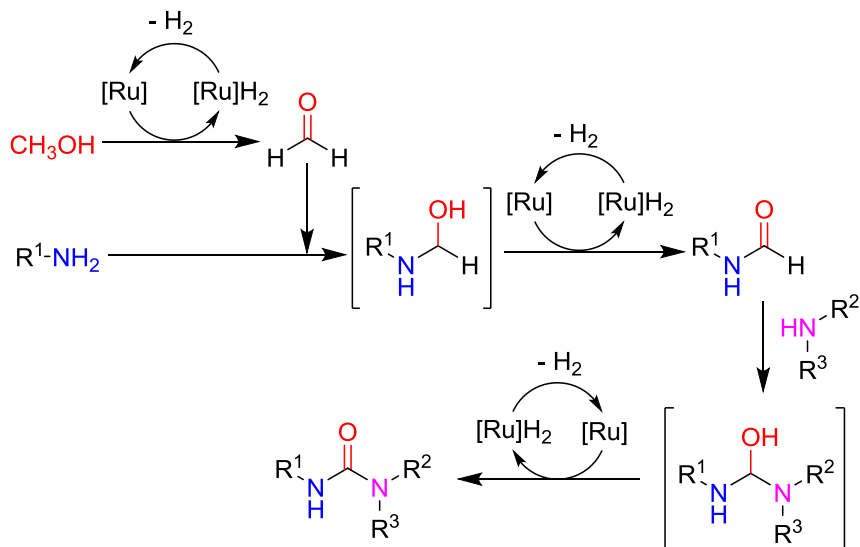
and **9av**, in very good yields. Notably, using secondary amines as the second cross partners was successful (**9at** and **9au**) although symmetrical urea synthesis of secondary amines was not possible; this implies that tertiary formamides are not reactive for further urea functionalization because of steric congestion. Unfortunately, the use of aniline in the reaction did not generate a urea derivative, as in the case of symmetrical urea synthesis. It is worthwhile to note that a diamine reacted with in situ-generated formamide to afford a diurea compound (**9aw**).

4.2.3 Possible mechanism



Scheme 4.3 Control experiments.

An independent reaction with paraformaldehyde and benzylamine under our reaction conditions gave 1,3-dibenzylurea (Scheme 4.3a). To investigate the possibility of isocyanate mediated mechanism, N-benzyl formamide was treated with aniline under the complex **1**, but no reaction occurred (Scheme 4.3b). Since benzyl isocyanate is easily reacted with aniline to form the corresponding urea,²³ isocyanate mediated urea formation pathway was ruled out. In addition, isocyanate was not observed at all from N-benzyl formamide under our reaction conditions (Scheme 4.3b). Involvement of amidine was also excluded as we could not observe the formation of amidine under our reaction conditions even in the presence of molecular sieves to remove water.



Scheme 4.4. Proposed mechanism.

Based on the results, the formation of urea is proposed to follow the pathway shown in Scheme 4.4. The primary amine is oxidatively coupled with formaldehyde, which is formed from dehydrogenation of methanol, to generate the formamide. Subsequent nucleophilic attack of an amine on the formamide generates the hemiaminal analogue, which is further dehydrogenated to the urea.

4.3 Conclusion

In summary, we reported a novel urea synthetic method directly from methanol and amines catalyzed by readily available ruthenium PNP catalyst with hydrogen as the sole byproduct. No additive, such as base, oxidant, or hydrogen acceptor, was required. Symmetrical and unsymmetrical urea derivatives were successfully obtained using methanol as the C1 feedstock by applying a dehydrogenative condensation strategy.

4.4 Experimental section

4.4.1 General information

Unless otherwise noted, all reactions were carried out using standard Schlenk techniques or in an argon-filled glove box. All symmetrical urea synthesis were performed in an oven-dried stainless steel

vessel under argon atmosphere (internal pressure of the reaction vessel was increased to about 3 bar during the reaction at 140 °C). In case of unsymmetrical urea synthesis a thick-wall glass tube was used with a safety shield. Ru complexes **3**^{14c} and **4**^{12a} were prepared according to the literature procedures. Unless otherwise noted, all reagents were obtained from Alfa Aesar, Strem, and Sigma Aldrich used as received. Analytical TLC was performed on a Merck 60 F254 silica gel plate (0.25mm thickness). Column chromatography was performed on Merck 60 silica gel (230–400 mesh). NMR spectra were recorded on a Bruker DPX–300 (300 MHz) spectrometer. Tetramethylsilane was used as reference, and the chemical shifts were reported in ppm and the coupling constant in Hz. Chiral compounds analysis were carried out on an Agilent LC chromatograph using CHIRALPAK AS–H column (particle size 5 μ m, dimensions 4.6 mm \times 250 mm). HRMS analysis was performed by Organic Chemistry Research Center in Sogang University.

4.4.2 General procedure for symmetrical urea synthesis

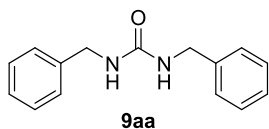
A stainless steel autoclave (50 mL) was charged with complex **1** (0.01 mmol, 5.9 mg), amine (2 mmol), methanol (2 mmol, 81 μ L), and toluene (1.5 mL) in an argon-filled glove box. The vessel was heated

to 140 °C (bath temperature) under closed conditions. After 24 h, the reaction was cooled to 0 °C for 30 min. The generated H₂ was carefully released in a fumehood. *n*-Hexane (40 mL) was then added to the reaction mixture. The resulting solid was collected and further washed with cold diethyl ether to afford the corresponding product.

4.4.3 General procedure for unsymmetrical urea synthesis

A Schlenk-type thick-wall round-bottom flask (50 mL) was charged with complex **1** (0.01 mmol, 5.9 mg), benzyl amine (0.5 mmol, 54 mg), and methanol (2 mL) in an argon-filled glove box. The reaction tube was heated to 150 °C (bath temperature) under closed conditions. After 12 h, the reaction was cooled to 0 °C for 1 h. Methanol was removed under vacuum. Complex **1** (0.017 mmol, 9.9 mg), amine (0.42 mmol), and toluene (1.5 mL) were then added to the reaction tube under an argon atmosphere. The vessel was heated to 120 °C (bath temperature) for 16 h under closed conditions and then cooled to 0 °C for 30 min. The generated H₂ was released carefully in a fumehood. *n*-Hexane (40 mL) was then added to the reaction mixture. The resulting solid was collected and further washed with cold diethyl ether to afford the corresponding product.

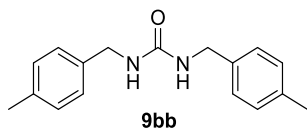
4.4.4 Characterization data of urea



1,3-dibenzylurea

White solid (223.9 mg 0.933 mmol, 93%). The compound was identified by spectral comparison with literature data.²⁴

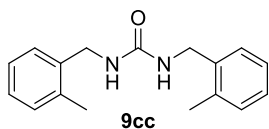
¹H NMR (300 MHz, DMSO-*d*₆, δ): 4.23 (s, 4H, 2CH₂), 6.45 (br, 2H, 2NH), 7.20 – 7.34 (m, 10H, 10CH) ppm.



1,3-bis(4-methylbenzyl)urea

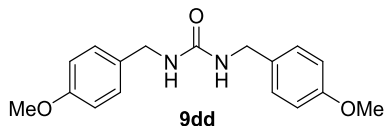
White solid (239.9 mg, 0.895 mmol, 90%). The compound was identified by spectral comparison with literature data.²⁵

¹H NMR (300 MHz, DMSO-*d*₆, δ): 2.28 (s, 6H, 2CH₃), 4.17 (d, *J* = 5.6 Hz, 4H, 2CH₂), 6.35 (br, 2 H, 2NH), 7.13 (m, 8H, 8CH) ppm.



1,3-bis(2-methylbenzyl)urea

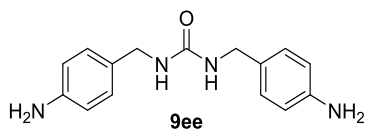
White solid (246.1 mg, 0.917 mmol, 92%). ^1H NMR (300 MHz, $\text{DMSO}-d_6$, δ): 2.27 (s, 6H, 2CH_3), 4.21 (d, $J = 3$ Hz, 4H, 2CH_2), 6.28 (br, 2H, 2NH), 7.15 – 7.23 (m, 8H, 8CH) ppm; ^{13}C NMR (75 MHz, $\text{DMSO}-d_6$, δ): 18.98, 41.53, 126.16, 127.10, 127.63, 130.32, 135.84, 138.85, 158.33 ppm, HRMS(ESI) calcd for $\text{C}_{17}\text{H}_{20}\text{N}_2\text{ONa}$: 291.1473 Found: 291.1468 $[\text{M}+\text{Na}]^+$.



1,3-bis(4-methoxybenzyl)urea

White solid (226.0 mg, 0.753 mmol, 75%). The compound was identified by spectral comparison with literature data.²⁶

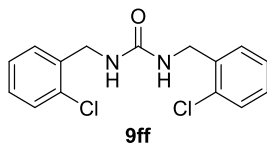
^1H NMR (300 MHz, $\text{DMSO}-d_6$, δ): 3.73 (s, 6H, 2CH_3), 4.14 (d, $J = 6.0$ Hz, 4H, 2CH_2), 6.29 (m, 2H, 2NH), 6.80 (d, $J = 8.4$ Hz, 4H, 4CH), 7.16 (d, $J = 8.5$ Hz, 4H, 4CH) ppm.



1,3-bis(4-aminobenzyl)urea

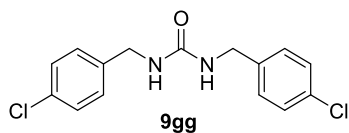
Reddish brown solid (227.1 mg, 0.841 mmol, 84%). The compound was identified by spectral comparison with literature data.^{3e}

¹H NMR (300 MHz, DMSO-*d*₆, δ): 4.01 (d, J = 5.5 Hz, 4H, 2CH₂), 4.93 (s, 4H, 2NH₂), 6.04 (br, 2H, 2NH), 6.49 (d, J = 8.3 Hz, 4H, 4CH), 6.89 (d, J = 8.3 Hz, 4H, 4CH) ppm.



1,3-bis(2-chlorobenzyl)urea

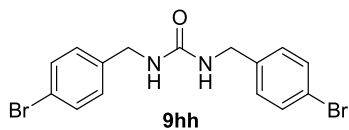
White solid (232.1 mg, 0.751 mmol, 75%). ¹H NMR (300 MHz, DMSO-*d*₆, δ): 4.28 (d, J = 5.9 Hz, 4H, 2CH₂), 7.07 (br, 2H, 2NH), 7.28 – 7.43 (m, 8H, 8CH) ppm; ¹³C NMR (75 MHz, DMSO-*d*₆, δ): 41.28, 127.54, 128.76, 129.03, 129.43, 132.26, 138.37, 158.53 ppm; HRMS(ESI) calcd for C₁₅H₁₄Cl₂N₂ONa: 331.0381 Found: 331.0375 [M+Na]⁺.



1,3-bis(4-chlorobenzyl)urea

White solid (216.3 mg, 0.700 mmol, 70%). The compound was identified by spectral comparison with literature data.^{3e}

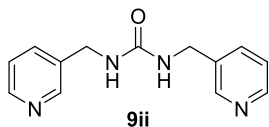
¹H NMR (300 MHz, DMSO-*d*₆, δ): 4.20 (d, J = 6.1 Hz, 4H, 2CH₂), 6.68 (br, 2H, 2NH), 7.25 (d, J = 8.4 Hz, 4H, 4CH), 7.36 (d, J = 8.4 Hz, 4H, 4CH) ppm.



1,3-bis(4-bromobenzyl)urea

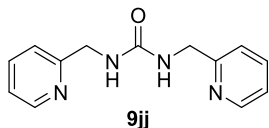
White solid (277.0 mg, 0.695 mmol, 70%). The compound was identified by spectral comparison with literature data.^{3e}

¹H NMR (300 MHz, DMSO-*d*₆, δ): 4.18 (d, J = 6.0 Hz, 4H, 2CH₂), 6.59 (br, 2H, 2NH), 7.19 (d, J = 8.2 Hz, 4H, 4CH), 7.49 (d, J = 8.3 Hz, 4H, 4CH) ppm.



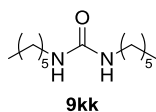
1,3-bis(pyridin-3-ylmethyl)urea

White solid (185.1 mg, 0.765 mmol, 77%). ^1H NMR (300 MHz, $\text{DMSO}-d_6$, δ): 4.24 (d, $J = 6.0$ Hz, 4H, 2CH_2), 6.62 (br, 2H, 2NH), 7.31 (m, 2H, 2CH), 7.63 (d, $J = 7.8$ Hz, 2H, 2CH), 8.43 (m, 4H, 4CH) ppm; ^{13}C NMR (75 MHz, $\text{DMSO}-d_6$, δ): 41.16, 123.83, 135.27, 135.74, 148.34, 149.06, 158.51 ppm; HRMS(ESI) calcd for $\text{C}_{13}\text{H}_{14}\text{N}_4\text{ONa}$: 265.1065 Found: 265.1060 $[\text{M}+\text{Na}]^+$.



1,3-bis(pyridin-2-ylmethyl)urea

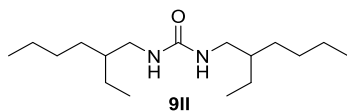
Yellowish solid (140.4 mg, 0.580 mmol, 58%). ^1H NMR (300 MHz, $\text{DMSO}-d_6$, δ): 4.33 (d, $J = 5.8$ Hz, 4H, 2CH_2), 6.74 (m, 2H, 2NH), 7.23 – 7.32 (m, 4H, 4CH), 7.73 – 7.79 (m, 2H, 2CH), 8.49 (d, $J = 4.6$ Hz, 2H, 2CH) ppm; ^{13}C NMR (75 MHz, $\text{DMSO}-d_6$, δ): 45.42, 121.30, 122.36, 137.08, 149.16, 158.59, 160.18 ppm; HRMS(ESI) calcd for $\text{C}_{13}\text{H}_{14}\text{N}_4\text{ONa}$: 265.1065 Found: 265.1060 $[\text{M}+\text{Na}]^+$.



1,3-di-*n*-hexylurea

Purification of the product was performed with silica gel column chromatography using DCM/methanol (20:1) as an eluent. Thick dark oil (199.1 mg, 0.873 mmol, 87%). The compound was identified by spectral comparison with literature data.²⁴

¹H NMR (300 MHz, CDCl₃, δ): 0.88 (t, J = 6.6 Hz, 6H, 2CH₃), 1.29 (m, 12H, 6CH₂), 1.48 (m, 4H, 2CH₂), 3.15 (br, 4H, 2CH₂), 4.30 (br, 2H, 2NH) ppm.

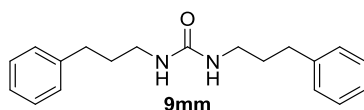


1,3-bis(2-ethylhexyl)urea

Purification of the product was performed with silica gel column chromatography using DCM/methanol (20:1) as an eluent. Thick dark oil (270.1 mg, 0.951 mmol, 95%).

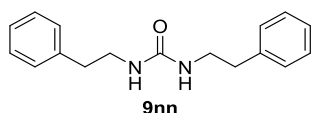
¹H NMR (300 MHz, CDCl₃, δ): 0.89 (t, J = 7.6 Hz, 12H, 4CH₃), 1.28 – 1.41 (m, 18H), 3.09 (d, J = 5.9 Hz, 4H, 2CH₂), 4.25 (br, 2H, 2NH) ppm; ¹³C NMR (75 MHz, CDCl₃, δ): 10.92, 14.07, 23.05, 24.22, 28.94,

31.01, 39.81, 43.54, 158.44 ppm; HRMS (ESI) calcd for $C_{17}H_{36}N_2ONa$:
307.2725 Found: 307.2720 $[M+Na]^+$.



1,3-bis(3-phenylpropyl)urea

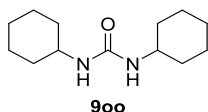
White solid (267.0 mg, 0.902 mmol, 90%). 1H NMR (300 MHz, $DMSO-d_6$, δ): 1.66 (m, 4H, $2CH_2$), 2.57 (m, 4H, $2CH_2$), 2.99 (m, 4H, $2CH_2$), 5.86 (m, 2H, $2NH$), 7.15 – 7.30 (m, 10H, $10CH$) ppm; ^{13}C NMR (75 MHz, $DMSO-d_6$, δ): 32.34, 32.97, 39.33, 126.13, 128.73, 142.32, 158.57 ppm; HRMS (ESI) calcd for $C_{19}H_{24}N_2ONa$: 319.1786 Found: 319.1781 $[M+Na]^+$.



1,3-bis(phenethyl)urea

White solid (252.0 mg, 0.942 mmol, 94%). The compound was identified by spectral comparison with literature data.^{3b}

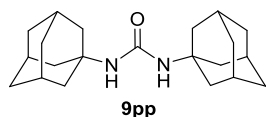
1H NMR (300 MHz, $DMSO-d_6$, δ): 2.64 (t, $J = 7.2$ Hz, 4H, $2CH_2$), 3.20 (dd, $J = 6.7$ Hz, $J = 13.3$ Hz, 4H, $2CH_2$), 5.88 (m, 2H, $2NH$), 7.13 – 7.31 (m, 10H, $10CH$) ppm.



1,3-dicyclohexylurea

White solid (182.3 mg, 0.813 mmol, 81%). The compound was identified by spectral comparison with literature data.²⁷

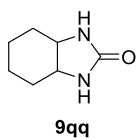
¹H NMR (300 MHz, MeOD-*d*₄, δ): 1.09 – 1.43 (m, 10H), 1.59 – 1.88 (m, 10H), 3.31 – 3.50 (m, 2H, 2CH) ppm.



1,3-di(1-adamantyl)urea

White solid (103.1 mg, 0.314 mmol, 31%). The compound was identified by spectral comparison with literature data.^{3c}

¹H NMR (300 MHz, CDCl₃, δ): 1.66 (m, 12H), 1.95 (m, 12H), 2.05 (m, 6H), 3.83 (br, 2H, 2NH) ppm.

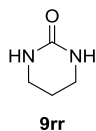


Octahydro-benzoimidazol-2-one

Purification of the product was performed with silica gel column chromatography using DCM/methanol (20:1) as an eluent. White solid

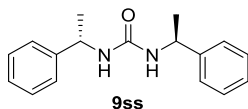
(105 mg, 0.751 mmol, 75%). The compound was identified by spectral comparison with literature data.²⁷

¹H NMR (300 MHz, MeOD-*d*₄, δ): 1.36 (m, 2H), 1.56 – 1.75 (m, 6H), 3.67 (m, 2H, 2CH) ppm.



Tetrahydropyrimidin-2(1H)-one

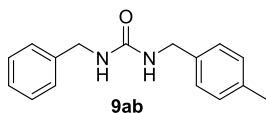
White solid (51.1mg, 0.511 mmol, 51%). ¹H NMR (300 MHz, D₂O, δ): 1.85 (m, 2H), 3.26 (m, 4H) ppm.



1,3-bis((S)-1-phenylethyl)urea

White solid (164.2 mg, 0.611 mmol, 61%). The compound was identified by spectral comparison with literature data.^{3b}

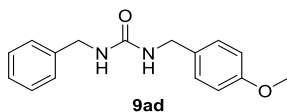
¹H NMR (300 MHz, DMSO-*d*₆, δ): 1.28 (s, *J* = 6.9 Hz, 6H, 2CH₃), 4.72 (m, 2H, 2CH), 6.26 (d, *J* = 8.0 Hz, 2H, 2NH), 7.19 – 7.34 (m, 10H, 10CH) ppm.



1-benzyl-3-(4-methylbenzyl)urea

Yellowish solid (94.9 mg, 0.373 mmol, 89%). The compound was identified by spectral comparison with literature data.^{4c}

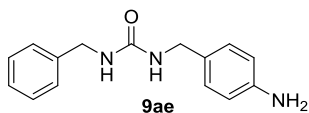
¹H NMR (300 MHz, CDCl₃, δ): 2.31 (s, 3H, CH₃), 4.32 (d, J = 6.0, 2H, CH₂), 4.37 (d, J = 5.8, 2H, CH₂), 4.80 (br, 2H, 2NH), 7.15 – 7.09 (m, 4H, 4CH), 7.25 – 7.32 (m, 5H, 5CH) ppm.



1-benzyl-3-(4-methoxybenzyl)urea

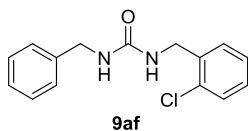
Yellowish solid (101.3 mg, 0.375 mmol, 90%). The compound was identified by spectral comparison with literature data.^{4c}

¹H NMR (300 MHz, CDCl₃, δ): 3.77 (s, 3H, CH₃), 4.29 (m, 2H, CH₂), 4.36 (m, 2H, CH₂), 4.71 (br, 2H, 2NH), 6.82 (d, J = 8.0, 2H, 2CH), 7.18 (d, J = 8.0, 2H, 2CH), 7.25 – 7.30 (m, 5H, 5CH) ppm.



1-(4-aminobenzyl)-3-benzylurea

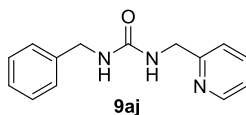
Light orange solid (94.2 mg, 0.369 mmol, 88%). ^1H NMR (300 MHz, $\text{DMSO}-d_6$, δ): 4.03 (d, $J = 5.7$ Hz, 2H, CH_2), 4.21 (d, $J = 5.9$, 2H, CH_2), 4.92 (s, 2H, NH_2), 6.20 (m, 1H, NH), 6.35 (m, 1H, NH), 6.49 (d, $J = 8.3$ Hz, 2H, 2CH), 6.90 (d, $J = 8.2$ Hz, 2H, 2CH), 7.20 – 7.34 (m, 5H, 5CH) ppm; ^{13}C NMR (75 MHz, $\text{DMSO}-d_6$, δ): 43.30, 43.38, 114.15, 126.98, 127.44, 127.98, 128.54, 128.65, 141.44, 147.85, 158.49 ppm; HRMS(ESI) calcd for $\text{C}_{15}\text{H}_{17}\text{N}_3\text{ONa}$: 278.1269 Found: 278.1264 $[\text{M}+\text{Na}]^+$.



1-benzyl-3-(2-chlorobenzyl)urea

White solid (67.4 mg, 0.246 mmol, 59%). The compound was identified by spectral comparison with literature data.^{4c}

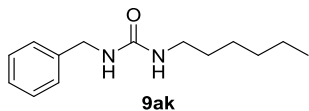
^1H NMR (300 MHz, CDCl_3 , δ): 4.37 (br, 2H, CH_2), 4.46 (br, 2H, CH_2), 4.80 (br, 1H, NH), 4.93 (br, 1H, NH), 7.17 – 7.40 (m, 9H, 9CH) ppm.



1-benzyl-3-(pyridin-2-ylmethyl)urea

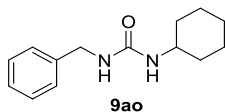
White solid (84.1 mg, 0.349 mmol, 83%). The compound was identified by spectral comparison with literature data.^{4c}

¹H NMR (300 MHz, CDCl₃, δ): 4.41 (d, J = 5.8, 2H, CH₂), 4.50 (d, J = 5.8, 2H, CH₂), 5.22 (br, 1H, NH), 5.67 (br, 1H, NH), 7.16 – 7.18 (m, 1H, 1CH), 7.28 – 7.36 (m, 6H, 6CH), 7.64 – 7.69 (m, 1H), 8.48 (d, J = 4.6, 1H) ppm.



1-benzyl-3-*n*-hexylurea

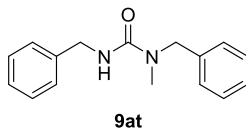
White solid (77.7 mg, 0.332 mmol, 79%). ¹H NMR (300 MHz, DMSO-*d*₆, δ): 0.87 (m, 3H, CH₃), 1.26 – 1.37 (m, 8H, 4CH₂), 2.97 (m, 2H, CH₂), 4.19 (m, 2H, CH₂), 5.91 (m, 1H, NH), 6.27 (m, 1H, NH), 7.21 – 7.34 (m, 5H, 5CH) ppm; ¹³C NMR (75 MHz, DMSO-*d*₆, δ): 14.38, 22.57, 26.51, 30.46, 31.51, 39.78, 43.33, 126.94, 127.42, 126.62, 141.52, 158.53 ppm; HRMS(ESI) calcd for C₁₄H₂₂N₂ONa: 257.1630 Found: 257.1624 [M+Na]⁺.



1-benzyl-3-cyclohexylurea

White solid (80.8 mg, 0.348 mmol, 83%). The compound was identified by spectral comparison with literature data.²⁵

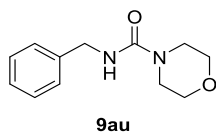
¹H NMR (300 MHz, DMSO-*d*₆, δ): 1.03 – 1.29 (m, 5H), 1.50 – 1.77 (m, 5H), 3.39 (m, 1H, CH), 4.18 (d, *J* = 5.9, 2H, CH₂), 5.81 (d, *J* = 7.9, 1H, NH), 6.17 (m, 1H, NH), 7.22 – 7.33 (m, 5H, 5CH) ppm.



1,3-dibenzyl-1-methylurea

Purification of the product was performed with silica gel column chromatography using EA/*n*-hexane (1:1) as an eluent. White solid (74.0 mg, 0.291 mmol, 70%). The compound was identified by spectral comparison with literature data.^{4c}

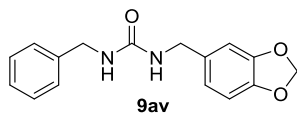
¹H NMR (300 MHz, CDCl₃, δ): 2.92 (s, 3H, CH₃), 4.47 (d, *J* = 5.5 Hz, 2H, CH₂), 4.55 (s, 2H, CH₂), 4.74 (br, 1H, NH), 7.26 – 7.38 (m, 10H, 10CH) ppm.



N-benzylmorpholine-4-carboxamide

Purification of the product was performed with silica gel column chromatography using DCM/methanol (20:1) as an eluent. White solid (68.4 mg, 0.311 mmol, 74%). The compound was identified by spectral comparison with literature data.^{4c}

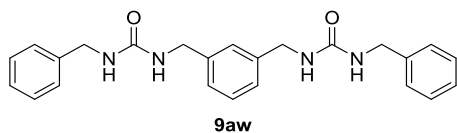
¹H NMR (300 MHz, CDCl₃, δ): 3.37 (t, J = 4.8 Hz, 4H, 2CH₂), 3.70 (t, J = 5.1 Hz, 4H, 2CH₂), 4.44 (d, J = 5.5 Hz, 2H, CH₂), 4.79 (br, 1H, NH), 7.27 – 7.39 (m, 5H, 5CH) ppm.



1-(benzo-1,3-dioxol-5-ylmethyl)-3-benzylurea

White solid (99.1 mg, 0.348 mmol, 83%). ¹H NMR (300 MHz, DMSO-*d*₆, δ): 4.12 (d, J = 6.0 Hz, 2H, CH₂), 4.22 (d, J = 6.0 Hz, 2H, CH₂), 5.98 (s, 2H, CH₂), 6.36 – 6.44 (m, 2H, 2NH), 6.71 – 6.74 (m, 1H, CH), 6.81 – 6.83 (m, 2H, 2CH), 7.22 – 7.34 (m, 5H, 5CH) ppm; ¹³C NMR (75 MHz, DMSO-*d*₆, δ): 43.22, 43.40, 101.19, 108.14, 108.40, 120.54, 127.00, 127.44, 126.66, 135.34, 141.36, 146.31, 147.64, 158.48 ppm; HRMS(ESI) calcd for C₁₆H₁₆N₂O₃Na: 307.1059 Found:

307.1053 $[M+Na]^+$.

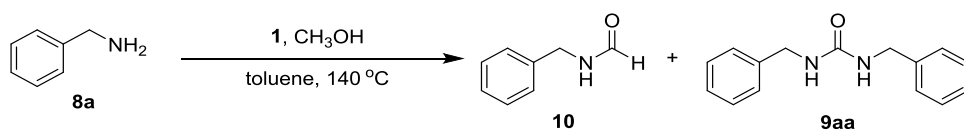


1,1'-(1,3-phenylenebis(methylene))bis(3-benzylurea)

White solid (75.1 mg, 0.187 mmol, 89%). ^1H NMR (300 MHz, $\text{DMSO}-d_6$, δ): 4.23 (t, J = 5.9 Hz, 8H, 4CH₂), 6.44 (m, 4H, 4NH), 7.11 – 7.35 (m, 14H, 14CH) ppm; ^{13}C NMR (75 MHz, $\text{DMSO}-d_6$, δ): 43.44, 43.49, 125.78, 126.21, 127.01, 127.46, 128.63, 128.68, 141.29, 141.38, 158.52 ppm; HRMS(ESI) calcd for C₂₄H₂₆N₄O₂Na: 425.1953
Found: 425.1948 $[M+Na]^+$.

4.4.5 Complementary reaction optimization data

Table 4.4 Screening experiment for symmetrical urea synthesis.^a



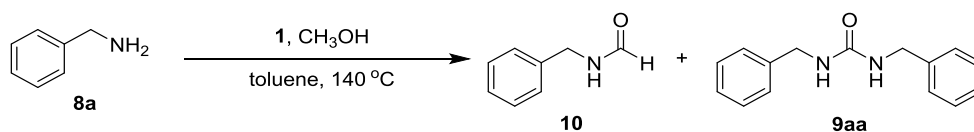
entry	loading	toluene	time	MeOH mmol	10 (%)	9aa (%)
1	0.5 mol %	1.5 mL	24 h	20	30	52
2	0.5 mol %	1.5 mL	24 h	10	17	82
3	0.5 mol %	4.0 mL	24 h	7.5	20	68
4	0.5 mol %	1.5 mL	24 h	7.5	14	84
5	0.5 mol %	1.0 mL	24 h	7.5	12	80
6	0.5 mol %	1.5 mL	12 h	7.5	22	63
7	0.5 mol %	1.5 mL	36 h	7.5	15	83
8	0.5 mol %	1.5 mL	24 h	4.0	10	88
9	0.5 mol %	1.5 mL	24 h	2.0	trace	97
10 ^b	0.5 mol %	1.5 mL	24 h	2.0	5	91
11 ^c	0.5 mol %	1.5 mL	24 h	2.0	11	31
10	0.3 mol %	1.5 mL	48 h	2.0	4	86
11	0.1 mol %	1.5 mL	48 h	2.0	5	6
12	0.5 mol %	1.5 mL	24 h	1.4	0	89

^aReaction conditions: benzyl amine (2.0 mmol, 1.0 equiv), **1**, methanol, toluene, $140\text{ }^\circ\text{C}$, NMR yield, *p*-xylene was used as a standard. ^b120

°C. ^c100 °C.

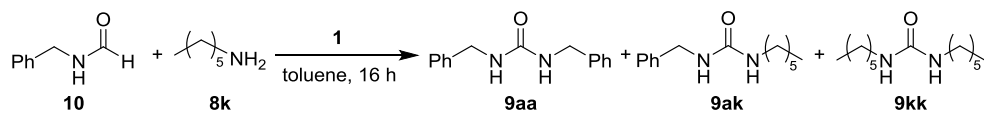
Table 4.5 Turnover numbers and turnover frequencies

measurement.^a



entry	loading	toluene	10 (%)	9aa (%)	TON	TOF(1/h)
1	0.5 mol %	1 h	2	12	12	12
2	0.5 mol %	3 h	2	32	32	10.7
3	0.5 mol %	6 h	3	63	63	10.5
4	0.5 mol %	12 h	4	78	78	6.5
5	0.3 mol %	12 h	2	53	88	7.3
6	0.5 mol %	24 h	trace	97	97	4.0
7	0.2 mol %	48 h	4	85	213	4.4
8	0.1 mol %	48 h	trace	59	295	6.1

^aReaction conditions: benzyl amine (2.0 mmol, 1.0 equiv), **1**, methanol (2.0 mmol), toluene, 140 °C, NMR yield, *p*-xylene was used as a standard, TONs and TOFs were calculated based on the amount of 1,3-dibenzyl urea.

Table 4.6 Screening experiment for unsymmetrical urea synthesis.^a

entry	loading	toluene	temperature	9aa (%)	9ak (%)	9kk (%)
1	1 mol %	1.5 mL	150 °C	12	63	12
2	1 mol %	0.75 mL	140 °C	8	69	8
3	1 mol %	1.5 mL	140 °C	5	68	5
4	4 mol %	1.5 mL	140 °C	3	85	3
5	4 mol %	1.5 mL	130 °C	2	88	2
6	4 mol %	1.5 mL	120 °C	trace	94	trace
7	2 mol %	1.5 mL	120 °C	11	85	4
8	1 mol %	1.5 mL	120 °C	5	44	4

^aReaction conditions: **10** (0.5 mmol, 1.0 equiv), **8k** (0.5 mmol), **1**, toluene, NMR yield, *p*-xylene was used as a standard.

Scheme 4.5 Screening experiment for unsymmetrical urea synthesis.

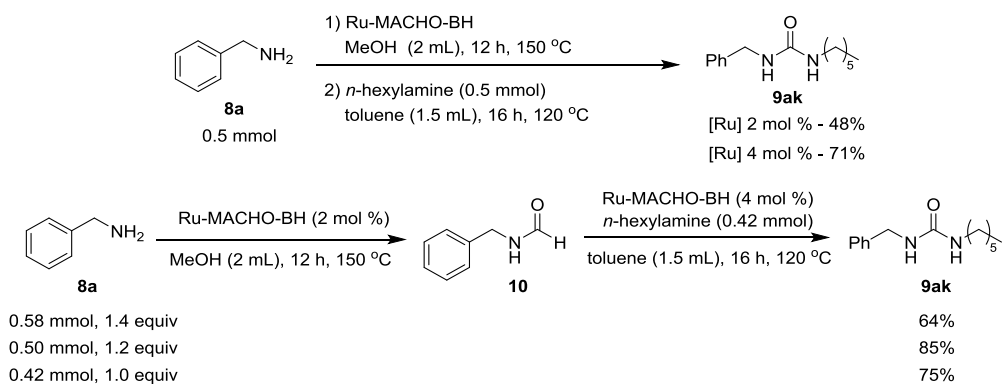


Figure 4.1 The LC chart for 1,3-bis(1-phenylethyl) urea.

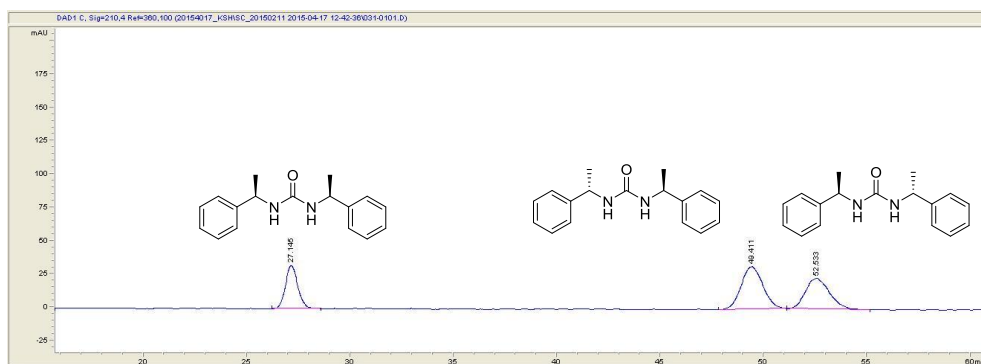
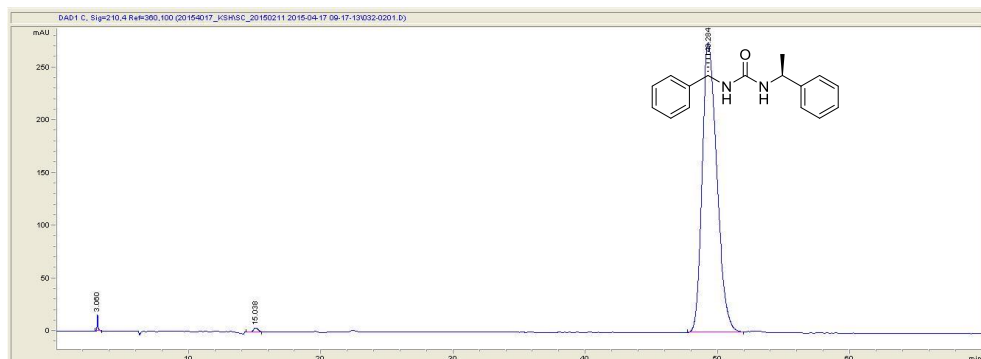


Figure 4.2 The LC chart for 1,3-bis((S)-1-phenylethyl) urea.



4.5 Reference

- (1) (a) Arasappan, A.; Bennett, F.; Bogen, S. L.; Venkatraman, S.; Blackman, M.; Chen, K. X.; Hendrata, S.; Huang, Y.; Huelgas, R. M.; Nair, L.; Padilla, A. I.; Pan, W.; Pike, R.; Pinto, P.; Ruan, S.; Sannigrahi, M.; Velazquez, F.; Vibulbhan, B.; Wu, W.; Yang, W.; Saksena, A. K.; Girijavallabhan, V.; Shih, N.-Y.; Kong, J.; Meng, T.; Jin, Y.; Wong, J.; McNamara, P.; Prongay, A.; Madison, V.; Piwinski, J. J.; Cheng, K.-C.; Morrison, R.; Malcolm, B.; Tong, X.; Ralston, R.; Njoroge, F. G. *ACS Med. Chem. Lett.* **2010**, *1*, 64. (b) Gallou, I. *Org. Prep. Proc. Int.* **2007**, *39*, 355. (c) Bankston, D.; Dumas, J.; Natero, R.; Riedl, B.; Monahan, M.-K.; Sibley, R. *Org. Process Res. Dev.* **2002**, *6*, 777. (d) Matsuda, K. *Med. Res. Rev.* **1994**, *14*, 271.
- (2) (a) Bigi, F.; Maggi, R.; Sartori, G. *Green Chem.* **2000**, *2*, 140. (b) Babad, H.; Zeiler, A. G. *Chem. Rev.* **1973**, *73*, 75.
- (3) (a) Guan, Z.-H.; Lei, H.; Chen, M.; Ren, Z.-H.; Bai, Y.; Wang, Y.-Y. *Adv. Synth. Catal.* **2012**, *354*, 489. (b) Park, J. H.; Yoon, J. C.; Chung, Y. K. *Adv. Synth. Catal.* **2009**, *351*, 1233. (c) Orito, K.; Miyazawa, M.; Nakamura, T.; Horibata, A.; Ushito, H.; Nagasaki, H.; Yuguchi, M.; Yamashita, S.; Yamazaki, T.; Tokuda, M. *J. Org. Chem.* **2006**, *71*, 5951. (d) Gabriele, B.; Salerno, G.; Mancuso, R.; Costa, M. *J. Org. Chem.* **2004**, *69*, 4741. (e) McCusker, J. E.; Main, A. D.;

Johnson, K. S.; Grasso, C. A.; McElwee–White, L. *J. Org. Chem.* **2000**, *65*, 5216.

(4) (a) Honda, M.; Sonehara, S.; Yasuda, H.; Nakagawa, Y.; Tomishige, K. *Green Chem.* **2011**, *13*, 3406. (b) Kong, D.–L.; He, L.–N.; Wang, J.–Q. *Synlett* **2010**, *2010*, 1276. (c) Peterson, S. L.; Stucka, S. M.; Dinsmore, C. J. *Org. Lett.* **2010**, *12*, 1340. (d) Wu, C.; Cheng, H.; Liu, R.; Wang, Q.; Hao, Y.; Yu, Y.; Zhao, F. *Green Chem.* **2010**, *12*, 1811. (e) Jiang, T.; Ma, X.; Zhou, Y.; Liang, S.; Zhang, J.; Han, B. *Green Chem.* **2008**, *10*, 465. (f) Ion, A.; Parvulescu, V.; Jacobs, P.; Vos, D. D. *Green Chem.* **2007**, *9*, 158.

(5) (a) Kalutharage, N.; Yi, C. S. *Org. Lett.* **2015**, *17*, 1778. (b) Lee, D.–H.; Kwon, K.–H.; Yi, C. S. *J. Am. Chem. Soc.* **2012**, *134*, 7325. (c) Lee, D. H.; Kwon, K. H.; Yi, C. S. *Science* **2011**, *333*, 1613.

(6) (a) Fujita, K.–i.; Kawahara, R.; Aikawa, T.; Yamaguchi, R. *Angew. Chem. Int. Ed.* **2015**, *54*, 9057. (b) Nielsen, M.; Alberico, E.; Baumann, W.; Drexler, H. J.; Junge, H.; Gladiali, S.; Beller, M. *Nature* **2013**, *495*, 85. (c) Kawahara, R.; Fujita, K.–i.; Yamaguchi, R. *J. Am. Chem. Soc.* **2012**, *134*, 3643. (d) Kawahara, R.; Fujita, K.–i.; Yamaguchi, R. *Angew. Chem. Int. Ed.* **2012**, *51*, 12790. (e) Fujita, K.–i.; Yoshida, T.; Imori, Y.; Yamaguchi, R. *Org. Lett.* **2011**, *13*, 2278. (f) Yi, C. S.; Lee, D. W. *Organometallics* **2009**, *28*, 947. (g) Fujita, K.–i.; Tanino,

N.; Yamaguchi, R. *Org. Lett.* **2007**, *9*, 109.

(7) (a) Gunanathan, C.; Milstein, D. *Chem. Rev.* **2014**, *114*, 12024.

(b) Gunanathan, C.; Milstein, D. *Science* **2013**, *341*. (c) Chen, C.;

Hong, S. H. *Org. Biomol. Chem.* **2011**, *9*, 20. (d) Dobereiner, G. E.;

Crabtree, R. H. *Chem. Rev.* **2010**, *110*, 681. (e) Guillena, G.; J. Ramón,

D.; Yus, M. *Chem. Rev.* **2010**, *110*, 1611.

(8) (a) Kabo, G. J.; Kozyro, A. A.; Diky, V. V.; Simirsky, V. V. *J.*

Chem. Eng. Data. **1995**, *40*, 371. (b) Davies, R. H.; Finch, A.; Hill, J.

O. *Thermochim. Acta* **1991**, *184*, 243.

(9) (a) Chan, L. K. M.; Poole, D. L.; Shen, D.; Healy, M. P. d.; Donohoe,

T. J. *Angew. Chem. Int. Ed.* **2014**, *53*, 761. (b) Ogawa, S.; Obora, Y.

Chem. Commun. **2014**, *50*, 2491. (c) Sun, C.; Zou, X.; Li, F. *Chem.–*

Eur. J. **2013**, *19*, 14030. (d) Li, F.; Xie, J.; Shan, H.; Sun, C.; Chen, L.

RSC Adv. **2012**, *2*, 8645. (e) Moran, J.; Preetz, A.; Mesch, R. A.;

Krische, M. J. *Nat. Chem.* **2011**, *3*, 287.

(10) (a) Oldenhuis, N. J.; Dong, V. M.; Guan, Z. *Tetrahedron* **2014**,

70, 4213. (b) Zhang, G.; Hanson, S. K. *Org. Lett.* **2013**, *15*, 650. (c)

Gnanaprakasam, B.; Zhang, J.; Milstein, D. *Angew. Chem. Int. Ed.*

2010, *49*, 1468.

(11) (a) Chen, C.; Zhang, Y.; Hong, S. H. *J. Org. Chem.* **2011**, *76*,

10005. (b) Ghosh, S. C.; Muthaiah, S.; Zhang, Y.; Xu, X.; Hong, S. H.

Adv. Synth. Catal. **2009**, *351*, 2643. (c) Nordstrøm, L. U.; Vogt, H.; Madsen, R. *J. Am. Chem. Soc.* **2008**, *130*, 17672. (d) Gunanathan, C.; Ben-David, Y.; Milstein, D. *Science* **2007**, *317*, 790.

(12) (a) Kang, B.; Hong, S. H. *Adv. Synth. Catal.* **2015**, *357*, 834. (b) Ortega, N.; Richter, C.; Glorius, F. *Org. Lett.* **2013**, *15*, 1776.

(13) (a) Spasyuk, D.; Smith, S.; Gusev, D. G. *Angew. Chem. Int. Ed.* **2013**, *52*, 2538. (b) Spasyuk, D.; Smith, S.; Gusev, D. G. *Angew. Chem. Int. Ed.* **2012**, *51*, 2772.

(14) (a) Zhang, L.; Han, Z.; Zhao, X.; Wang, Z.; Ding, K. *Angew. Chem. Int. Ed.* **2015**, *54*, 6186. (b) Kim, S. H.; Hong, S. H. *ACS Catal.* **2014**, *4*, 3630. (c) Han, Z. B.; Rong, L. C.; Wu, J.; Zhang, L.; Wang, Z.; Ding, K. L. *Angew. Chem. Int. Ed.* **2012**, *51*, 13041. (d) Kuriyama, W.; Matsumoto, T.; Ogata, O.; Ino, Y.; Aoki, K.; Tanaka, S.; Ishida, K.; Kobayashi, T.; Sayo, N.; Saito, T. *Org. Process Res. Dev.* **2012**, *16*, 166.

(15) Vinogradova, E. V.; Fors, B. P.; Buchwald, S. L. *J. Am. Chem. Soc.* **2012**, *134*, 11132.

(16) Gallou, I.; Eriksson, M.; Zeng, X.; Senanayake, C.; Farina, V. *J. Org. Chem.* **2005**, *70*, 6960.

(17) (a) Donovan, A. C.; Valliant, J. F. *J. Org. Chem.* **2009**, *74*, 8133. (b) Lebel, H.; Leogane, O. *Org. Lett.* **2006**, *8*, 5717.

- (18) Dubé, P.; Nathel, N. F. F.; Vetelino, M.; Couturier, M.; Aboussafy, C. L.; Pichette, S.; Jorgensen, M. L.; Hardink, M. *Org. Lett.* **2009**, *11*, 5622.
- (19) Wei, Y.; Liu, J.; Lin, S.; Ding, H.; Liang, F.; Zhao, B. *Org. Lett.* **2010**, *12*, 4220.
- (20) Li, F.; Sun, C.; Shan, H.; Zou, X.; Xie, J. *ChemCatChem* **2013**, *5*, 1543.
- (21) Breitler, S.; Oldenhuis, N. J.; Fors, B. P.; Buchwald, S. L. *Org. Lett.* **2011**, *13*, 3262.
- (22) Kumar, G. S.; Kumar, R. A.; Kumar, P. S.; Reddy, N. V.; Kumar, K. V.; Kantam, M. L.; Prabhakar, S.; Reddy, K. R. *Chem. Comm.* **2013**, *49*, 6686.
- (23) Lengyel, I.; Patel, H. J.; Stephani, R. A. *Heterocycles* **2007**, *73*, 349.
- (24) Mizuno, T.; Mihara, M.; Iwai, T.; Ito, T.; Ishino, Y. *Synthesis* **2006**, *2006*, 2825.
- (25) Artuso, E.; Degani, I.; Fochi, R.; Magistris, C. *Synthesis* **2007**, *2007*, 3497.
- (26) Mizuno, T.; Mihara, M.; Nakai, T.; Iwai, T.; Ito, T. *Synthesis* **2007**, *2007*, 3135.
- (27) Zhang, M.; Imm, S.; Bähn, S.; Neubert, L.; Neumann, H.; Beller,

M. *Angew. Chem. Int. Ed.* **2012**, *51*, 3905.

Chapter 5. Abnormal N–Heterocyclic Carbene Gold(I) Complexes: Synthesis, Structure, and Catalysis in Hydration of Alkynes*

5.1 Introduction

The use of N–heterocyclic carbene ligands (NHCs) in homogeneous catalysis has now become one of the most extensively studied fields in organometallic chemistry.¹ A breakthrough came when Arduengo isolated stable free carbenes derived from imidazolium salts.^{1f} It is considered that NHCs behave like tertiary phosphines in many aspects with stronger σ –donor properties.² The strong σ –donating ability of NHCs confers several advantages such as stronger binding, greater thermal stability and increased basicity.³ Although many examples show that NHC binds to the metal through C2, it has been shown that C4 and C5 of carbene can also be used for the binding, since the first discovery by Crabtree and co–workers.⁴ Carbenes of the latter type, so–called "abnormal" NHCs or mesoionic NHCs, are considered as even stronger σ –donors than traditional imidazolin–

* The majority of this work has been published: Xiangya Xu+, Seung Hyo Kim+, Xi Zhang, Atanu Das, Hajime Hirao, and Soon Hyeok Hong (+equal contribution) *Organometallics* **2013**, 32, 164–171

2-ylidenes, which may offer new opportunities in catalysis.^{4–5} Recently, Bertrand and co-workers have successfully crystallized a free mesoionic carbene and its Au(I) complex, thereby providing a detailed structural insight into these molecules.⁶ Our group has recently shown that abnormal NHCs could be more effective than traditional NHCs in the Pd-catalyzed Suzuki–Miyaura reactions.⁷

In the past decade, great progress has been made in developing efficient and selective Au-catalyzed transformations, as evidenced by a great number of articles and reviews available on the various aspects of this field.⁸ In particular, NHC–Au(I) complexes⁹ have emerged as highly efficient catalysts, leading to the realization of many transformations including cycloisomerization,¹⁰ alkene or allene activation,¹¹ and cross coupling reactions¹² with high yield and selectivity.^{9a} In continuation of our research on aNHC–Pd complexes,⁷ herein, we report the structurally characterized aNHC–Au(I) complexes and their catalytic activity in alkyne hydration.

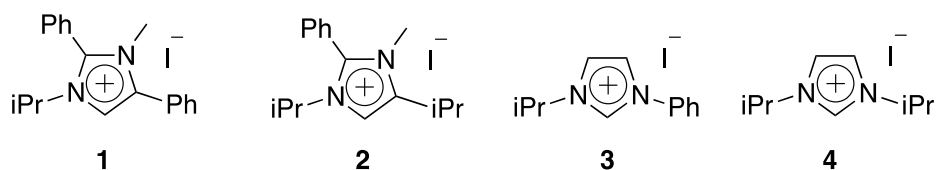


Figure 5.1 Imidazolium salts used as traditional and mesoionic NHC precursors.

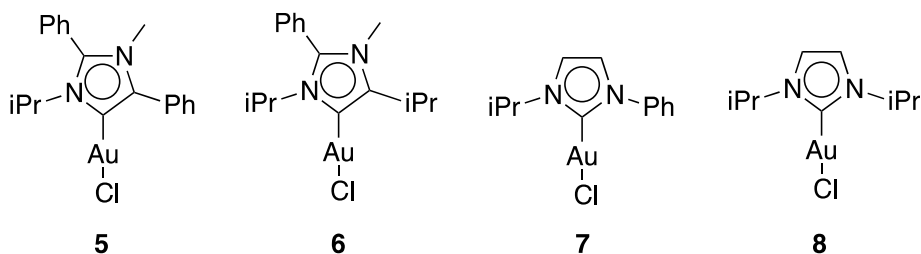


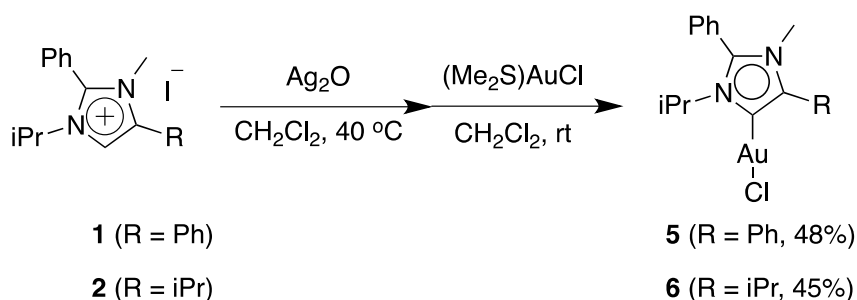
Figure 5.2 Traditional and mesoionic NHC – based Au complexes.

5.2 Results and Discussion

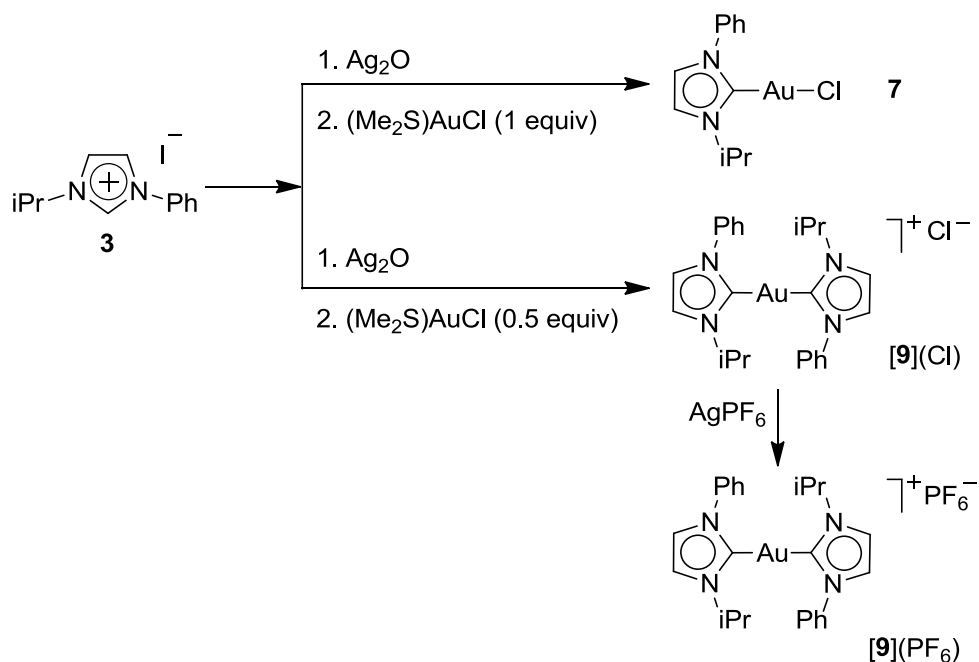
5.2.1 Synthesis of abnormal NHC based Au complexes

To investigate the difference in structure and catalytic activity between aNHC – and NHC – based Au complexes with similar steric hindrance, NHC precursors **1–4**, which would exert similar steric effect near the Au center, were chosen. A straightforward reaction between AuCl and free aNHC was initially attempted, as it should potentially be the most direct route to synthesize (aNHC)AuCl complexes. This route proved unsuccessful with poor yields and a problem of metallic gold production. A similar observation was reported in the attempted preparation of (I^tBu)Au(X) (I^tBu = 1,3-di-*tert*-butylimidazol-2-ylidene; X = BF₄, ClO₄).¹³ Therefore, we examined an alternative approach using transmetallation from silver where an equimolar amount of (SMe₂)AuCl is reacted with the respective in situ generated aNHC – Ag(I) salt. More specifically, **1** and **2** were reacted with Ag₂O in dichloromethane followed by

(Me₂S)AuCl, and subsequent recrystallization from dichloromethane/pentane solution yielded complexes **5** and **6** as off-white solids in 48% and 45% yields, respectively (Scheme 5.1). Hashmi and co-workers recently reported a [3+2] cycloaddition strategy using azomethane ylides and isonitrile gold (I) complexes to synthesize saturated aNHC–Au complexes.¹⁴ Complexes **5** and **6** were air stable both in solid state and in solution. The diastereotopic isopropyl methyl resonances observed in the ¹H NMR spectrum indicate hindered rotation about the gold–carbon bond. A similar synthetic procedure was applied to obtain complexes **7** and **8**.¹⁵ When 0.5 equiv of (Me₂S)AuCl instead of 1 equiv was used, a dicarbene–Au(I) complex [**9**] (PF₆) was obtained (Scheme 5.2).



Scheme 5.1 Synthesis of aNHC–Au complexes **5** and **6**.



Scheme 5.2 Synthesis of (NHC) – Au complexes **7** and **9**.

5.2.2 Structure analysis

The structures of complexes **5** – **9** were confirmed by X-ray crystallography (Figures 5.3, 5.4, 5.7). The bond lengths and angles of complexes **5**–**8** are given in Table 5.1. X-ray quality crystals of **5**–**9** were obtained by layering a dichloromethane solution with pentane. The crystal structure analyses confirmed that a carbene ligand binds to Au through C5 in both **5** and **6**. Each of the complexes possessed a (quasi-) linear two-coordinate geometry with $\text{C}_{\text{carbene}}\text{--Au--Cl}$ coordination. The $\text{Au--C}_{\text{carbene}}$ distances in the abnormal carbene complexes, **5** [2.002(6) Å] and **6** [2.020(8) Å], were slightly longer

than those in the normally bound Au–NHC complexes **7** [1.989(6) Å] and **8** [1.986(6) Å] (Table 5.1). These bond lengths indicate a single–bond character of the Au–C_{carbene} bonds. The slightly longer Au–C_{carbene} distance in **5** and **6** was contrary to our expectation based on the reported greater electron–donating ability of the same type of mesoionic carbenes.⁵ Hashmi also reported that Au–C_{carbene} bond lengths of saturated aNHC–gold complexes range between [1.957(6) Å] and [1.977(3) Å],¹⁴ which are shorter than the length [1.979(3)] in SIPr–Au–Cl.¹⁶ In addition, irregularity was observed in the Au–Cl distances of these carbene complexes. The Au–Cl distance [2.310(2) Å] in **5** was longer than that [2.301(2) Å] in **7**, but that [2.289(3) Å] in **6** was shorter than that [2.3124(12) Å] in **8**. It has been reported that bond distances would not be very sensitive to the small change in the bond order in NHC transition metal complexes.^{7a}

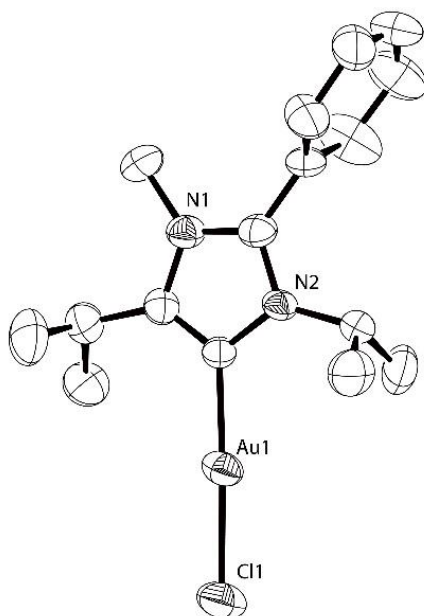
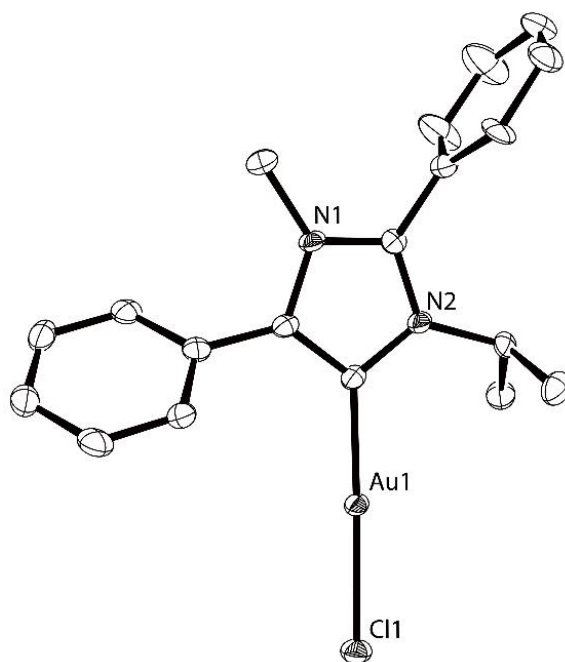


Figure 5.3 Molecular structure of complexes **5** and **6** showing 50% probability ellipsoids.

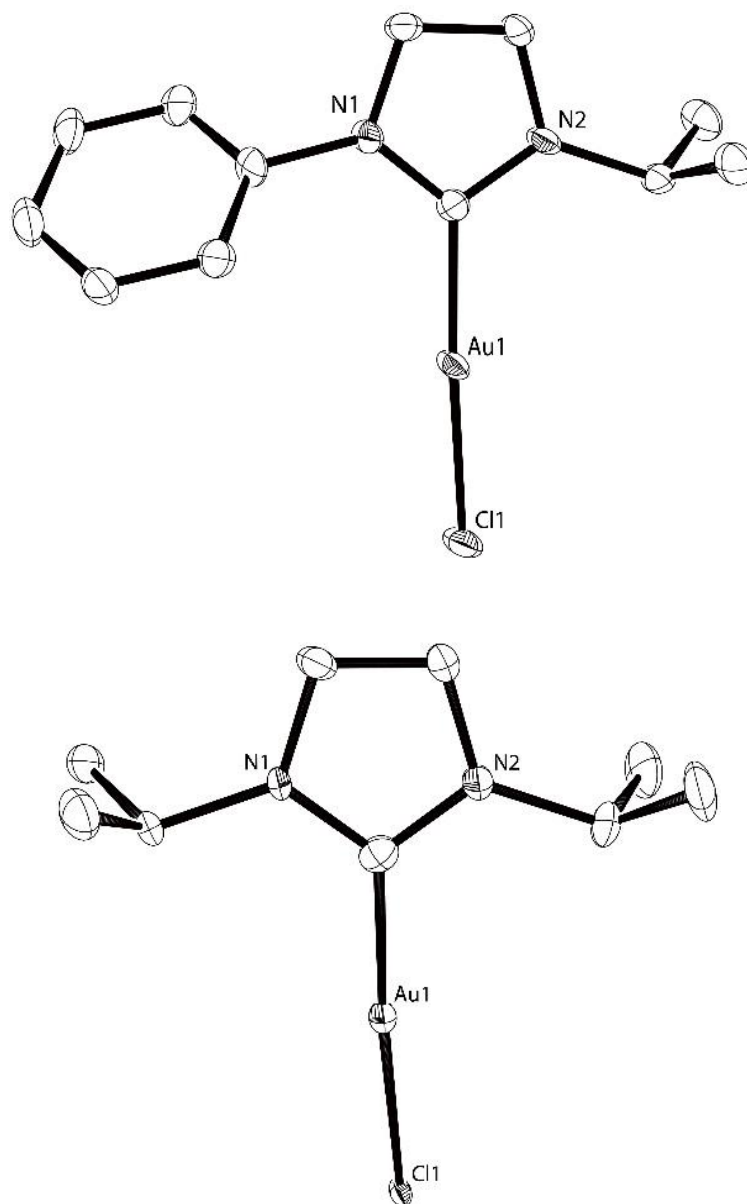
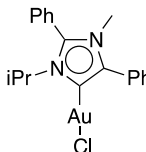
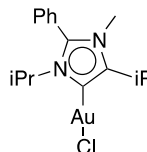
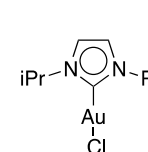
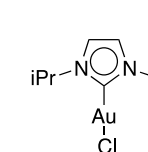
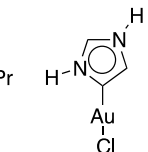
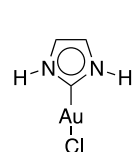


Figure 5.4 Molecular structure of complex 7 and 8 showing 50% probability ellipsoids.

5.1.3 Computational analysis[†]

Table 5.1 Summary of computationally and experimentally obtained values of selected bond lengths (Å) and bond angles (deg) for complexes **5–8**, **10**, and **11**.

	5		6		7		8		10		11
	meth od	5	6	7	8	10	11				
C _{carbene} – Au	DFT1	2.024	2.027	2.015	2.018	2.009	2.001				
	DFT2	2.010	2.013	1.999	2.002	1.994	1.985				
	Exp.	2.002 (6)	2.020 (8)	1.989 (8)	1.986 (6)	NA	NA				
Au–Cl	DFT1	2.338	2.339	2.322 1	2.322 4	2.326	2.315				
	DFT2	2.318	2.319	2.302 8	2.303 4	2.306	2.296				
	Exp.	2.310 (2)	2.289 (3)	2.301 7(19)	2.312 4(12)	NA	NA				
C _{carbene} – Au–Cl	DFT1	179.1	179.2	179.5	179.9	179.8	179.8				
	DFT2	179.0	179.2	179.5	179.7	180	179.8				
	Exp.	178.4 (2)	177.7 (3)	176.2 (2)	175.2 (2)	NA	NA				
Au– C _{carbene} – N2	DFT1	127.3	126.7	127.3	127.5	124.0	128.5				
	DFT2	127.1	126.4	127.2	127.3	124.1	128.3				
	Exp.	126.4 (5)	124.4 (7)	124.9 (6)	125.3 (5)	NA	NA				

[†] Computational analysis was mainly carried out in the Dr. Hajime Hirao group.

Density functional theory (DFT) calculations were performed to gain a deeper understanding of the structure and bonding in complexes **5–8**, as well as their unsubstituted analogs **10** (aNHC) and **11** (NHC). Two levels of DFT methods, i.e. DFT1 and DFT2, were employed (see the Experimental section for details). In Table 5.1, computationally obtained geometric parameters are shown alongside the respective experimental values. The experimentally observed longer Au-C_{carbene} distances in **5** and **6** than in **7** and **8** were reproduced by both DFT1 and DFT2 calculations. Overall, better agreement with the experimental values for **5–8** was obtained by the DFT2 method that employs a larger basis set.

Table 5.2 HOMO energy of free carbene, Mulliken atomic charge of C_{carbene} (q(C_{carbene})), and binding energy (BE) for **10** and **11**, as obtained with DFT1/DFT2.

entry	HOMO level [Eh] ^a	q(C _{carbene}) ^a	BE [kcal/mol] ^b
10	−0.168 / −0.194	−0.056 / −0.403	85.7 / 79.6
11	−0.199 / −0.223	0.101 / −0.198	79.4 / 74.5

^aValues for optimized free carbenes. ^bCalculating from the energies of a complex and isolated fragments.

Interestingly, the calculated Au-C_{carbene} distance in **10** was longer than that in **11** by both DFT methods, which is consistent with the geometric trend seen in **5–8**. This indicates that the fundamental nature of the Au-C_{carbene} bonding is determined by which carbon atom in carbene is used for the binding to Au and by the configuration of the carbene ring, rather than by the substituent effect. Therefore, further analysis was undertaken on the simplest carbene complexes **10** and **11**, to scrutinize the Au-C_{carbene} bonding in aNHCs and NHCs. Table 5.2 summarizes a few key theoretical quantities that are deemed relevant to the strength of the Au-C_{carbene} bond. The data clearly show that the energy level of HOMO (C_{carbene} lone-pair orbital) is higher in free **10** than in free **11**, suggesting that free aNHC has a greater electron-donating ability. Furthermore, C_{carbene} in **10** had a larger negative charge, which should permit larger electrostatic attraction to a slightly positive Au atom in AuCl. The HOMO levels and Mulliken charges therefore suggest that aNHC should bind more strongly to AuCl than NHC. Indeed, DFT calculated binding energy was larger for **10** than for **11** by 5–6 kcal/mol (Table 5.2). These results are in accord with a previous finding that aNHC has a higher electron-donating ability than NHC.^{4–5} However, our data apparently present an interesting yet puzzling relationship between the Au–

C_{carbene} distance and the binding energy, as aNHC, which has a longer Au- C_{carbene} distance, actually has a larger binding strength.

To gain additional insights into the somewhat counterintuitive trend of Au- C_{carbene} bonding, population analysis has been performed with the atomic-orbital (AO) basis and with the fragment molecular orbital (FO) basis. In the AO-based population analysis, we assessed how the electron population of each basis AO changes upon the formation of the Au(I)-aNHC or Au(I)-NHC complex. To simplify the interpretation, we used the same geometries of free carbene and AuCl as in the complex geometry for the analysis. In addition, the coordinate system was defined in such a way that the Au- C_{carbene} is aligned to the z axis and the y axis is perpendicular to the molecular plane (see Scheme 5.3a). As shown in Scheme 5.3b, for the interaction between carbene and AuCl, we can consider two-way orbital interactions, namely, (a) normal electron delocalization from the carbene lone-pair orbital to the s-type unoccupied molecular orbital (MO) of AuCl, and (b) back-donation from d_{yz} -type MO of AuCl to the π^* MO of carbene.¹⁷ As there are multiple p_z AOs placed on C_{carbene} , for example, in the 6-31G* basis set, p_z population was calculated by taking the sum of the populations of all p_z AOs. Electron delocalization of type (a) should result in a decrease in p_z population

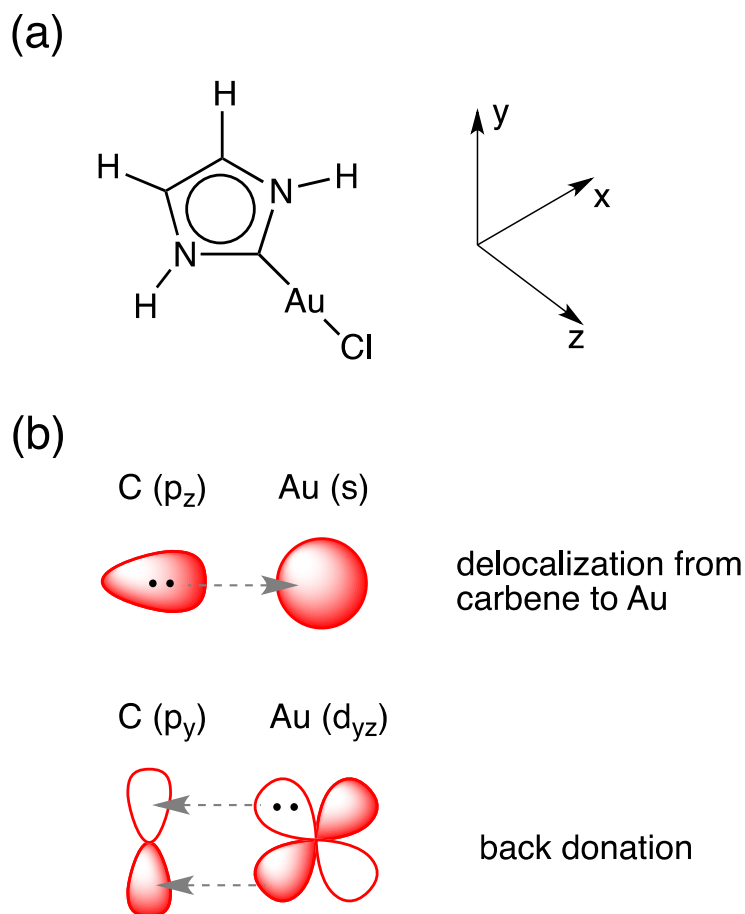
on C_{carbene} . This was indeed the case, as shown in Figure 5.5a, where we can see a decreased p_z population. Concomitantly, the s -AO population on Au increased in the Au(I) – carbene complexes. These results are consistent with the view that electrons are delocalized as described above (type (a)). Closer inspection reveals that the extent of this type of electron delocalization is larger in **10**, which is also consistent with the stronger Au(I) – carbene binding in **10**. In contrast, stronger back-donation in **11** can be seen from the larger decrease in Au d_{yz} population and the slightly larger increase in the C_{carbene} p_y population in **11**. From these results, we suggest that the shorter Au– C_{carbene} distances in NHCs is partly due to the stronger back-donation in these complexes.

A similar picture was obtained from the FO-based population analysis (Figure 5.5b). In this population analysis, MOs of the carbene – AuCl complexes were expanded by the MOs (FOs) of the carbene and AuCl fragments. Changes in electron population in each FO upon the complex formation were analyzed. The decrease in the lone-pair MO of carbene and the increase in the AuCl s -type MO population were larger in **10**. In contrast, the decrease in the Au d_{yz} -type MO population and the increase in carbene π^* MO population were larger in **11**, indicative of a larger degree of back-donation in

NHC complexes. More efficient back – donation in **11** is attributed to the fact that the π^* MO is more stable in **11**.

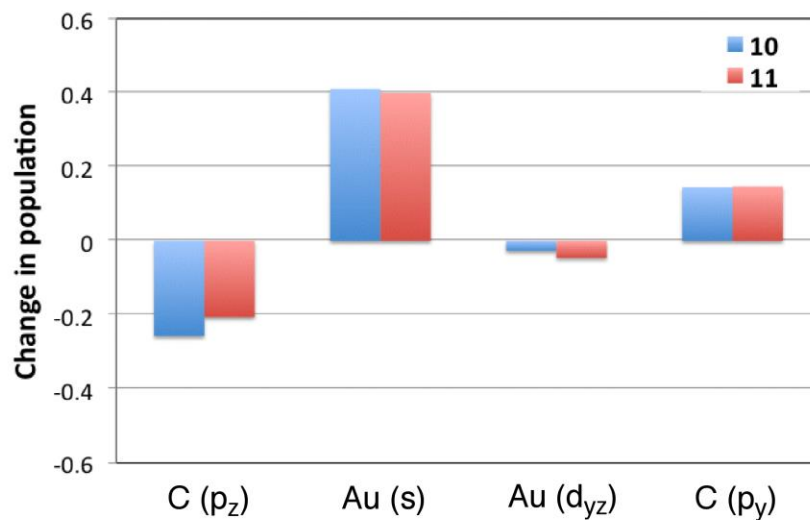
Additional energy decomposition analysis by the reduced variational space (RVS) method verified that electron delocalization (or charge transfer) from carbene to AuCl is greater in **10**, while the back – donation is stronger in **11**. As one can surmise from the larger negative charge on C_{carbene} in **10**, the electrostatic attraction was larger in **10**, and the electrostatic effect was the major reason **10** has a larger binding energy. Despite the larger electrostatic attraction in **10**, however, the higher electron density on C_{carbene} in **10** may cause a stronger repulsion against the electrons in the d_{z2} – type MO of AuCl. In fact, the exchange repulsion was larger in **10**, which seems to be another reason aNHC complexes have longer Au – C_{carbene} distances. To further evaluate the exchange effect, we slightly moved the AuCl moiety in **10** toward carbene along the z axis until the Au – Cl distance became 2.001 Å. The Au – C_{carbene} distance in the resultant structure (**10'**) is the same as that in **11**. The shortening of the Au – C_{carbene} distance resulted in an increase in electrostatic interaction energy by 2.1 kcal/mol but an increase in exchange repulsion by 4.1 kcal/mol. Thus, a shorter Au – C_{carbene} distance does not give a net gain of stabilization to the system. Instead, complex **10** prefers a slightly

longer Au–C_{carbene} distance in order to mitigate the exchange repulsion that is brought by the high electron density on C_{carbene}. As the electrostatic energy is a long–range interaction and decays slowly, a slight increase in the Au–C_{carbene} distance in **10** does not cause a significant loss of attractive electrostatic effect.



Scheme 5.3 (a) Coordinate system for population analysis, and (b) schematic illustration of orbital interactions between carbene and AuCl.

(a) AO basis



(b) FO basis

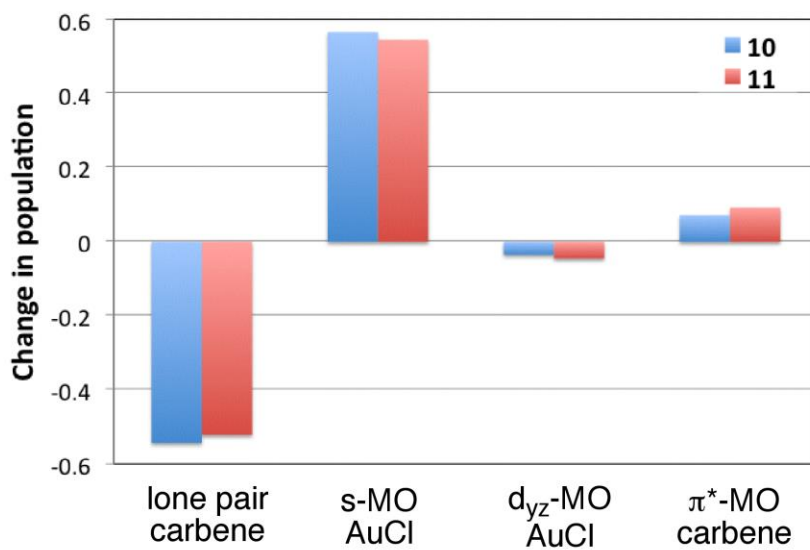


Figure 5.5 Population analyses (a) with the AO basis and (b) with the FO basis. DFT1 data are presented.

5.2.4 Hydration of alkyne

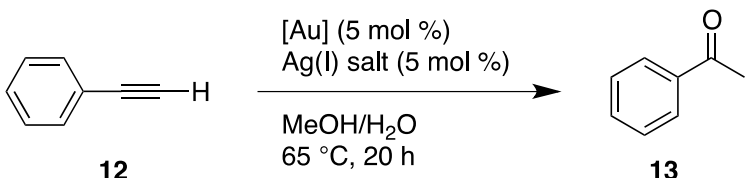
α NHC–Au complexes **5** and **6**, and NHC–Au complexes **7** and **8** contain two different types of *N*-heterocyclic carbenes with a similar topological framework but with a different electron–donating ability. To investigate the activity difference between the (NHC)AuCl complexes, we have chosen a well–known gold–catalyzed reaction, hydration of alkyne, as a benchmark reaction for the assessment of catalytic activity.¹⁸ The alkyne hydration reaction has long been known, dating back to 1881,¹⁹ and more recent interest lies in the use of transition–metal–based catalytic systems,²⁰ of which gold complexes have outperformed other complexes such as toxic mercury(II) salts. Utimoto was a pioneer in this field, who applied gold salts and complexes as a catalyst for the hydration of alkynes in 1991.²¹ In 1998, Teles experimentally discovered a significant fact that electron–poor ligands lead to an increase in activity.²² Hayashi and Tanaka reported the use of a [(Ph₃P)AuMe]/H⁺ catalytic system which showed a high turnover frequency (TOF) in the hydration of alkynes.^{18b} More recently, Nolan reported a highly active catalytic system for alkyne hydration, using (NHC)AuCl/AgSbF₆ as a catalyst. Although NHCs are stronger σ -donors than phosphines, NHC–Au complexes displayed high efficiency even at part–per–million

catalyst loadings, at variance with the discovery by Teles that of the hydration of alkynes is facilitated by electron poor ligands.^{18a,22} These results indicate that protodeauration or/and catalyst stability as well as electronic activation of alkyne is/are also important in the gold (I) catalyzed hydration of alkyne reaction as Xu and co-workers reported the studies on ligand effects in homogeneous gold (I) catalysis.²³ Inspired by the fact that N-heterocyclic carbene gold complexes have been remarkably successful in catalyzing the hydration of alkynes, we conducted a comparative study of the hydration activity between normal and abnormal carbene-based Au complexes.

Hydration of phenylacetylene using the catalytic system (NHC) AuCl/Ag-salt in MeOH was chosen as a model reaction. The results obtained for different catalysts, water/alkyne ratio and different Ag(I)-salt are shown in Table 5.3. The equimolar combination of **5**/AgSbF₆ (5 mol %) in MeOH was found to be the most effective combination resulting in 91% yield. Nolan also reported that AgSbF₆ was the most effective silver salt in the (NHC) AuCl catalyzed hydration of alkynes.^{18a} Substitution by isopropyl at the C4 position of aNHC complex resulted in decreased activity of **6** compared to that of **5**. Addition of more water decreased

the yield when AgSbF₆ salt was used (Table 5.3). Compared with **7** and **8**, their sterically similar aNHC-based counterparts **5** and **6** showed decreased activities in the hydration of phenyl acetylene (Table 5.4), demonstrating that aNHCs do not promote the reaction better than traditional NHCs. Furthermore, we investigated the reaction rates in the two different catalytic systems to make detailed comparisons of their catalytic activity (Figure 5.6). Traditional NHC–Au–Cl complexes enhanced the reaction rate to a larger extent than their aNHC analogs did. The catalytic reactions using **7** and **8** were completed in 300 and 100 min, respectively, both of which gave the product in 100% yield, whereas the reactions using **5** and **6** gave the product in 91% and 77% yield, respectively.

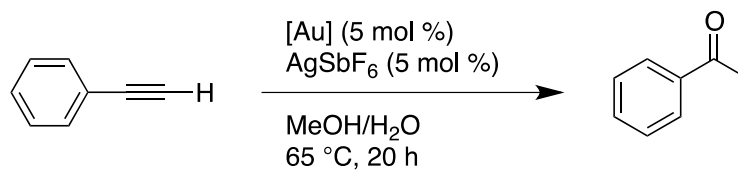
Table 5.3 Hydration of phenylacetylene with different Ag (I) –salt using (aNHC) AuCl.

				
GC–yield ^a				
entry	Ag–salt	H ₂ O (eqv)	5	6
1	AgSbF ₆	4	91	77
2	AgSbF ₆	8	69	70
3	AgOTf	4	63	80

4	AgOTf	8	71	82
5	AgPF ₆	4	48	43
6	Ag(CF ₃ COO)	4	62	54

^a GC yields are average of at least two runs using dodecane as an internal standard.

Table 5.4 Hydration of phenylacetylene.



entry	[Au]	^a GC yield (%)
1	5	91
2	6	77
3	7	100
4	8	100

^a GC yields are average of at least two runs using dodecane as an internal standard.

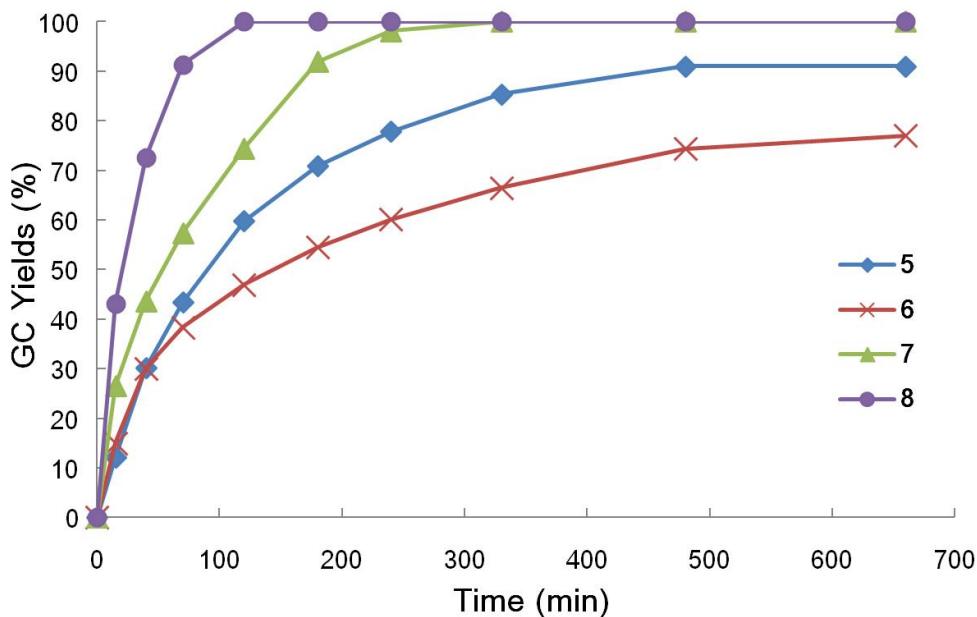


Figure 5.6 Comparison of reaction progress with complex 5–8 using GC

5.3 Conclusion

We have prepared two new air stable (aNHC) AuCl complexes by the transmetallation from the corresponding silver–carbene performed complexes. Contrary to our expectation, the X–ray analysis and DFT calculations confirmed slightly longer Au–C_{carbene} bond lengths in aNHC–Au complexes than in traditionally bound NHC–Au complexes. Curiously, however, DFT calculations showed that the former complexes have stronger Au–C_{carbene} bonds than the latter complexes. Additional theoretical analyses suggested that the longer Au–C_{carbene} distances in aNHC–Au complexes is due to the less efficient back–donation of electrons from AuCl to carbene and the larger exchange

repulsion between them. The stronger Au-C_{carbene} bonding in the aNHC-Au complexes was attributed to the higher electron-donating ability of the carbene lone-pair orbital and the larger electrostatic attraction between carbene and AuCl that originates from the larger electron density on C_{carbene}. Abnormal gold complexes **5** and **6** showed worse activities in the hydration of alkynes than their normal analogs **7** and **8**. This work hence lays a foundation for further studies on the structure and prominent catalytic activity of gold-carbene complexes.

5.4 Experimental Section

5.4.1 General information

All reactions were carried out in oven-dried glassware under an inert atmosphere of dry argon or nitrogen. Phenylacetylene, AuCl and SMe₂ were obtained from Alfa Aesar, Strem and Acros respectively and used as received. [(Me₂S)AuCl],²⁴ imidazolium salts,⁵ gold complex **7** and **8**¹⁵ were prepared according to the reported procedure. Anhydrous methanol was purchased from Sigma-Aldrich and used as received. Dichloromethane, pentane and toluene were dried over Pure Solv solvent purification system. Analytical TLC was performed on a Merck 60 F254 silica gel plate (0.25mm thickness). Column

chromatography was performed on Merck 60 silica gel (230–400 mesh). NMR spectra were recorded on a JEOL ECA400 (^1H -NMR at 400MHz; ^{13}C -NMR at 100 MHz) spectrometer. Tetramethysilane was used as reference, and the chemical shifts were reported in ppm and the coupling constant in Hz. GC yields were obtained on an Agilent 7890A instrument equipped with a HP-5 column. Mass spectrometry was performed by Waters Q-ToF Premier Micromass instrument, using Electro Spray Ionization (ESI) mode.

5.4.2 Synthetic method of abnormal NHC based Au complexes

Synthesis of (1-Isopropyl-3-methyl-2,4-diphenylimidazolin) gold chloride (I) (5)

A mixture of 1-isopropyl-3-methyl-2,4-diphenylimidazolium iodide (100 mg, 0.25 mmol), silver(I) oxide (34.7 mg, 0.15 mmol) and MS4A^o in dichloromethane (18 mL) was stirred for 12 h under an argon atmosphere at 40 °C in dark. The mixture was filtered through Celite and (dimethylsulphide)gold(I) chloride (70.7 mg, 0.24 mmol) was added. The resulting mixture was stirred for 6 h at room temperature and filtered through Celite. The solvent was removed in vacuo, and then dichloromethane (5 mL) was added. Pentane (10 mL) was added to the solution, resulting in an immediate precipitation of

a bright white solid. The solid was further washed with pentane (3 × 5 mL) and recrystallized from dichloromethane/pentane (1:3) to obtain analytically pure compound. Crystals Suitable for X-ray analysis studies were grown by diffusion of concentrated solution of complex **5** layered with pentane. Yield: 63.5 mg 48%. ¹H NMR (400 MHz, CD₂Cl₂): δ 7.66 (m, 5H, CH_{arom}), 7.55 (m, 5H, CH_{arom}), 4.52 (sept, ³J_{H-H} = 6.8 Hz, 1H, CH_{iPr}), 2.94 (s, 3H, NCH₃), 1.75 (d, ³J_{H-H} = 6.8, 6H, CH_{3-iPr}). ¹³C NMR (400 MHz, CD₂Cl₂): δ 144.7, 136.8, 133.2, 131.1, 130.9, 130.5, 130.4, 129.7, 126.1, 122.2, 116.8 (C_{arom}), 53.7 (CH_{iPr}), 35.0 (NCH₃), 23.4 (CH_{3-iPr}). Anal Calcd for C₁₉H₂₀AuClN₂•0.5(CH₂Cl₂) (550.08): C, 42.49; H, 03.84; N, 5.08. Found: C, 42.84; H, 2.44; N, 5.24.

Synthesis of (1,4-Diisopropyl-3-methyl-2-phenylimidazolin) gold chloride (I) (**6**)

A mixture of 1,4-diisopropyl-3-methyl-2-phenylimidazolium iodide (100 mg, 0.27 mmol), silver(I) oxide (36.9 mg, 0.16 mmol) and MS4A° in dichloromethane (18 mL) was stirred for 12 h under an argon atmosphere at 40 °C in dark. The mixture was filtered through Celite and (dimethylsulphide)gold(I) chloride (73.6 mg, 0.25 mmol) was added. The resulting mixture was stirred for 6 h and filtered

through Celite. The solvent was removed in vacuo, and then dichloromethane (5 mL) was added. Pentane (10 mL) was added to the solution, resulting in an immediate precipitation of a bright white solid. The solid was further washed with pentane (3 × 5 mL) and recrystallized from dichloromethane/pentane (1:3) to obtain analytically pure compound. Crystals Suitable for X-ray analysis studies were grown by diffusion of concentrated solution of complex **6** layered with pentane. Yield: 53.5 mg 45%. ¹H NMR (400 MHz, CD₂Cl₂): δ 7.69 (m, 5H, CH_{arom}), 4.32 (sept, ³J_{H-H} = 6.8 Hz, 1H, CH_{iPr}), 3.25 (s, 3H, NCH₃), 3.18 (sept, ³J_{H-H} = 6.8 Hz, 1H, CH_{iPr}), 1.50 (d, ³J_{H-H} = 6.8, 6H, CH_{3-iPr}), 1.38 (d, ³J_{H-H} = 6.8 Hz, 6H, CH_{3-iPr}). ¹³C NMR (400 MHz, CD₂Cl₂): δ 143.5, 142.3, 132.9, 130.4, 130.1, 121.5, 114.1 (C_{arom}), 51.7 (CH_{iPr}), 33.2 (NCH₃), 24.8, 22.8, 21.5 (CH_{3-iPr}). Anal Calcd for C₁₆H₂₂AuClN₂ (474.11): C, 40.48; H, 04.67; N, 5.90. Found: C, 40.92; H, 03.92; N, 05.12.

Synthesis of (3-Isopropyl-1-phenylimidazolin-2-ylidene) gold chloride (I) (**7**)

A mixture of 1-phenyl-3-isopropylimidazolium iodide (100 mg, 0.32 mmol), silver(I) oxide (44.5 mg, 0.19 mmol) and MS4A^o in dichloromethane (18 mL) was stirred for 12 h under an argon

atmosphere at room temperature in dark. The mixture was filtered through celite and (dimethylsulphide) gold(I) chloride (94.2 mg, 0.32 mmol) was added. The resulting mixture was stirred for 3h and filtered through celite. The solvent was removed in vacuo and then dichloromethane (5 mL) was added. Pentane (10 mL) was added to the solution, resulting in an immediate precipitation of a bright white solid. The solid was further washed with pentane (3 × 5 mL) and recrystallized from dichloromethane/pentane (1 : 3) to obtain analytically pure compound. Crystals Suitable for X-ray analysis studies were grown by slow diffusion of concentrated solution of complex **7** layered with pentane. Yield: 85.3 mg 64%. ^1H NMR (CD_2Cl_2): δ 7.64–7.47 (m, 5H, CH_{arom}), 7.22–7.17 (m, 2H, $\text{CH}_{\text{imidazole}}$), 5.16 (sept, $^3J_{\text{H-H}} = 6.8$ Hz, 1H, CH_{IPr}), 2.09, 1.53 (d, $^3J_{\text{H-H}} = 6.8$, 6H, $\text{CH}_3\text{-IPr}$). ^{13}C NMR (CD_2Cl_2): δ 169.2, 129.6, 129.0, 125.0, 122.1, 117.2 (C_{arom}), 30.6 (CH_{IPr}), 23.1 ($\text{CH}_3\text{-IPr}$). HRMS (ESI) calcd for $\text{C}_{12}\text{H}_{15}\text{AuClN}_2$: 419.0589. Found: 419.0594 [MH^+].

Synthesis of (1, 3-diisopropylimidazolin-2-ylidene)gold chloride (I) (8)

A mixture of 1, 3-diisopropylimidazolium iodide (100 mg, 0.36 mmol) and silver(I) oxide (49.2 mg, 0.21 mmol) in dichloromethane (18 mL) was stirred for 12 h under an argon atmosphere at room temperature in dark. The mixture was filtered through celite and (dimethylsulphide) gold(I) chloride (105.9 mg, 0.36 mmol) was added. The resulting mixture was stirred for 3 h and filtered through celite. The solvent was removed in vacuum, and then dichloromethane (5 mL) was added. Pentane (15 mL) was added to the solution. The resulting white crystalline solid was collected, washed with pentane (3 × 5 mL) and recrystallized from dichloromethane/pentane (1 : 3) to yield **8**. Crystals Suitable for X-ray analysis studies were grown by slow diffusion of concentrated solution of complex **8** layered with pentane. Yield: 57.5 mg 42%. ^1H NMR (CD_2Cl_2): δ 6.99 (s, 2H, $\text{CH}_{\text{imidazole}}$), 4.98 (sept, $^3J_{\text{H-H}} = 6.8$ Hz, 2H, CH_{Pr}), 1.48 (d, $^3J_{\text{H-H}} = 6.8$, 6H, $\text{CH}_{3-\text{Pr}}$).

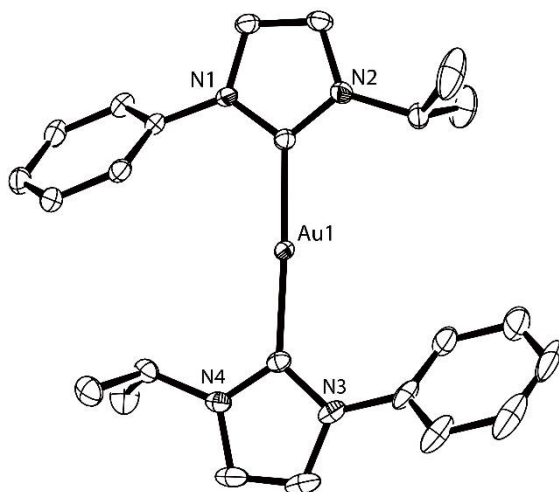


Figure 5.7 Molecular structure of complex **9** showing 50% probability ellipsoids. Selected bond lengths (Å) and bond angles (deg): Au1–C_{carbene} : 2.023(2), Au1–C13 : 2.018(2).

5.4.3 Computational investigation of the nature of the Au–C bond

All DFT calculations were done using the Gaussian 09 program.²⁵ Two levels of DFT methods, i.e. DFT1 and DFT2, were employed. DFT1 is a combination of the B3LYP DFT functional²⁶ and the SDD effective-core potential (ECP) basis set for Au and the 6–31G* basis set for the other atoms.²⁷ DFT2 is a combination of B3LYP and the LANL2TZ(f) ECP basis set for Au and the 6–311+G(2d,p) basis set for the other atoms.²⁸ Fragment orbital analysis was performed on **10** and **11** by using MATLAB software.²⁹ Energy decomposition

analysis using the RVS scheme, which is an extension of the Kitaura–Morokuma scheme, was performed with the [SDD(Au),6–31G(6d) (others)] basis set using GAMESS.³⁰ The use of a somewhat smaller basis set was necessary to obtain numerically convergent results.

5.5 Reference

- (1) (a) Arduengo, A. J.; Bertrand, G. *Chem. Rev.* **2009**, *109*, 3209.
(b) de Frémont, P.; Marion, N.; Nolan, S. P. *Coord. Chem. Rev.* **2009**, *253*, 862. (c) Hahn, F. E.; Jahnke, M. C. *Angew. Chem. Int. Ed.* **2008**, *47*, 3122. (d) *N-Heterocyclic Carbenes in Synthesis*; Nolan, S. P., Ed.; Wiley–VCH: Weinheim, Germany, 2006. (e) Crabtree, R. H. *Coord. Chem. Rev.* **2007**, *251*, 595. (f) Arduengo, A. J.; Harlow, R. L.; Kline, M. *J. Am. Chem. Soc.* **1991**, *113*, 361.
- (2) Díez–González, S.; Nolan, S. P. *Coord. Chem. Rev.* **2007**, *251*, 874.
- (3) (a) Dorta, R.; Stevens, E. D.; Hoff, C. D.; Nolan, S. P. *J. Am. Chem. Soc.* **2003**, *125*, 10490. (b) Huang, J. K.; Schanz, H. J.; Stevens, E. D.; Nolan, S. P. *Organometallics* **1999**, *18*, 5375.
- (4) (a) Gründemann, S.; Kovacevic, A.; Albrecht, M.; Faller, J. W.;

Crabtree, R. H. *Chem. Commun.* **2001**, 2274. (b) Schuster, O.; Yang, L. R.; Raubenheimer, H. G.; Albrecht, M. *Chem. Rev.* **2009**, *109*, 3445.

(c) Albrecht, M. *Chem. Commun.* **2008**, 3601. (d) Arnold, P. L.; Pearson, S. *Coord. Chem. Rev.* **2007**, *251*, 596. (e) Crabtree, R. H. *Pure Appl. Chem.* **2003**, *75*, 435.

(5) Chianese, A. R.; Kovacevic, A.; Zeglis, B. M.; Faller, J. W.; Crabtree, R. H. *Organometallics* **2004**, *23*, 2461.

(6) Aldeco–Perez, E.; Rosenthal, A. J.; Donnadieu, B.; Parameswaran, P.; Frenking, G.; Bertrand, G. *Science* **2009**, *326*, 556.

(7) (a) Xu, X.; Xu, B.; Li, Y.; Hong, S. H. *Organometallics* **2010**, *29*, 6343. (b) Huang, J.; Hong, J.–T.; Hong, S. H. *Eur. J. Org. Chem.* **2012**, DOI: 10.1002/ejoc.201201075.

(8) (a) Hashmi, A. S. K. *Angew. Chem. Int. Ed.* **2005**, *44*, 6990. (b) Hashmi, A. S. K. *Chem. Rev.* **2007**, *107*, 3180. (c) Hashmi, A. S. K.; Hutchings, G. J. *Angew. Chem. Int. Ed.* **2006**, *45*, 7896. (d) Hashmi, A. S. K.; Rudolph, M. *Chem. Soc. Rev.* **2008**, *37*, 1766. (e) Hoffmann–Roder, A.; Krause, N. *Org. Biomol. Chem.* **2005**, *3*, 387. (f) Dyker, G. *Angew. Chem. Int. Ed.* **2000**, *39*, 4237. (g) Arcadi, A. *Chem. Rev.* **2008**, *108*, 3266. (h) Gorin, D. J.; Sherry, B. D.; Toste, F. D. *Chem. Rev.* **2008**, *108*, 3351. (i) Li, Z. G.; Brouwer, C.; He, C. *Chem. Rev.* **2008**, *108*, 3239.

- (9) (a) Marion, N.; Nolan, S. P. *Chem. Soc. Rev.* **2008**, *37*, 1776. (b) Raubenheimer, H. G.; Cronje, S. *Chem. Soc. Rev.* **2008**, *37*, 1998. (c) Lin, I. J. B.; Vasam, C. S. *Can. J. Chem. – Rev. Can. Chim.* **2005**, *83*, 812. (d) Lin, J. C. Y.; Huang, R. T. W.; Lee, C. S.; Bhattacharyya, A.; Hwang, W. S.; Lin, I. J. B. *Chem. Rev.* **2009**, *109*, 3561.
- (10) (a) Kim, S. M.; Park, J. H.; Kang, Y. K.; Chung, Y. K. *Angew. Chem. Int. Ed.* **2009**, *48*, 4532. (b) Kim, S. M.; Park, J. H.; Choi, S. Y.; Chung, Y. K. *Angew. Chem. Int. Ed.* **2007**, *46*, 6172. (c) Jimenez–Nunez, E.; Raducan, M.; Lauterbach, T.; Molawi, K.; Solorio, C. R.; Echavarren, A. M. *Angew. Chem. Int. Ed.* **2009**, *48*, 6152. (d) Witham, C. A.; Mauleon, P.; Shapiro, N. D.; Sherry, B. D.; Toste, F. D. *J. Am. Chem. Soc.* **2007**, *129*, 5838.
- (11) (a) Corma, A.; Gutiérrez–Puebla, E.; Iglesias, M.; Monge, A.; Pérez–Ferreras, S.; Sánchez, F. *Adv. Synth. Catal.* **2006**, *348*, 1899. (b) Corberán, R.; Ramirez, J.; Poyatos, M.; Peris, E.; Fernández, E. *Tetrahedron: Asymmetry* **2006**, *17*, 1759. (c) Bender, C. F.; Widenhoefer, R. A. *Chem. Commun.* **2008**, 2741. (d) Marion, N.; Gealageas, R.; Nolan, S. P. *Org. Lett.* **2007**, *9*, 2653. (e) Shi, Y.; Roth, K. E.; Ramgren, S. D.; Blum, S. A. *J. Am. Chem. Soc.* **2009**, *131*, 18022.

- (12) (a) Lavallo, V.; Frey, G. D.; Kousar, S.; Donnadieu, B.; Bertrand, G. *Proc. Natl. Acad. Sci. U. S. A.* **2007**, *104*, 13569. (b) Corma, A.; González–Arellano, C.; Iglesias, M.; Pérez–Ferreras, S.; Sánchez, F. *Synlett* **2007**, 1771. (c) Hashmi, A. S. K.; Lothschutz, C.; Dopp, R.; Rudolph, M.; Ramamurthi, T. D.; Rominger, F. *Angew. Chem. Int. Ed.* **2009**, *48*, 8243.
- (13) Barnard, P. J.; Baker, M. V.; Berners–Price, S. J.; Skelton, B. W.; White, A. H. *Dalton Trans.* **2004**, 1038.
- (14) Hashmi, A. S.; Riedel, D.; Rudolph, M.; Rominger, F.; Oeser, T. *Chem. Eur. J.* **2012**, *18*, 3827.
- (15) Baker, M. V.; Barnard, P. J.; Berners–Price, S. J.; Brayshaw, S. K.; Hickey, J. L.; Skelton, B. W.; White, A. H. *J. Organomet. Chem.* **2005**, *690*, 5625.
- (16) de Fremont, P.; Scott, N. M.; Stevens, E. D.; Nolan, S. P. *Organometallics* **2005**, *24*, 2411.
- (17) Benitez, D.; Shapiro, N. D.; Tkatchouk, E.; Wang, Y. M.; Goddard, W. A.; Toste, F. D. *Nat. Chem.* **2009**, *1*, 482.
- (18) (a) Marion, N.; Ramon, R. S.; Nolan, S. P. *J. Am. Chem. Soc.* **2009**, *131*, 448. (b) Mizushima, E.; Sato, K.; Hayashi, T.; Tanaka, M. *Angew. Chem. Int. Ed.* **2002**, *41*, 4563.
- (19) Kucherov, M. *Chem. Ber.* **1881**, *14*, 1540.

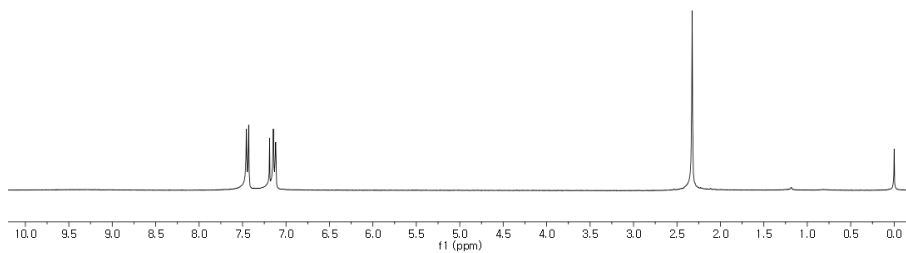
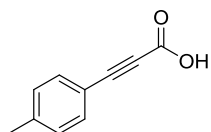
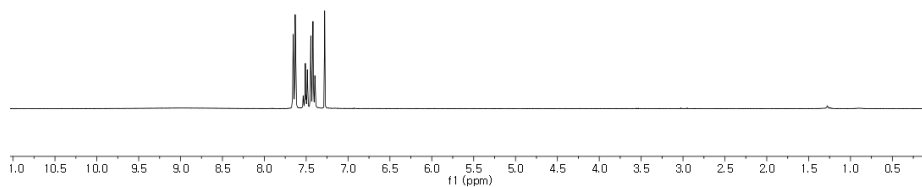
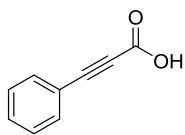
- (20) Hintermann, L.; Labonne, A. *Synthesis* **2007**, 1121.
- (21) Fukuda, Y.; Utimoto, K. *J. Org. Chem.* **1991**, *56*, 3729.
- (22) Teles, J. H.; Brode, S.; Chabanas, M. *Angew. Chem. Int. Ed.* **1998**, *37*, 1415.
- (23) Wang, W.; Hammond, G. B.; Xu, B. *J. Am. Chem. Soc.* **2012**, *134*, 5697.
- (24) Dash, K. C.; Schmidba.H *Chem. Ber.* **1973**, *106*, 1221.
- (25) Frisch, M. J.; Trucks, G. W.; Schlegel, H. B.; Scuseria, G. E.; Robb, M. A.; Cheeseman, J. R.; Scalmani, G.; Barone, V.; Mennucci, B.; Petersson, G. A., et al. Gaussian 09, revision B.01; Gaussian, Inc.: Wallingford, CT, 2010.
- (26) (a) Becke, A. D. *J. Chem. Phys.* **1993**, *98*, 5648. (b) Lee, C. T.; Yang, W. T.; Parr, R. G. *Phys. Rev. B* **1988**, *37*, 785. (c) Vosko, S. H.; Wilk, L.; Nusair, M. *Can. J. Phys.* **1980**, *58*, 1200.
- (27) (a) Dolg, M.; Wedig, U.; Stoll, H.; Preuss, H. *J. Chem. Phys.* **1987**, *86*, 866. (b) Hehre, W. R., L.; Schleyer, P. v. R.; Pople, J. Ed. *Ab Initio Molecular Orbital Theory*; John Wiley & Sons: New York, 1986.
- (28) Roy, L. E.; Hay, P. J.; Martin, R. L. *J. Chem. Theory Comput.* **2008**, *4*, 1029.
- (29) MATLAB, version R2011b; The MathWorks Inc.: Natick, MA,

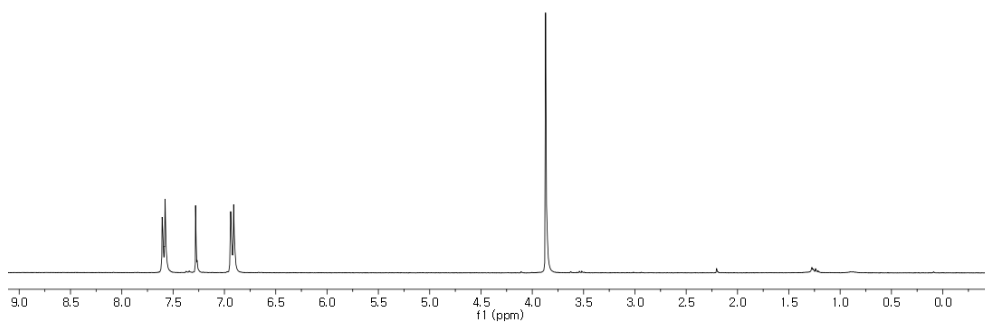
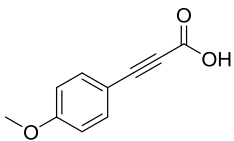
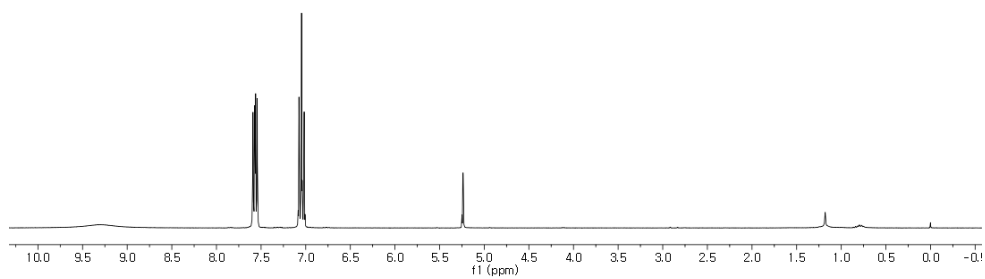
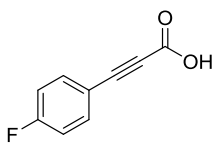
September 1, 2011.

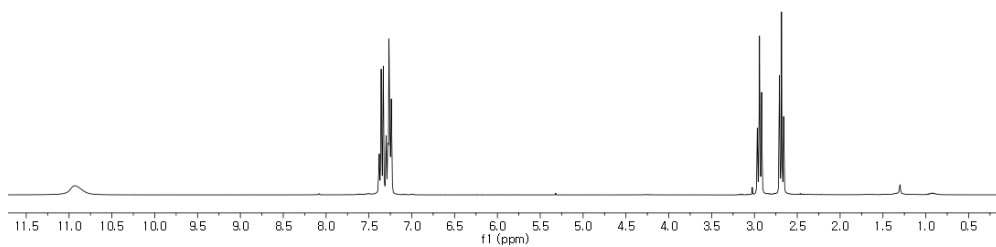
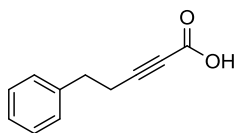
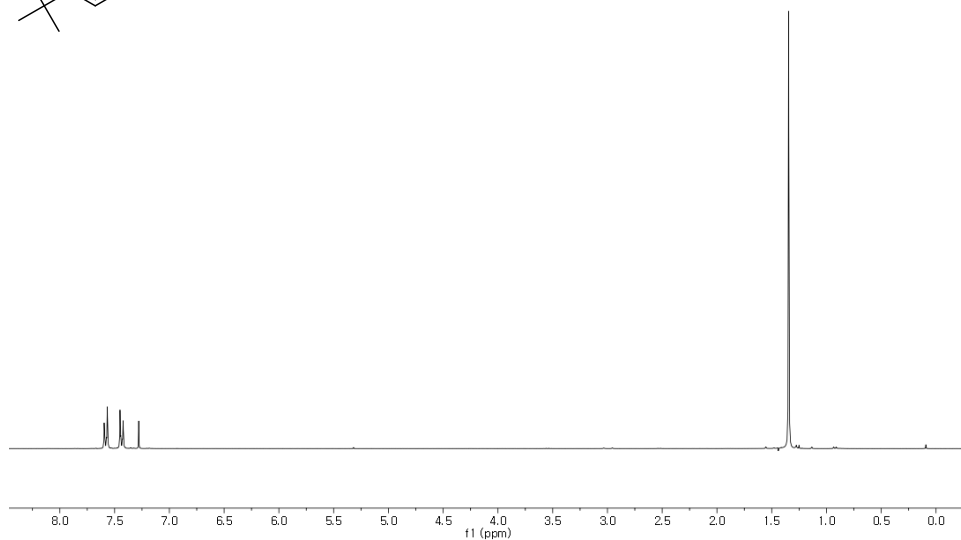
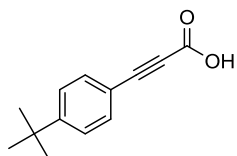
- (30) (a) Stevens, W. J.; Fink, W. H. *Chem. Phys. Lett.* **1987**, *139*, 15.
- (b) Kitaura, K.; Morokuma, K. *Int. J. Quantum Chem.* **1976**, *10*, 325.
- (c) Schmidt, M. W.; Baldridge, K. K.; Boatz, J. A.; Elbert, S. T.; Gordon, M. S.; Jensen, J. H.; Koseki, S.; Matsunaga, N.; Nguyen, K. A.; Su, S. J.; Windus, T. L.; Dupuis, M.; Montgomery, J. A. *J. Comput. Chem.* **1993**, *14*, 1347.

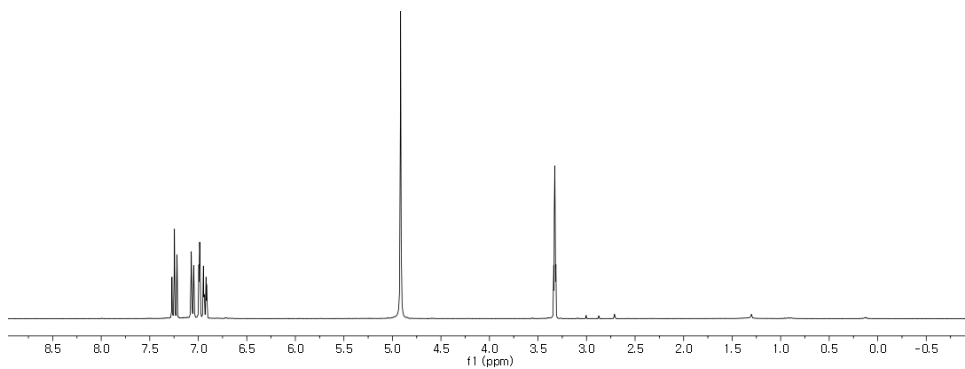
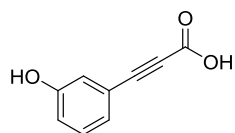
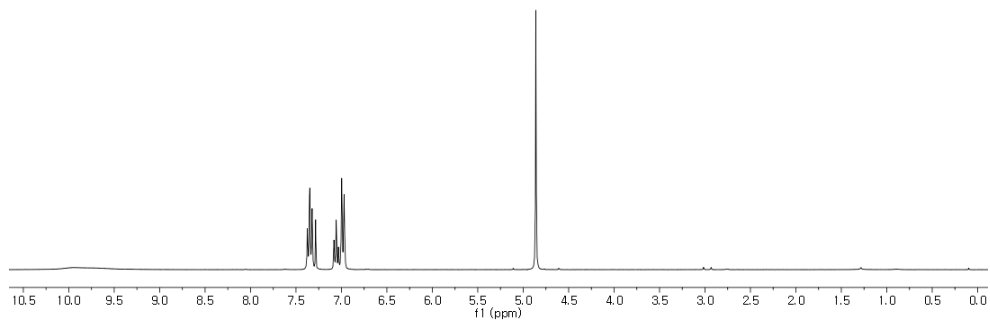
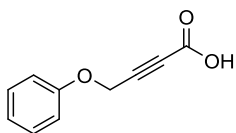
Appendix – NMR Spectra

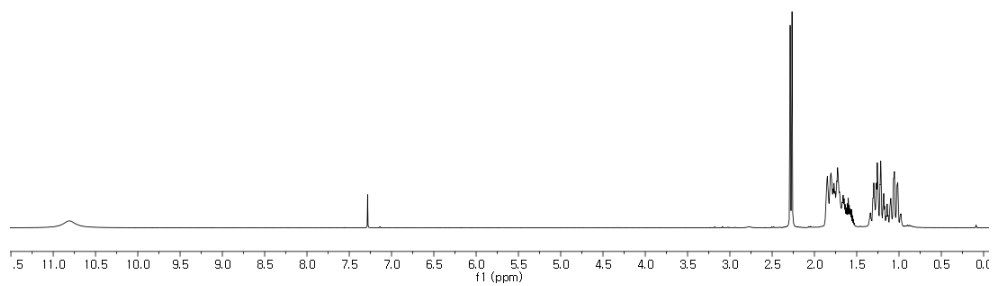
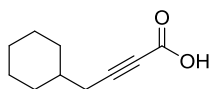
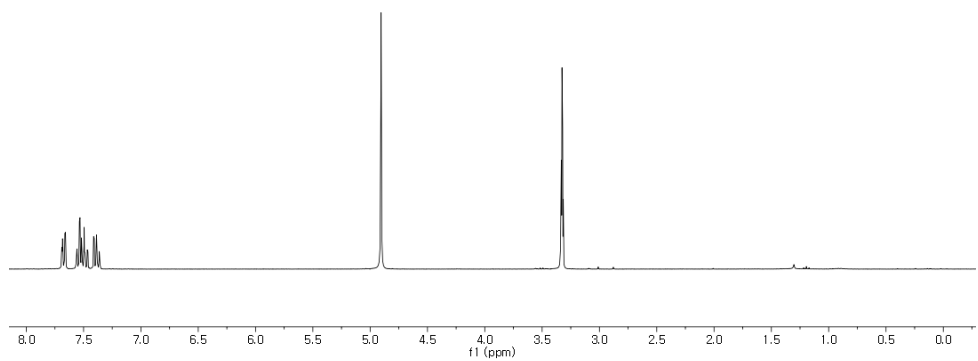
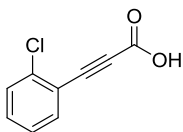
Chapter – 2

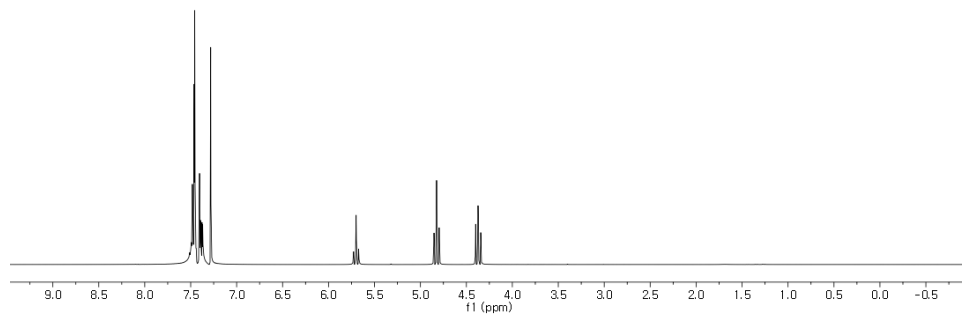
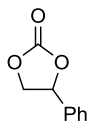
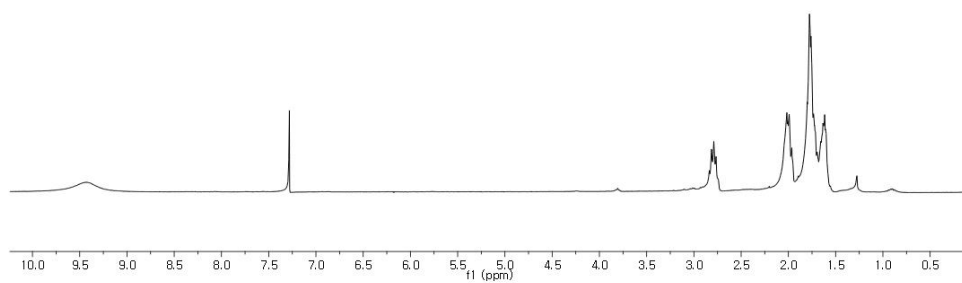
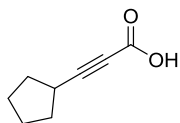


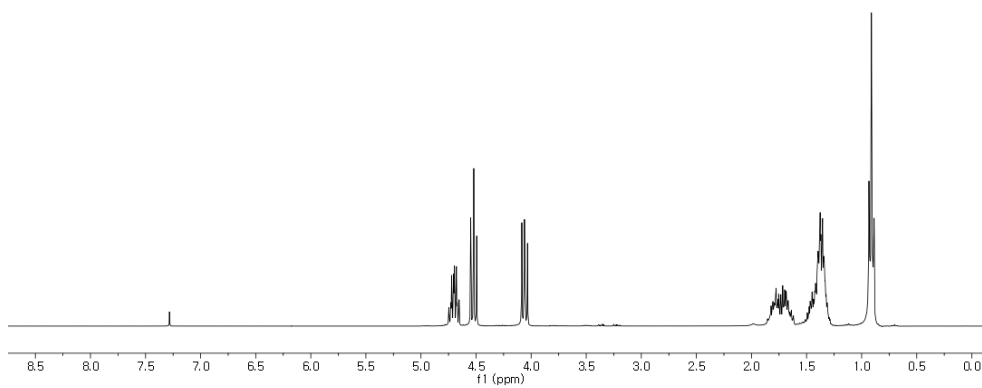
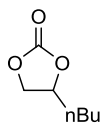
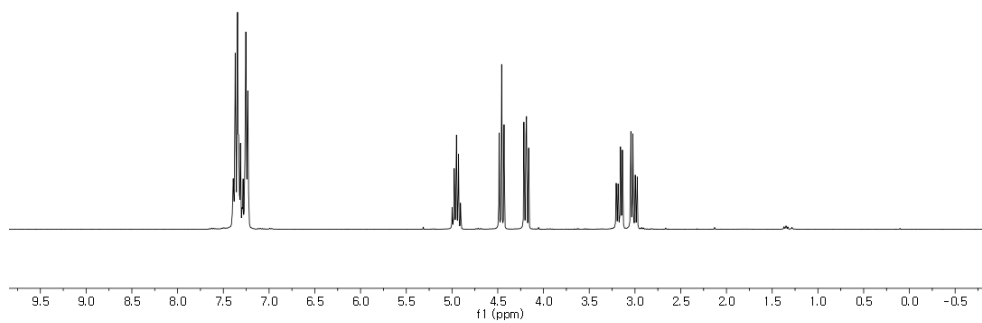
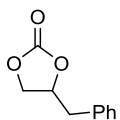


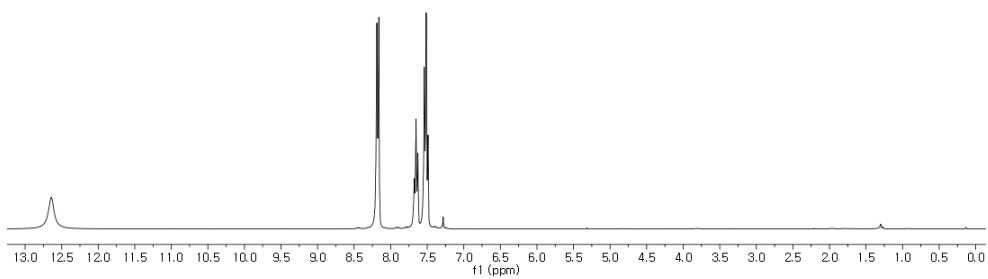
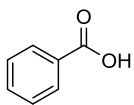
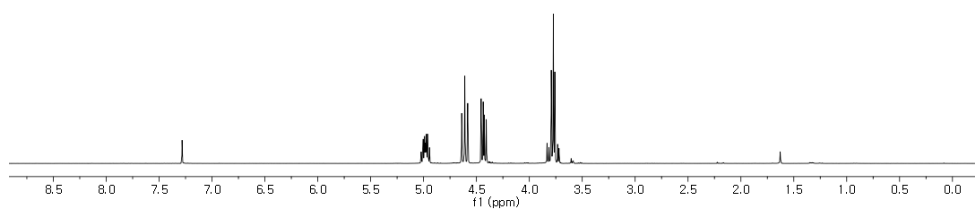
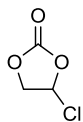


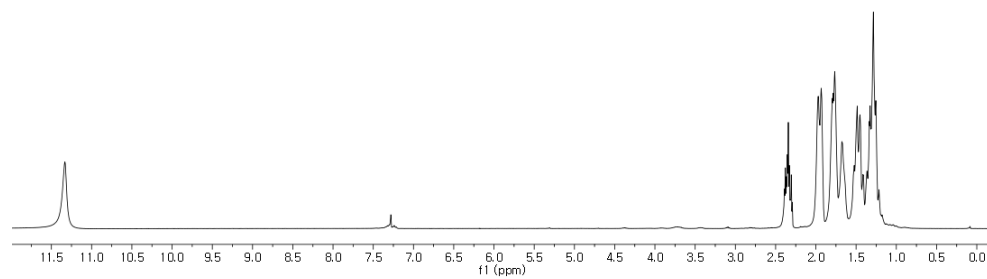
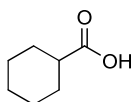
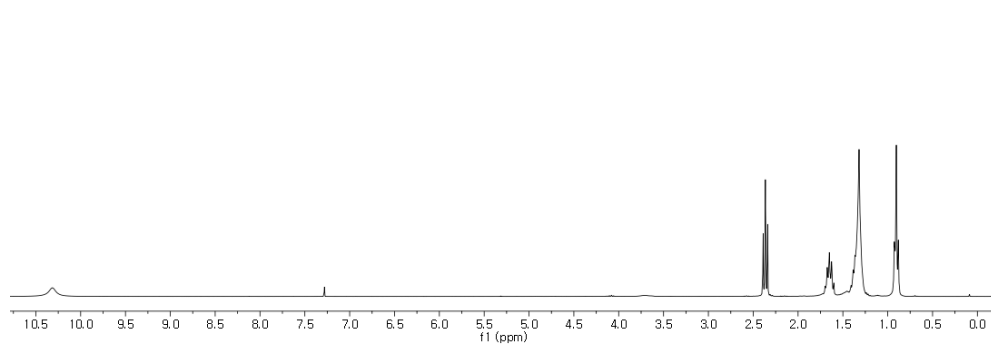
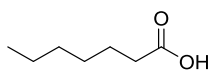




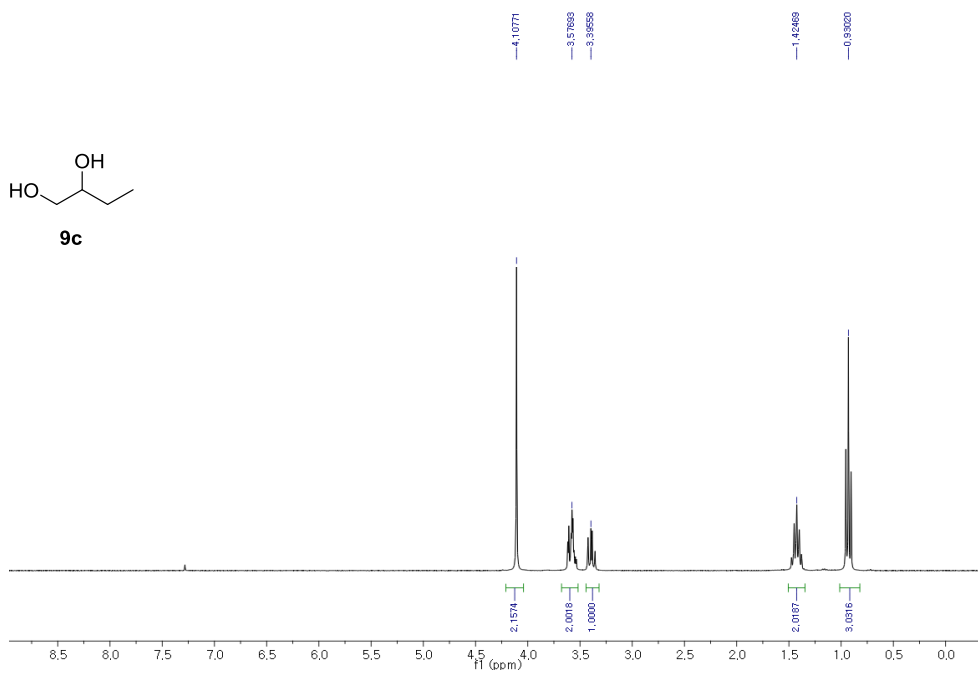
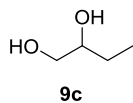
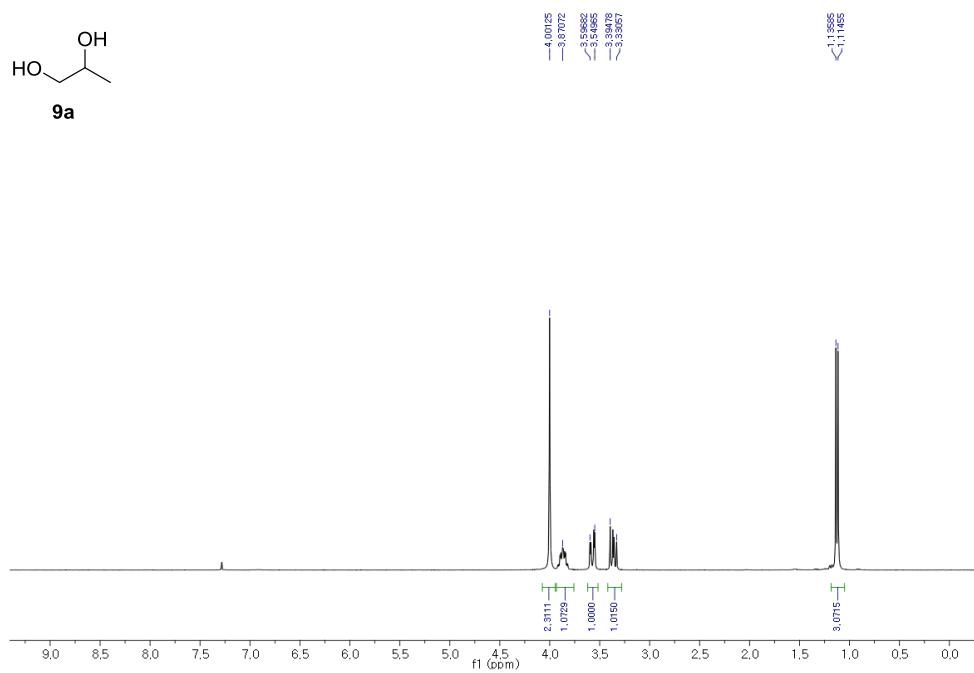
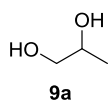


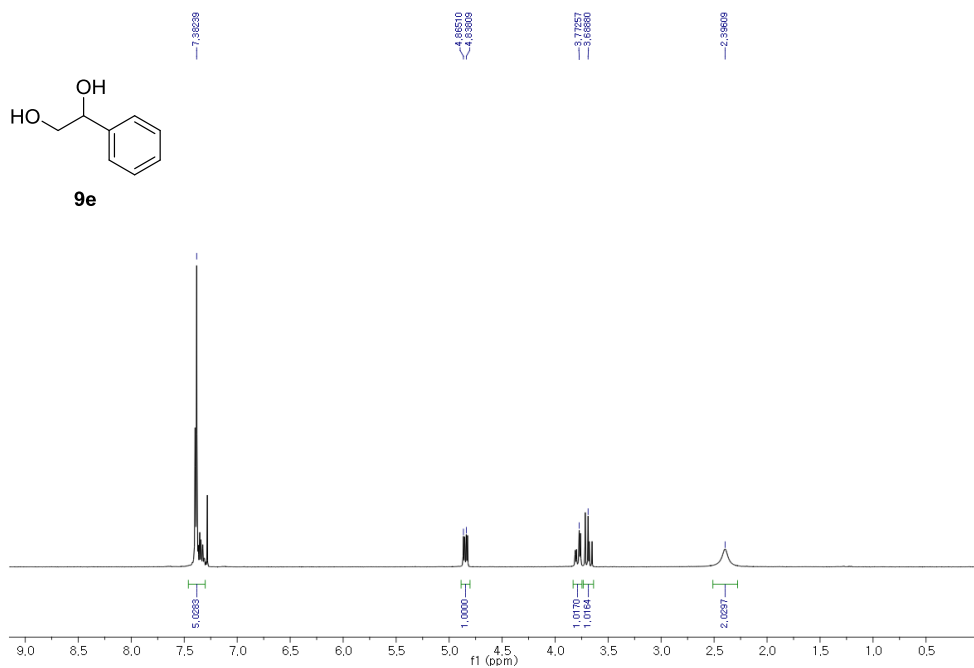
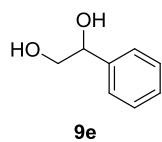
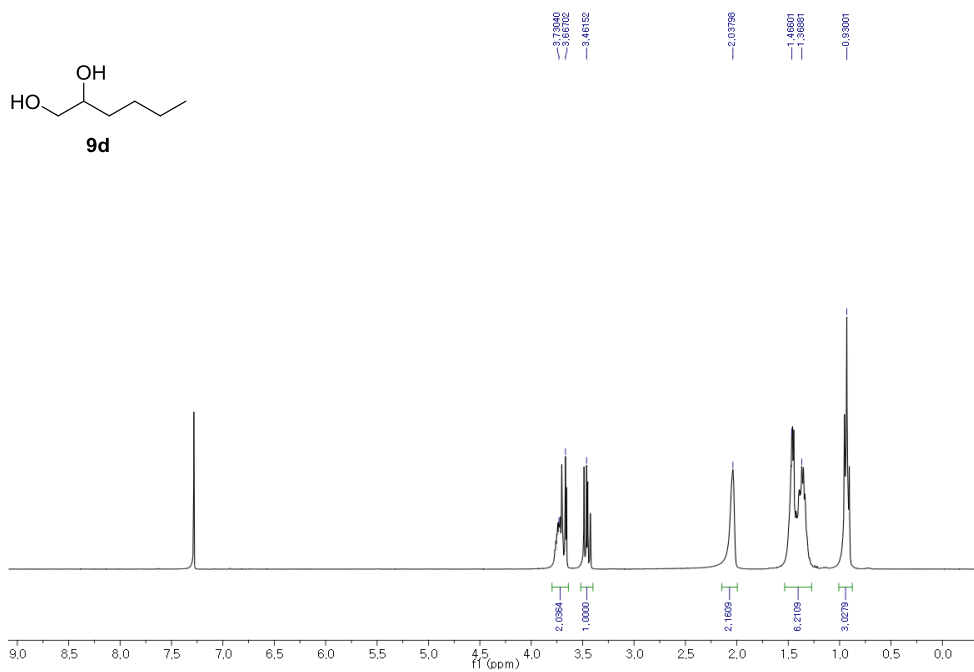
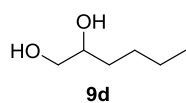




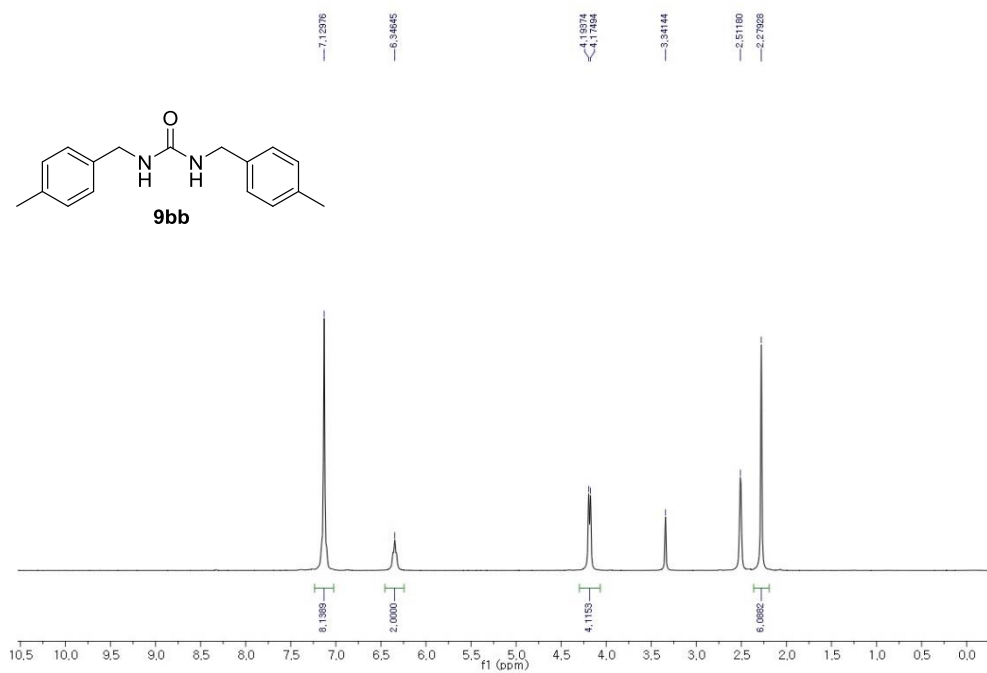
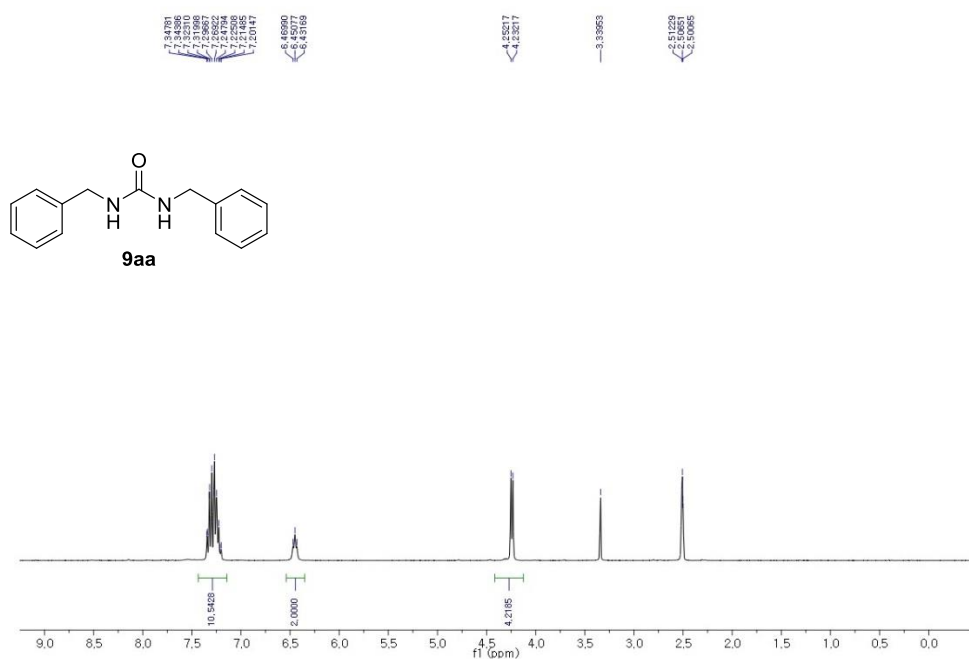


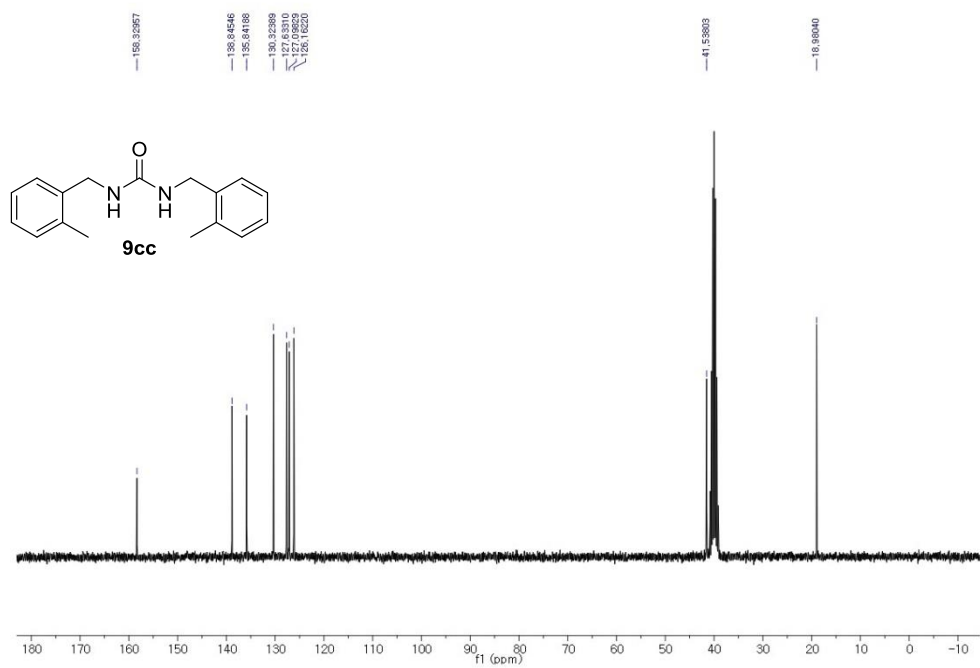
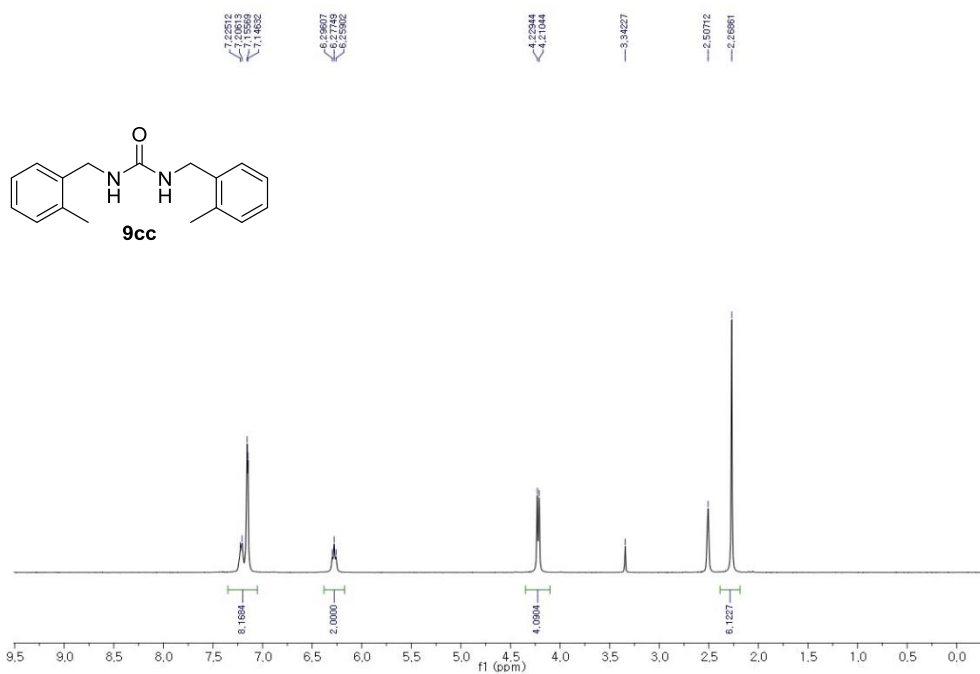
Chapter – 3

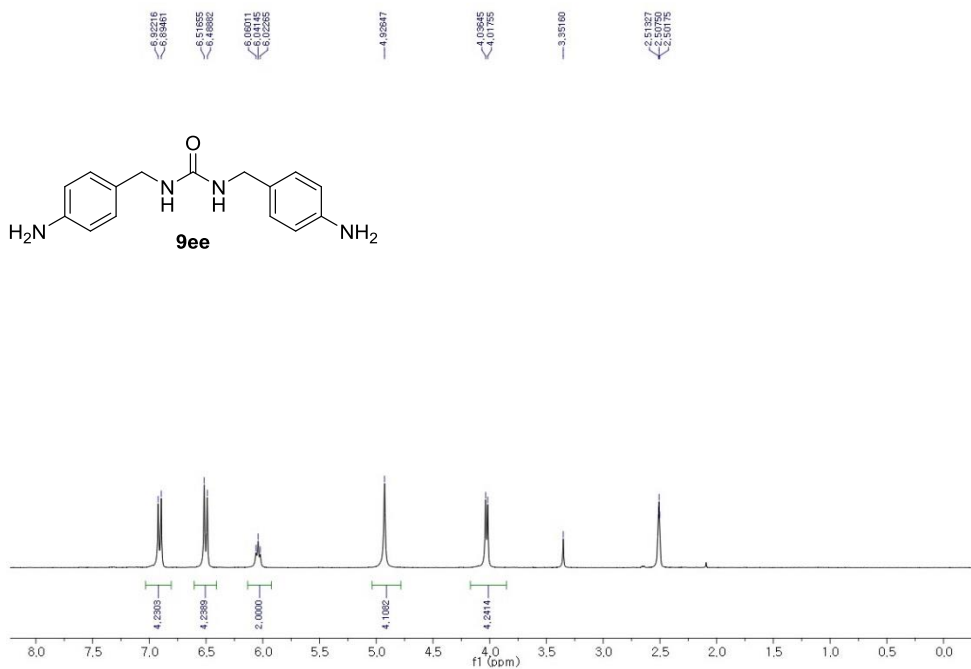
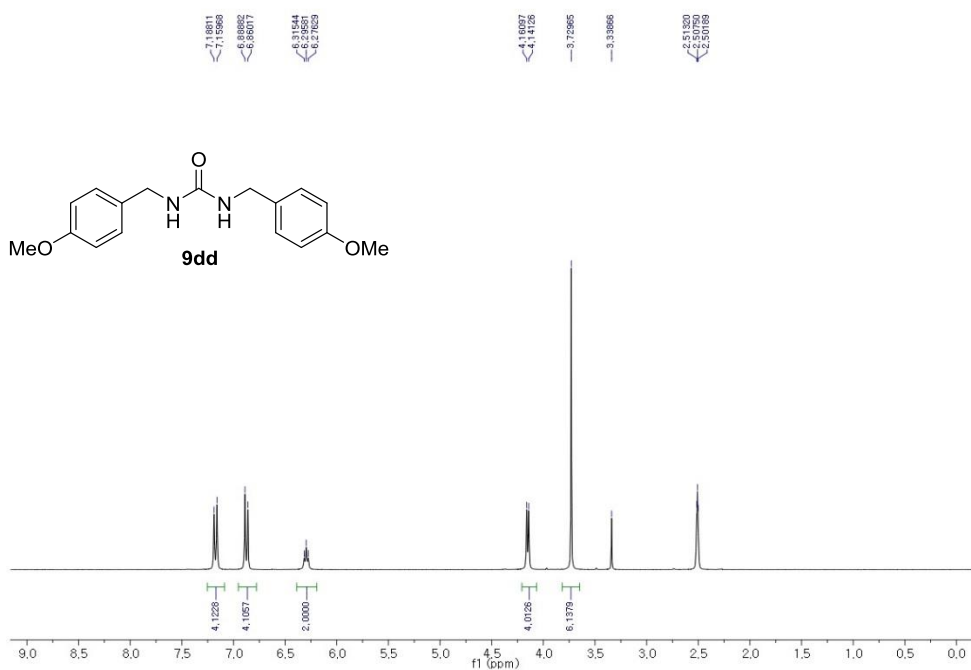


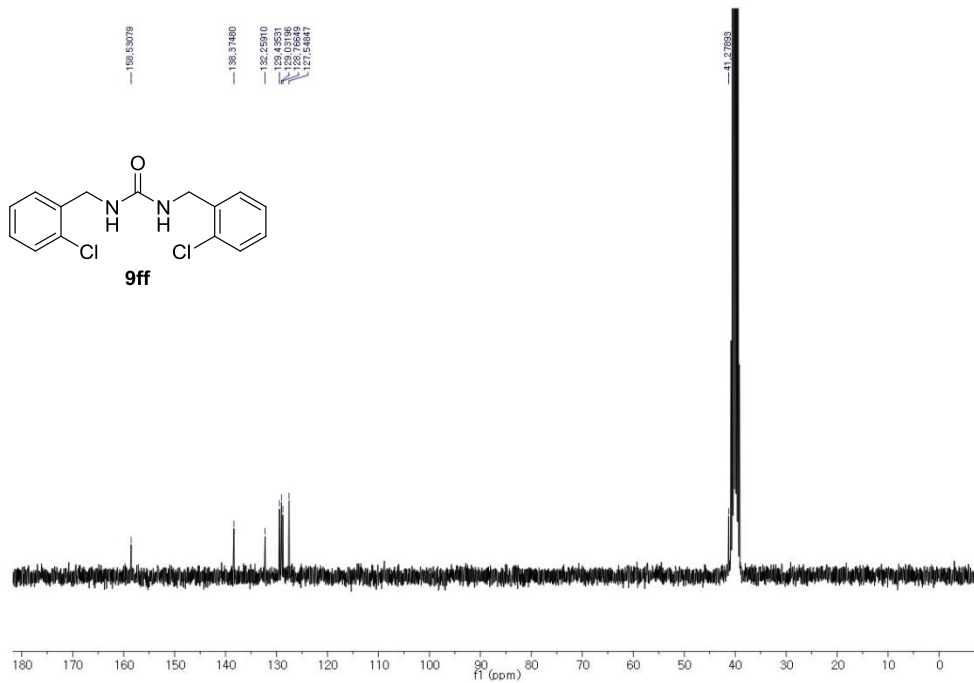


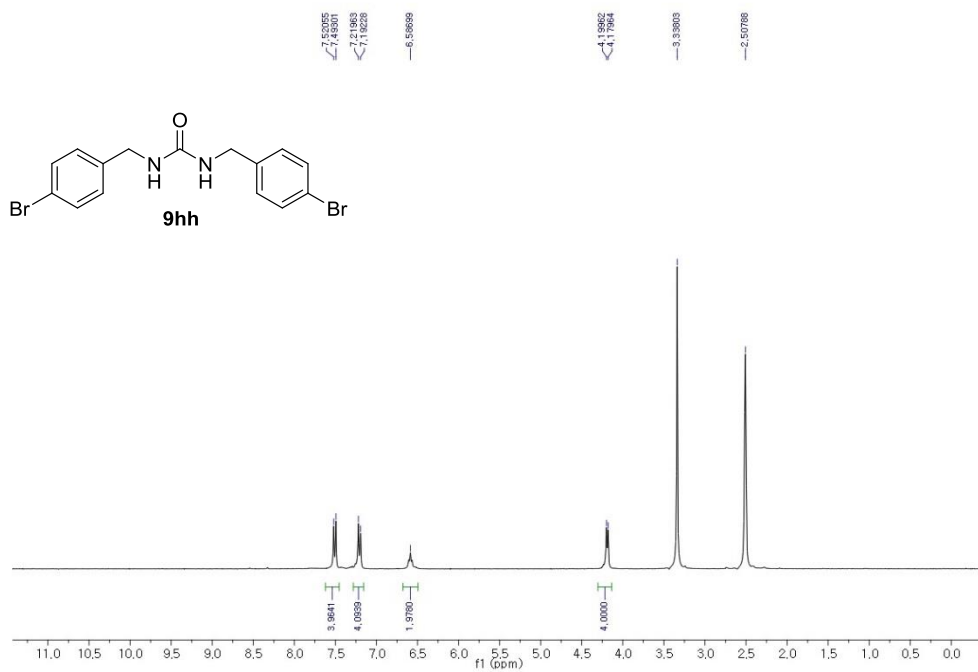
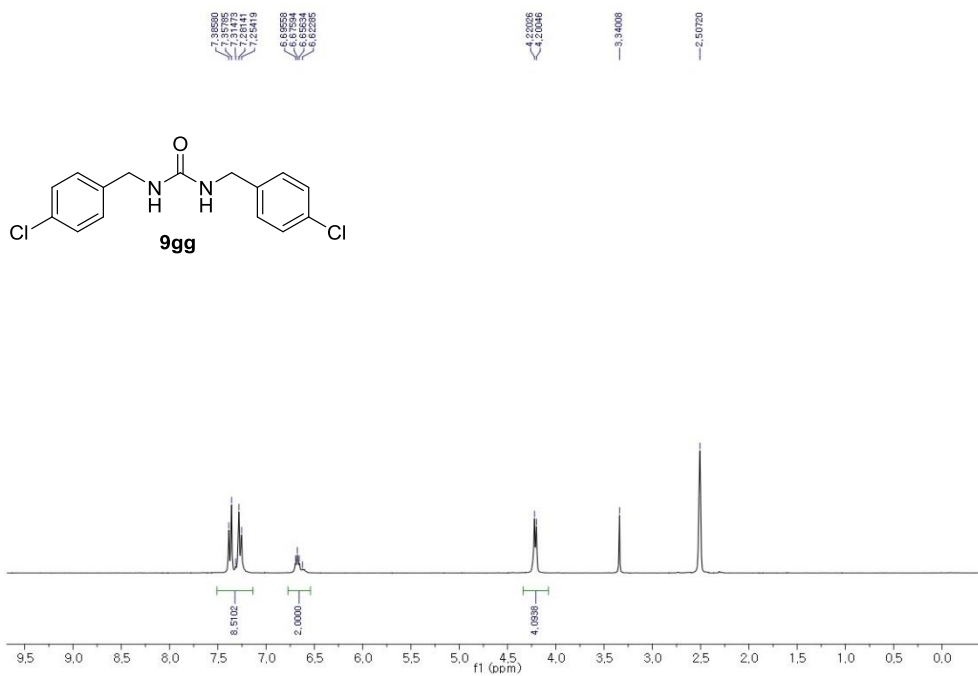
Chapter – 4

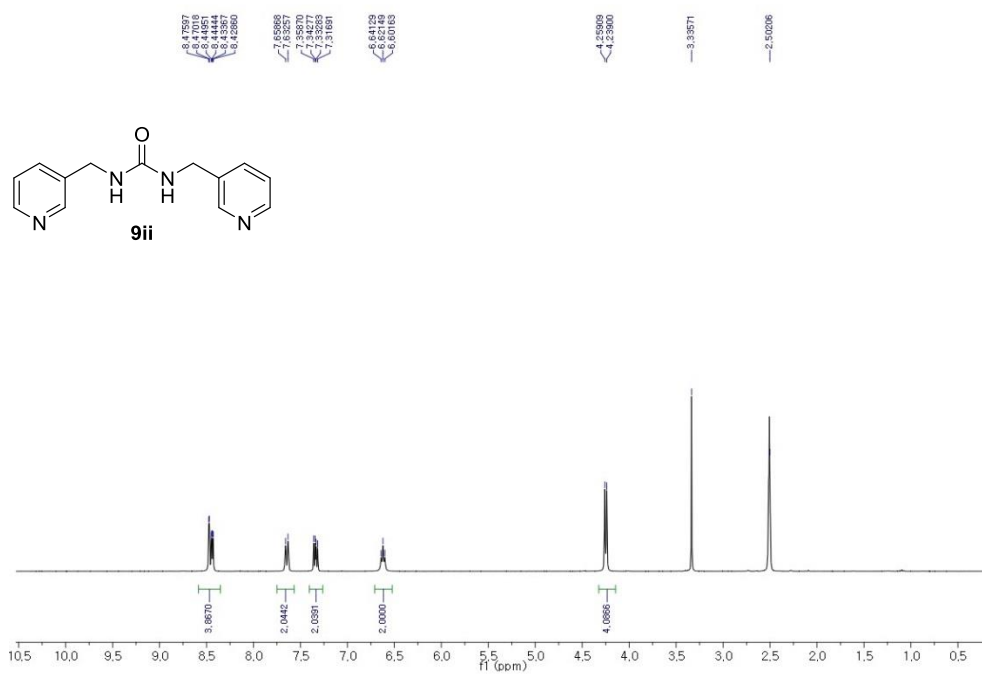


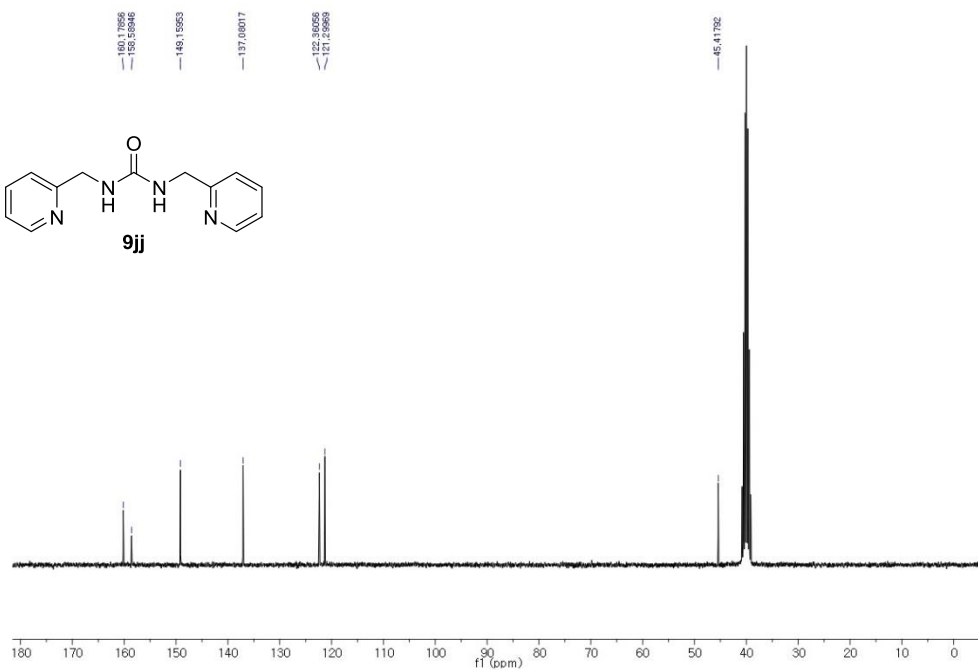
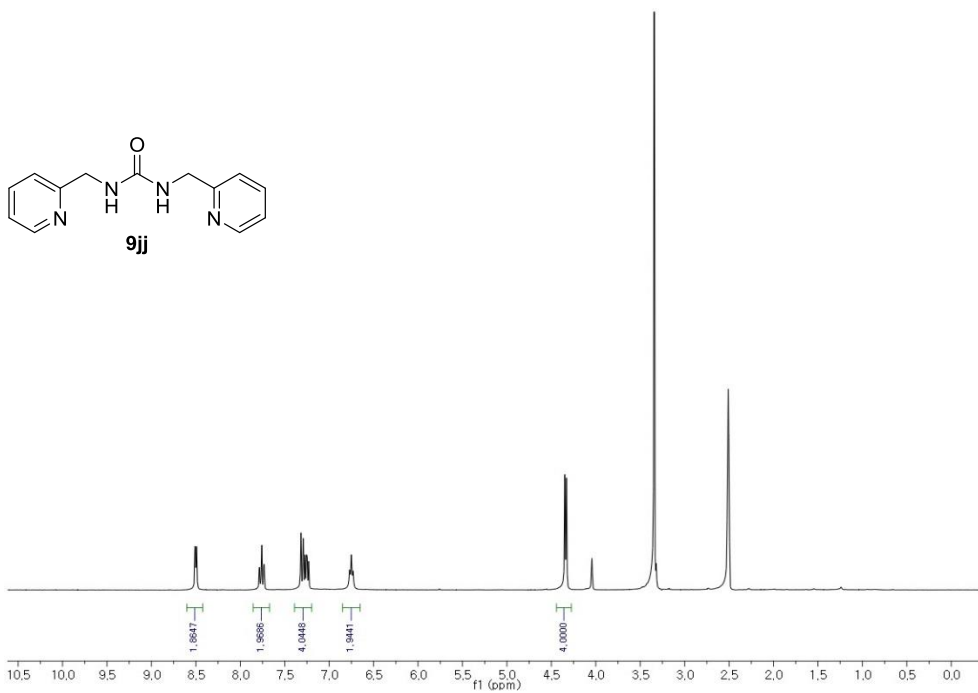


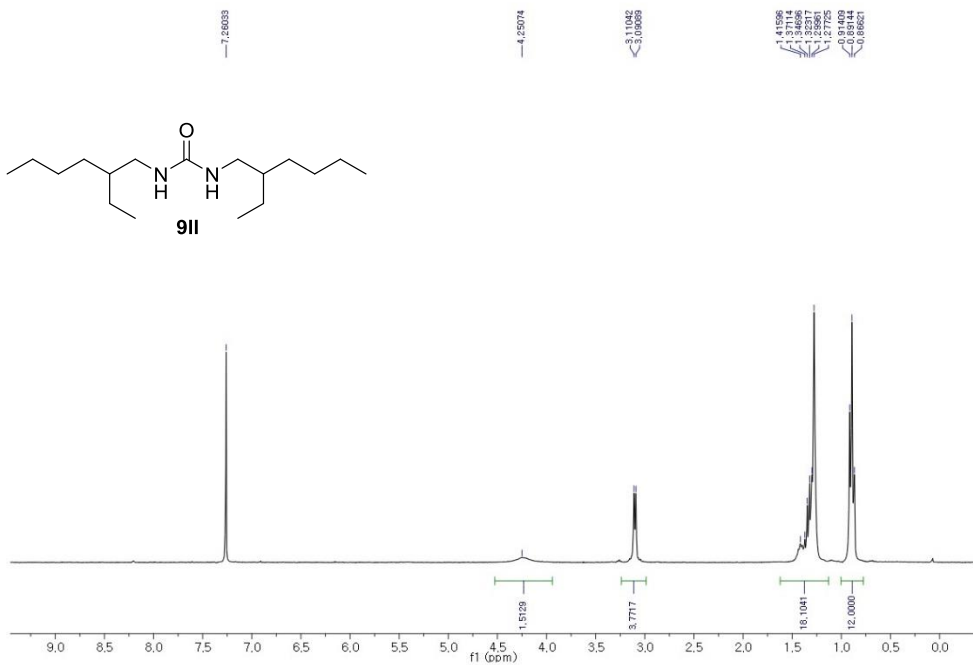
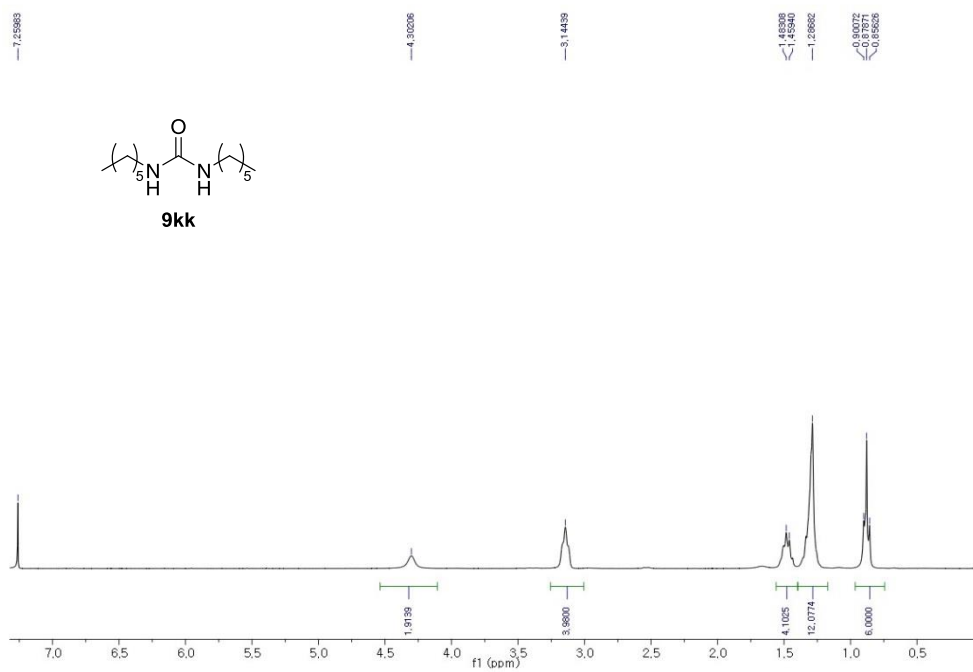


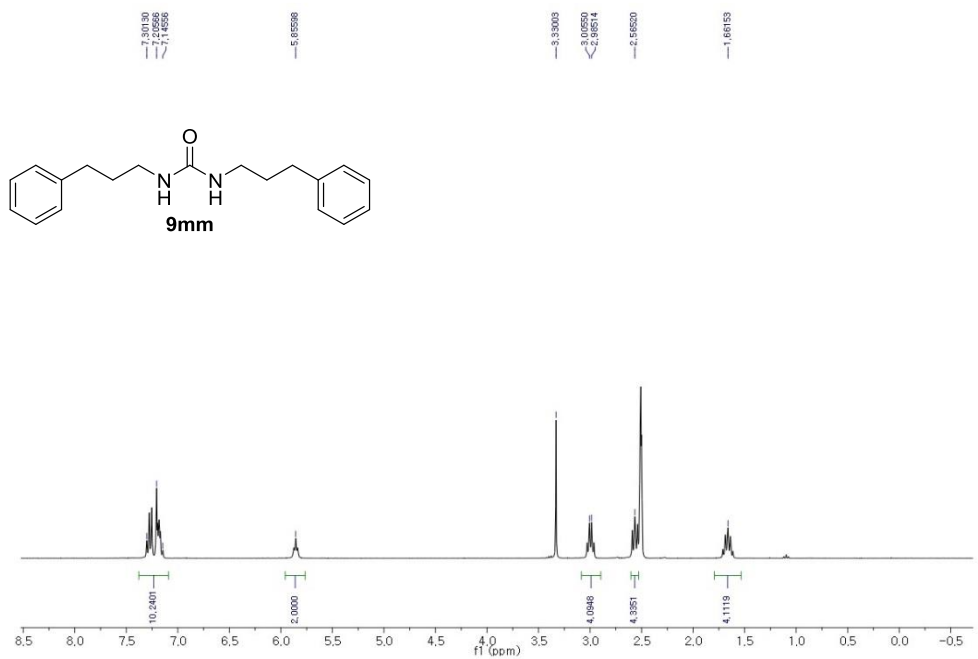
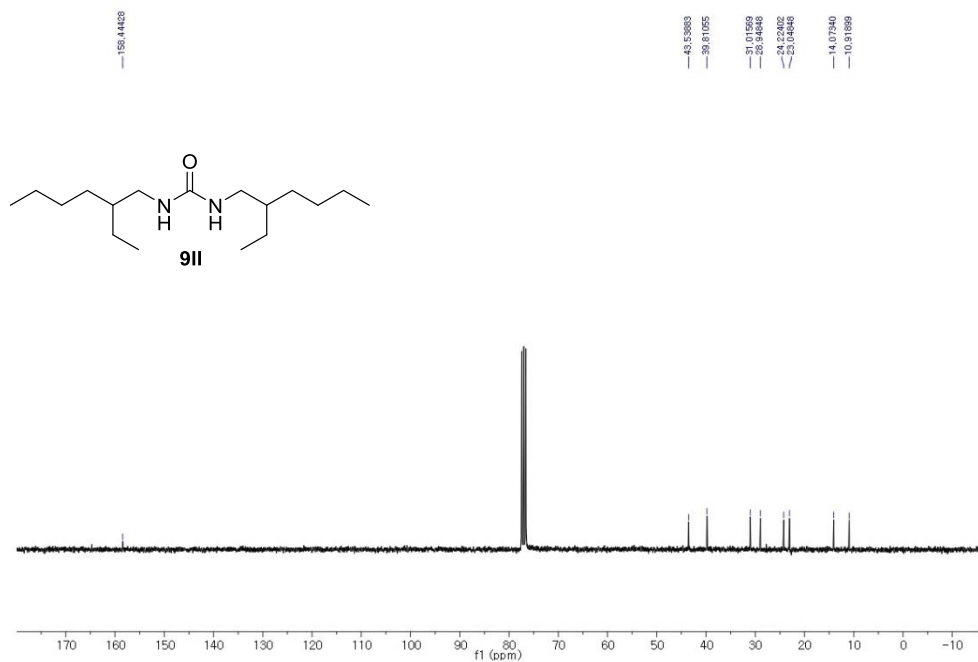


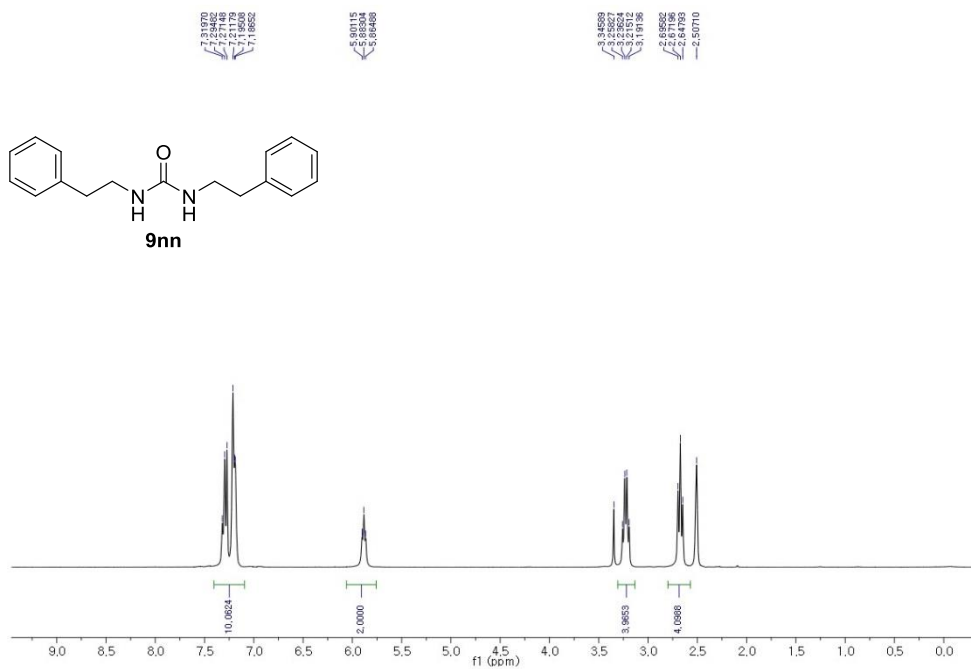
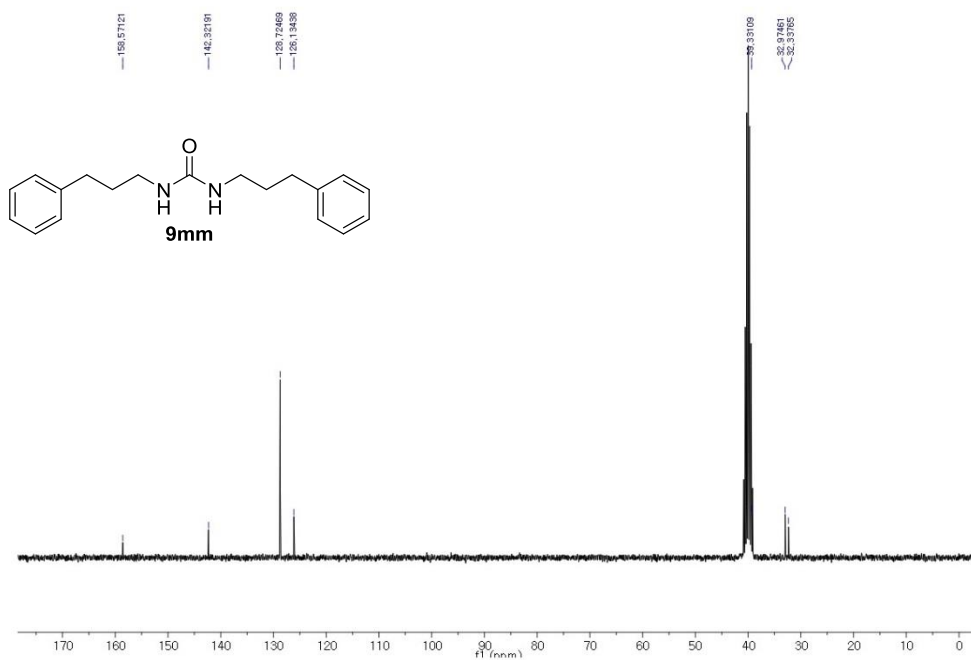


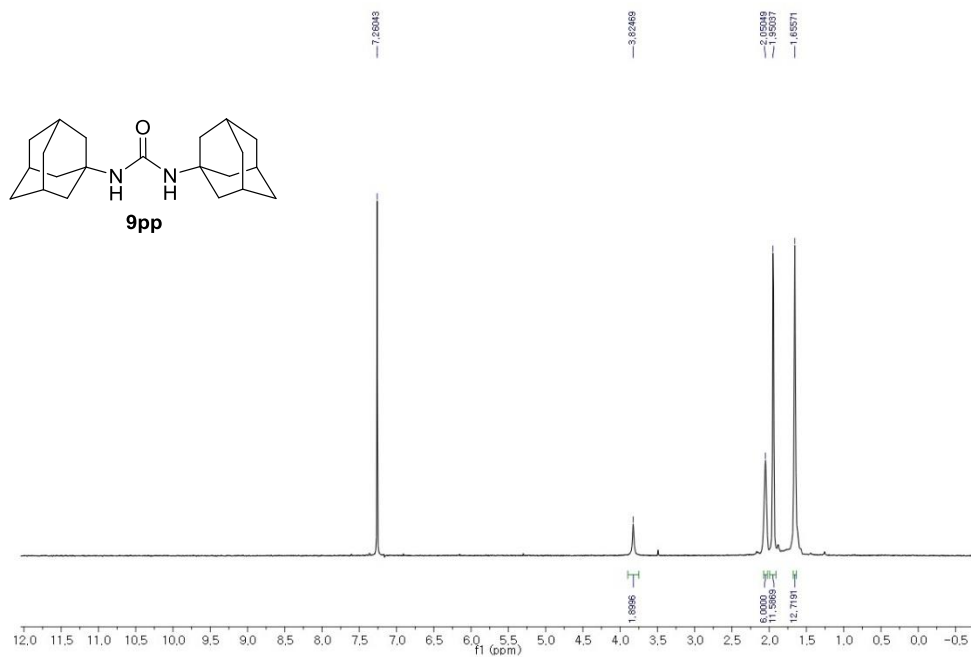
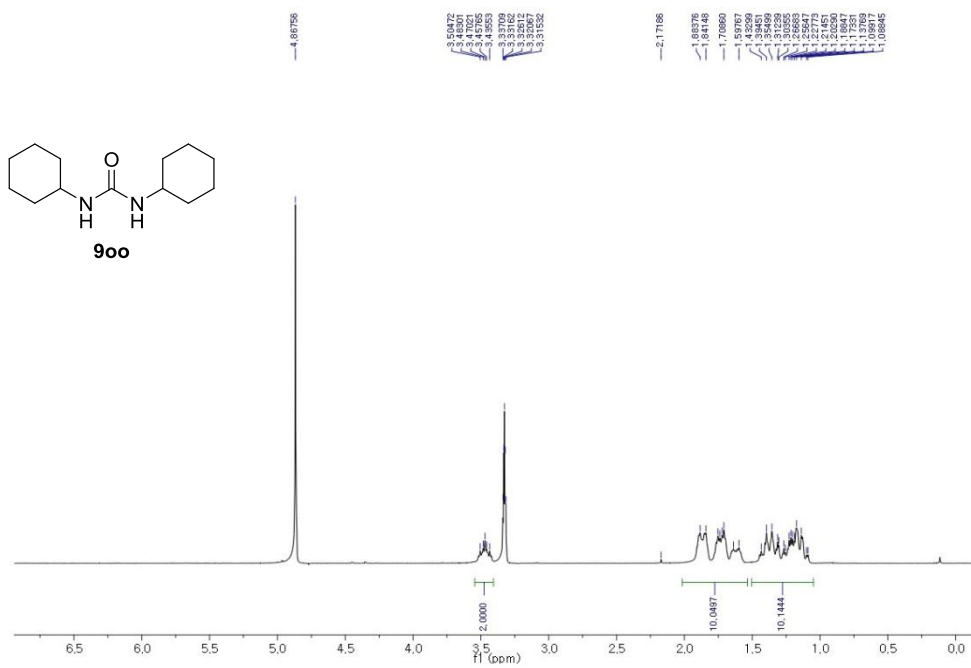


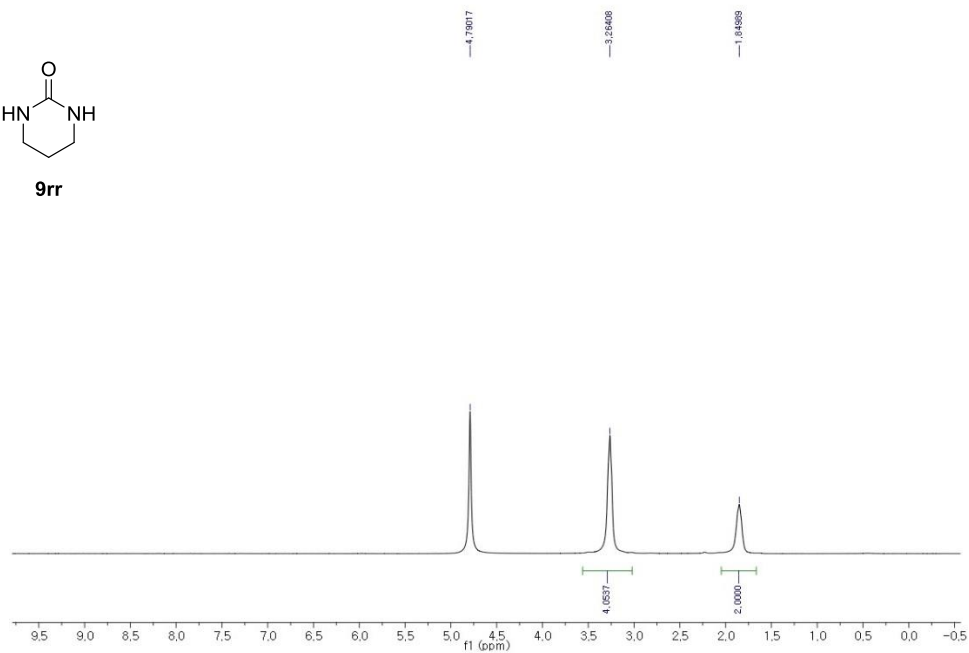
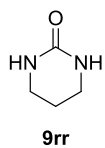
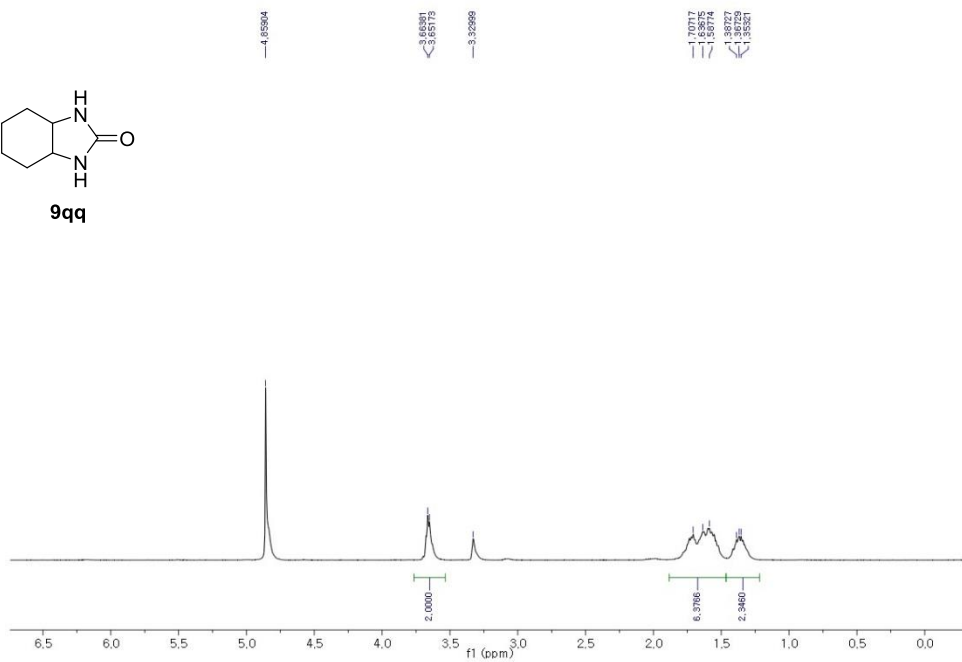
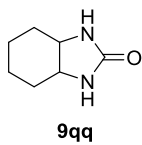


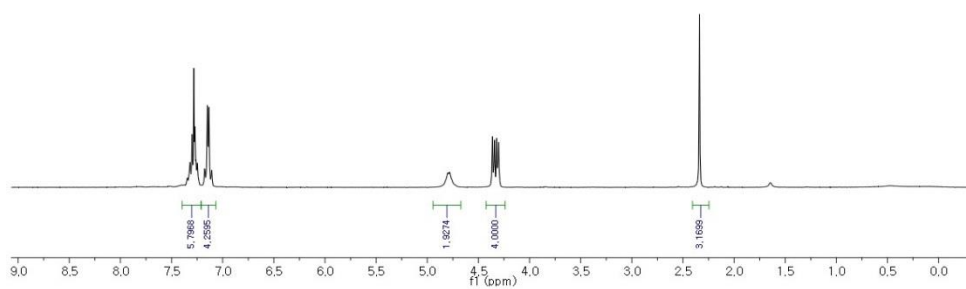
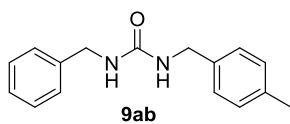
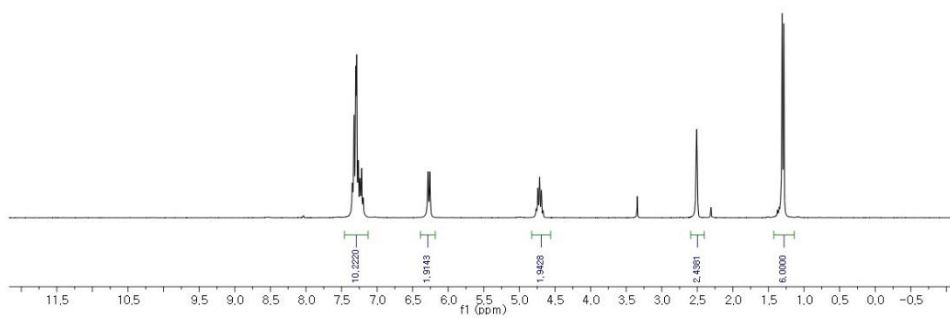
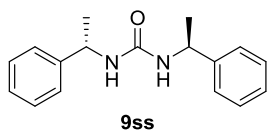


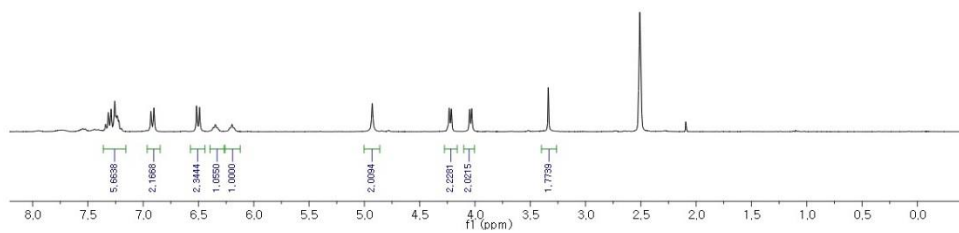
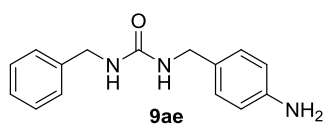
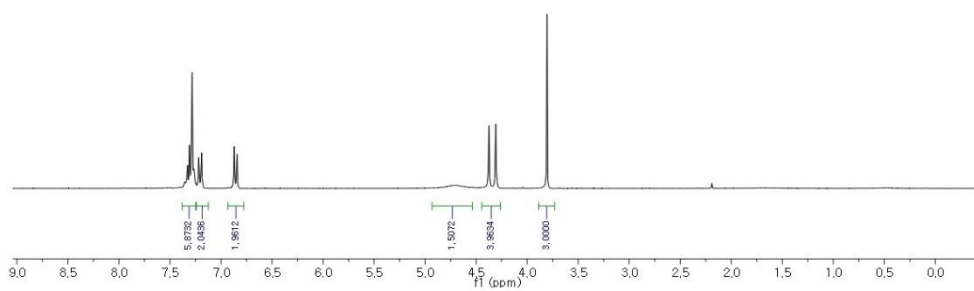
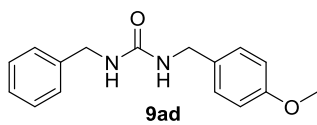


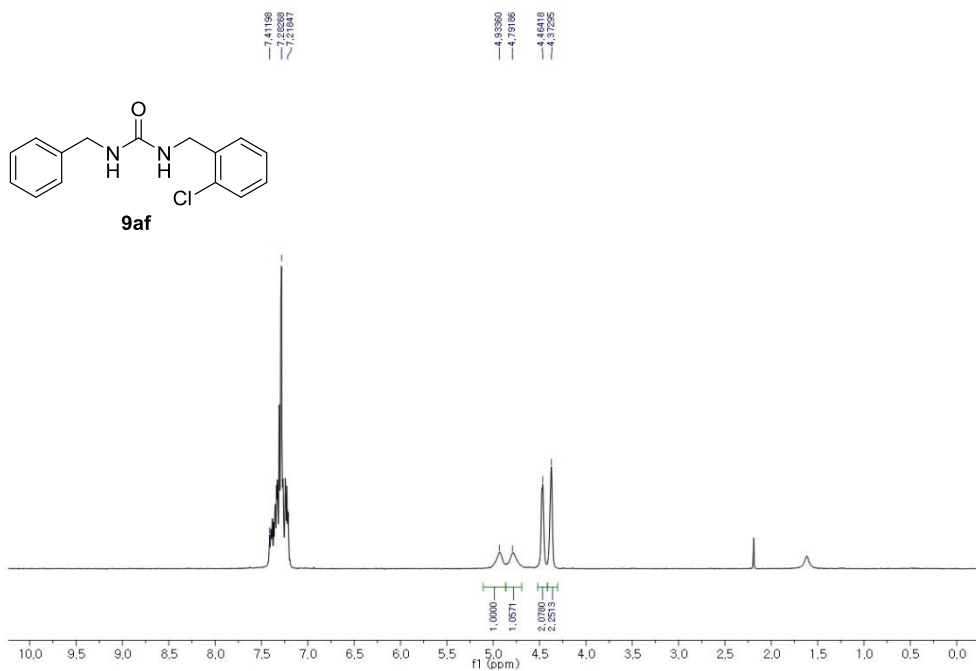
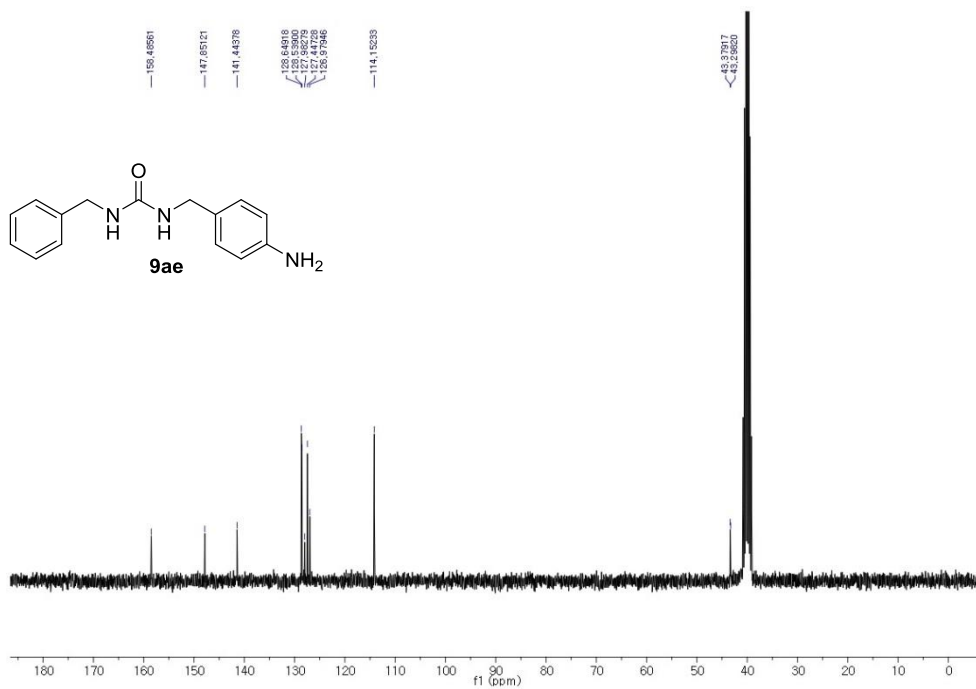


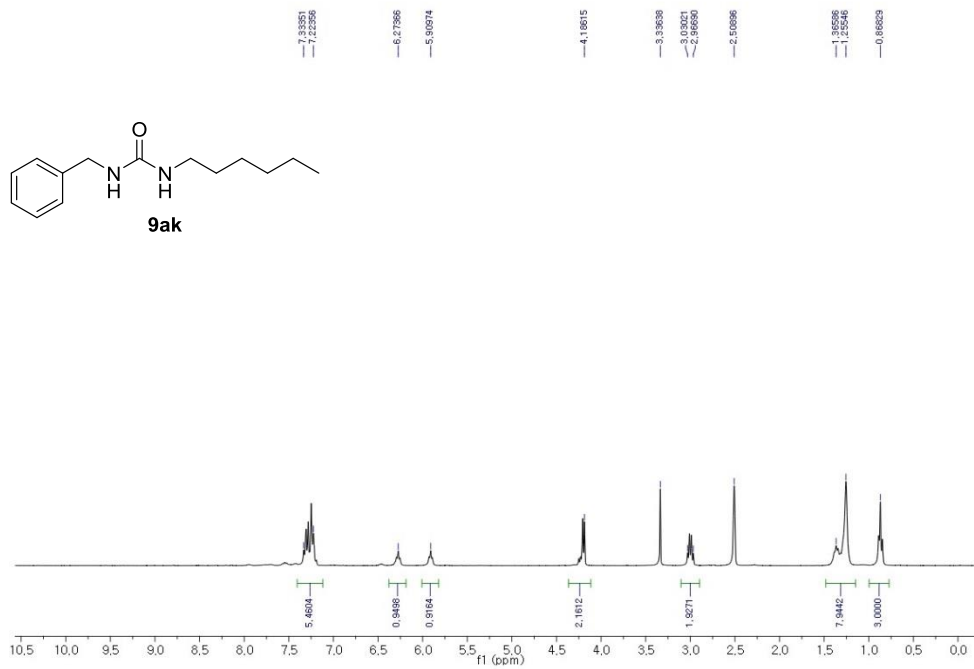
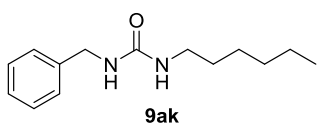
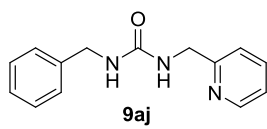


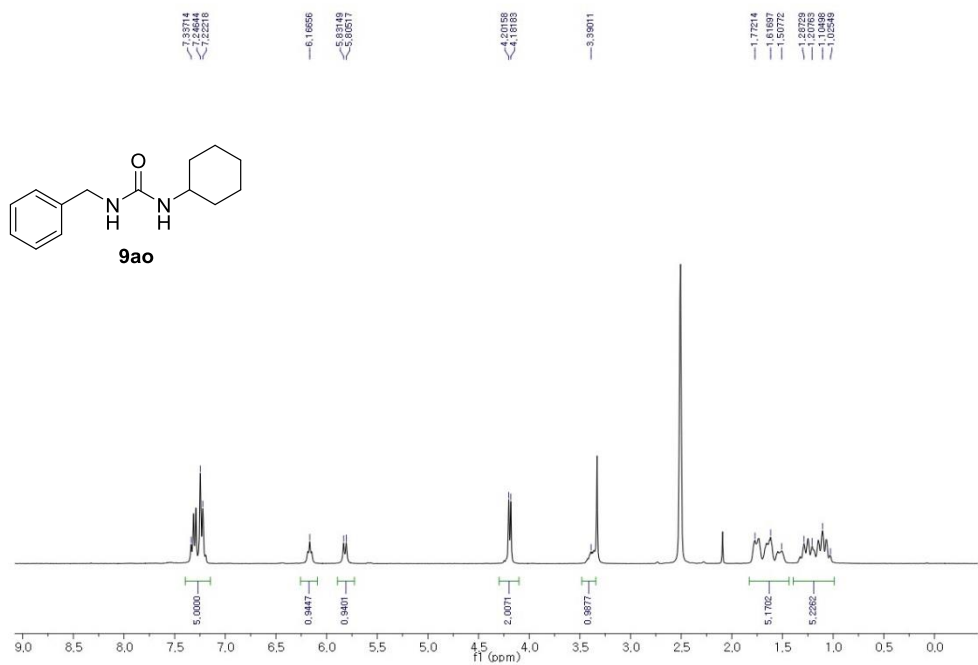
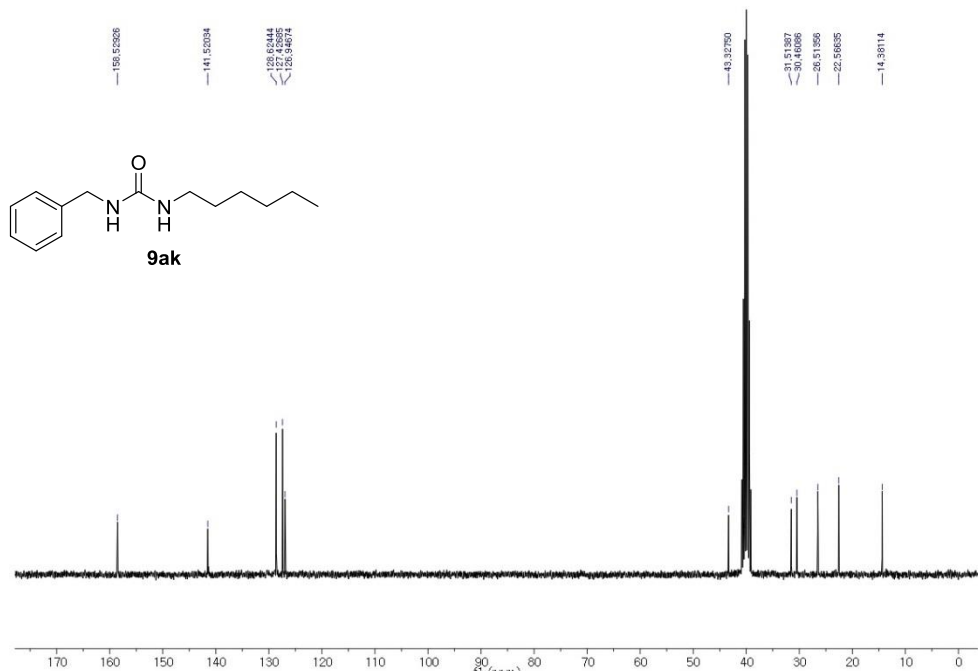




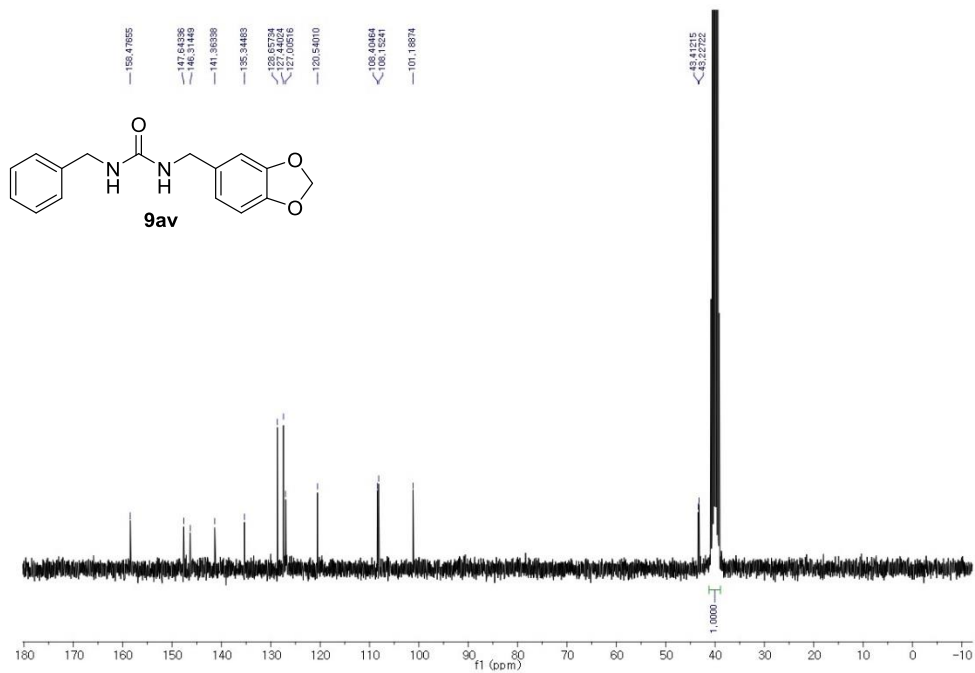


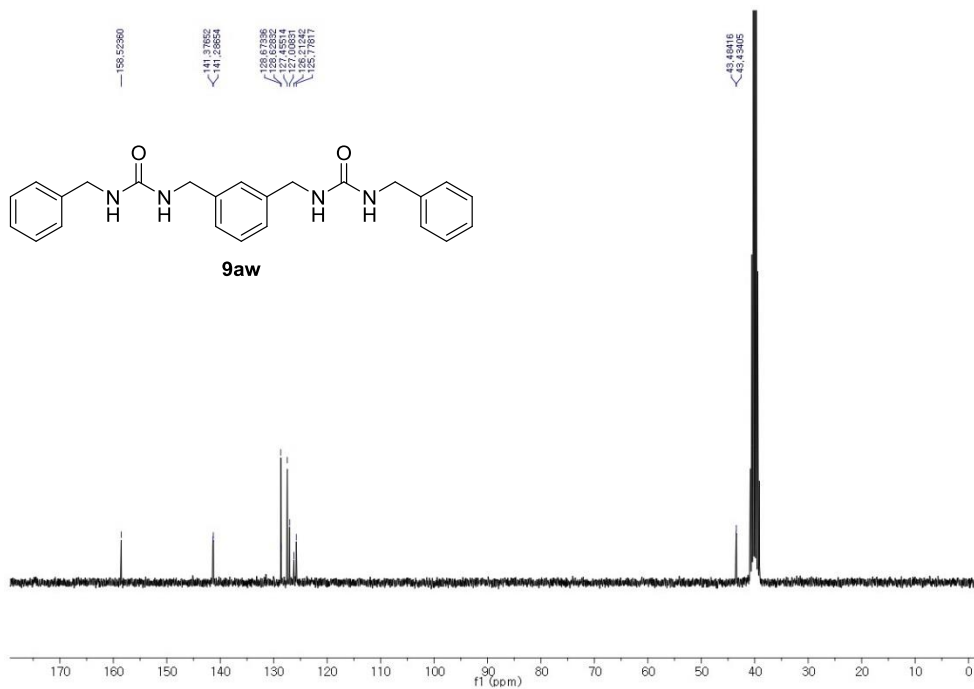
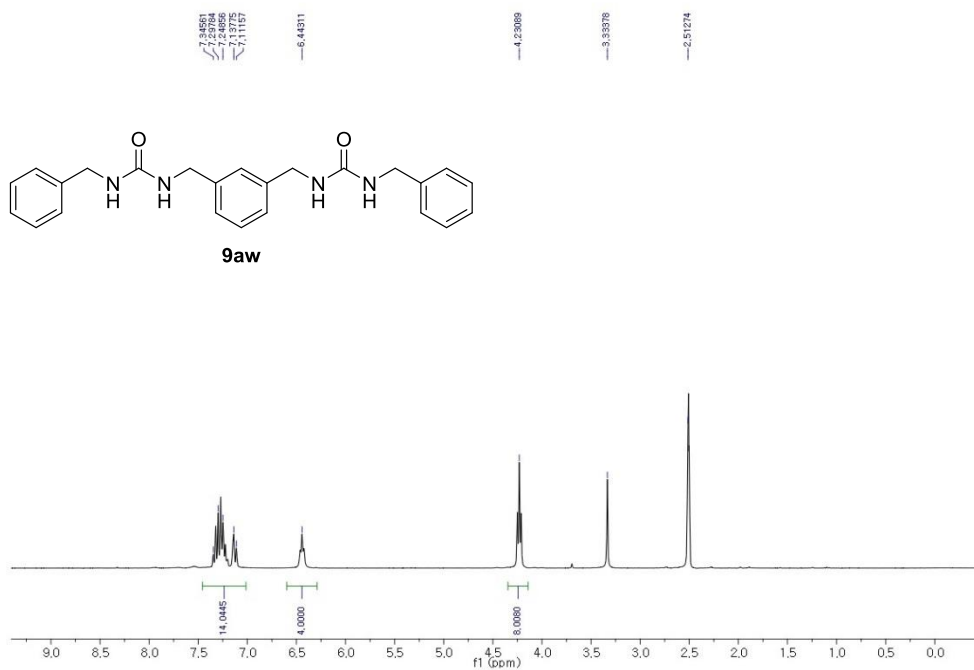


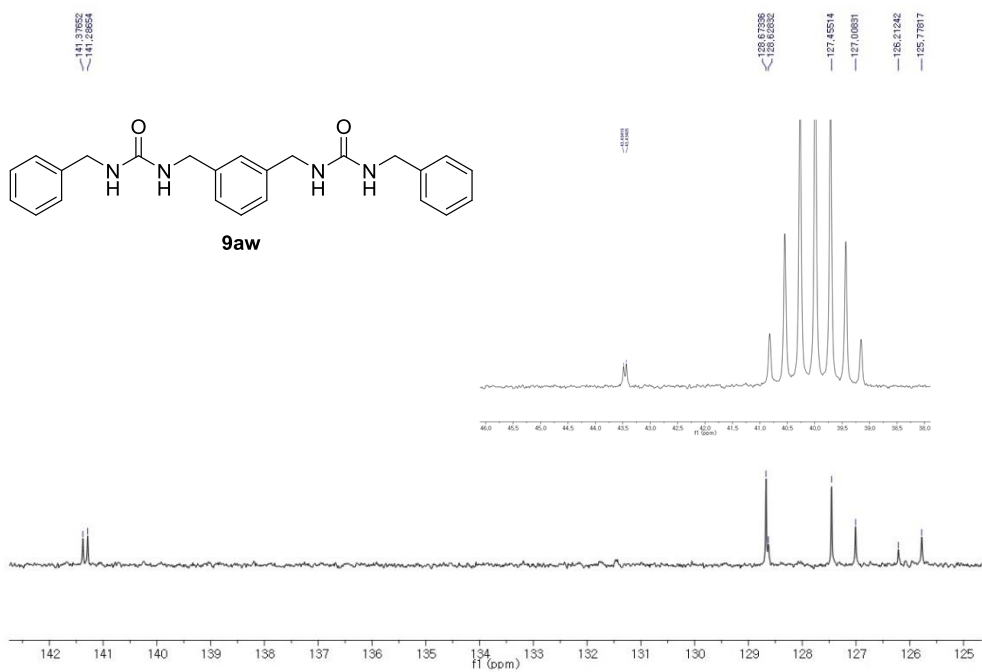




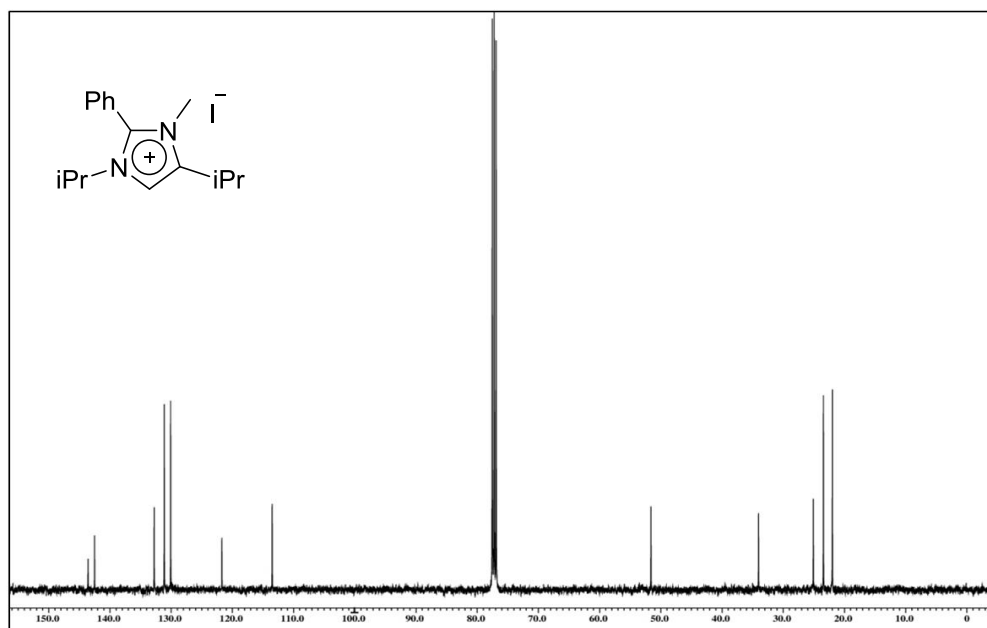
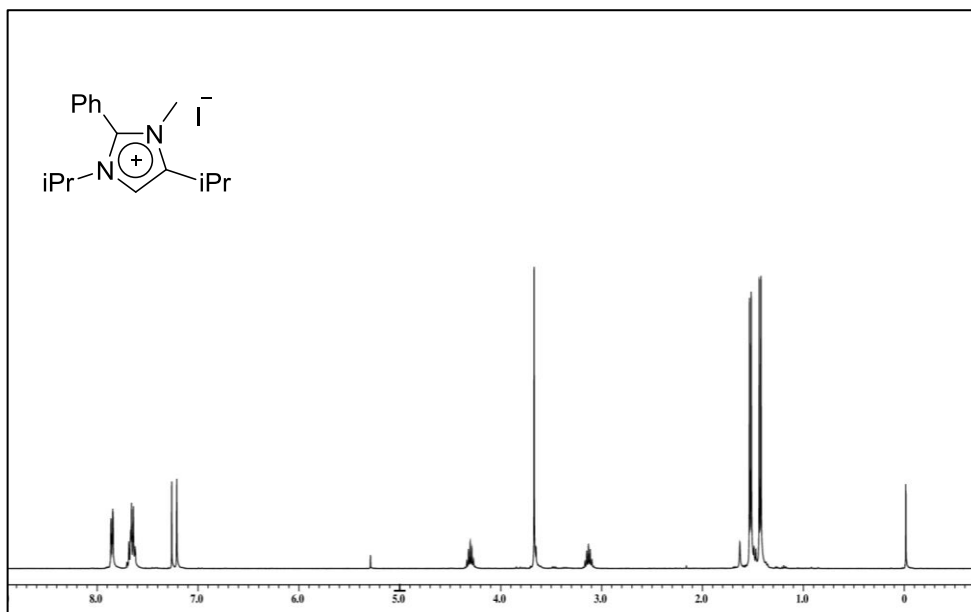


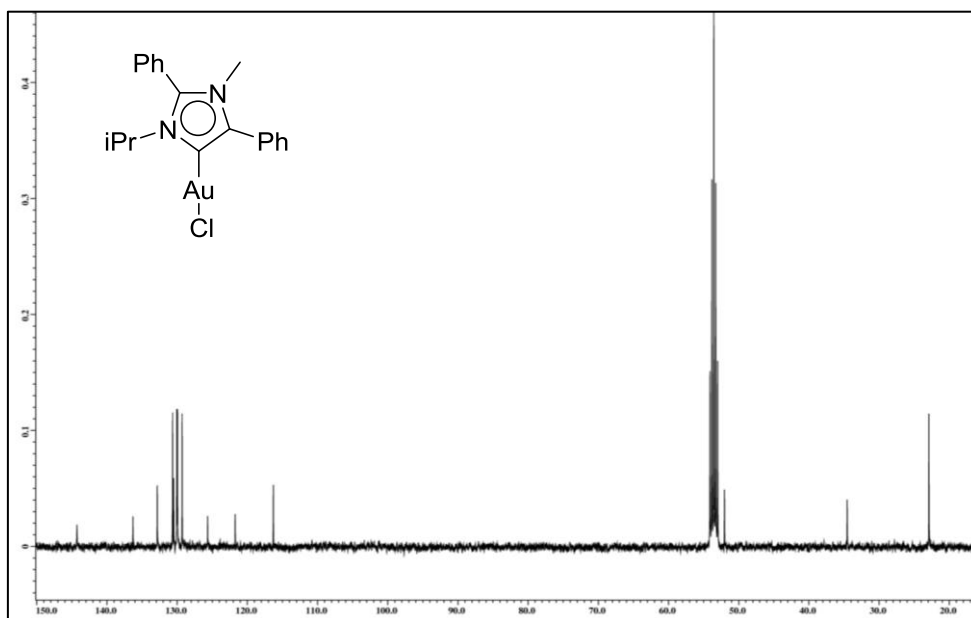
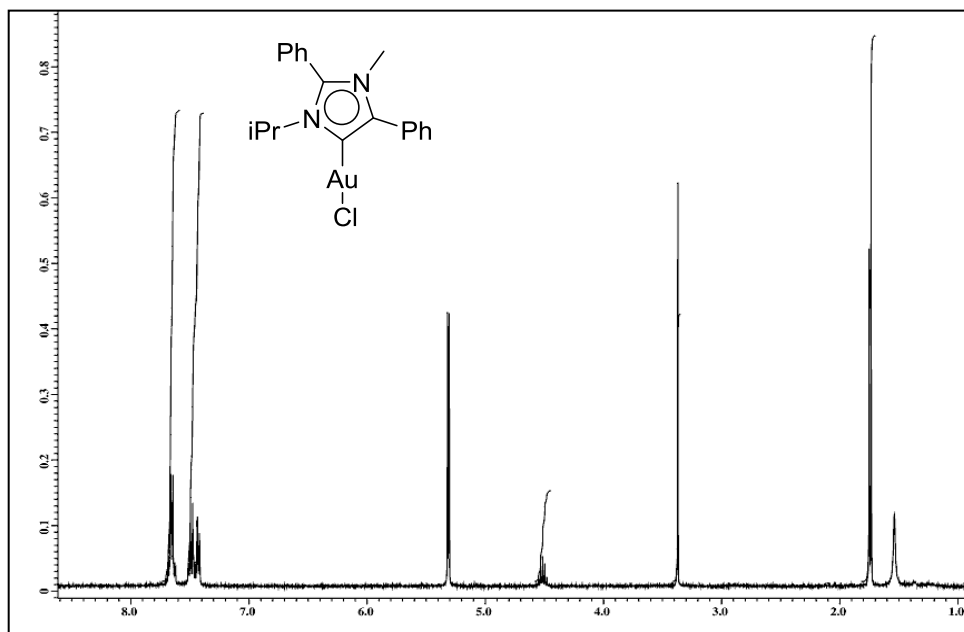


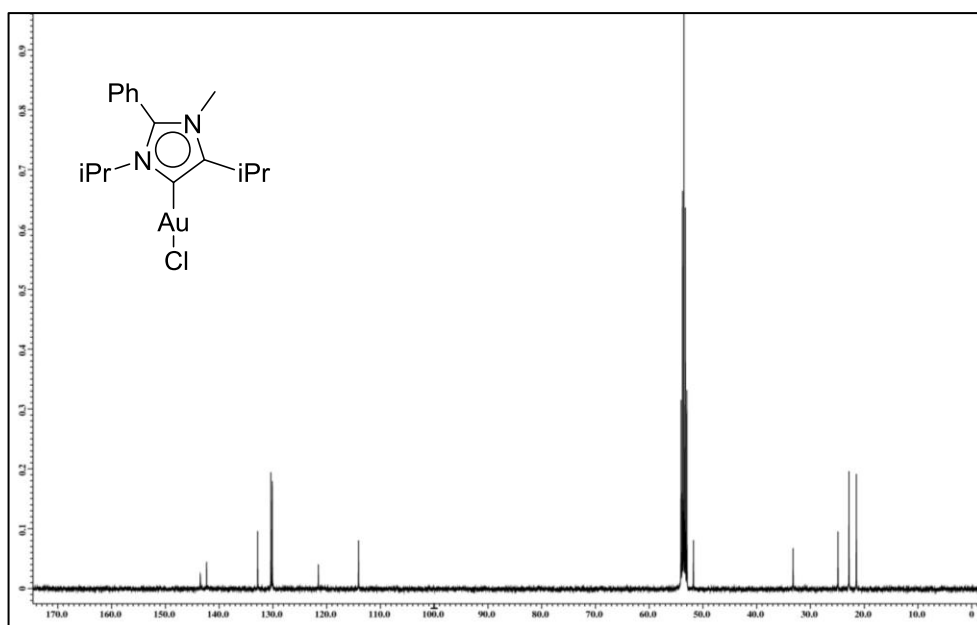
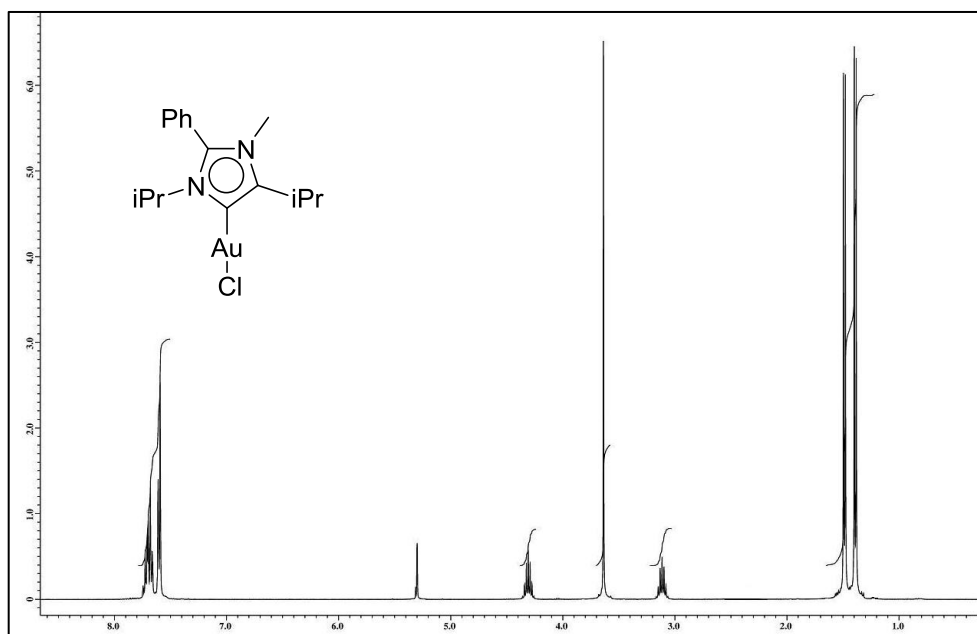


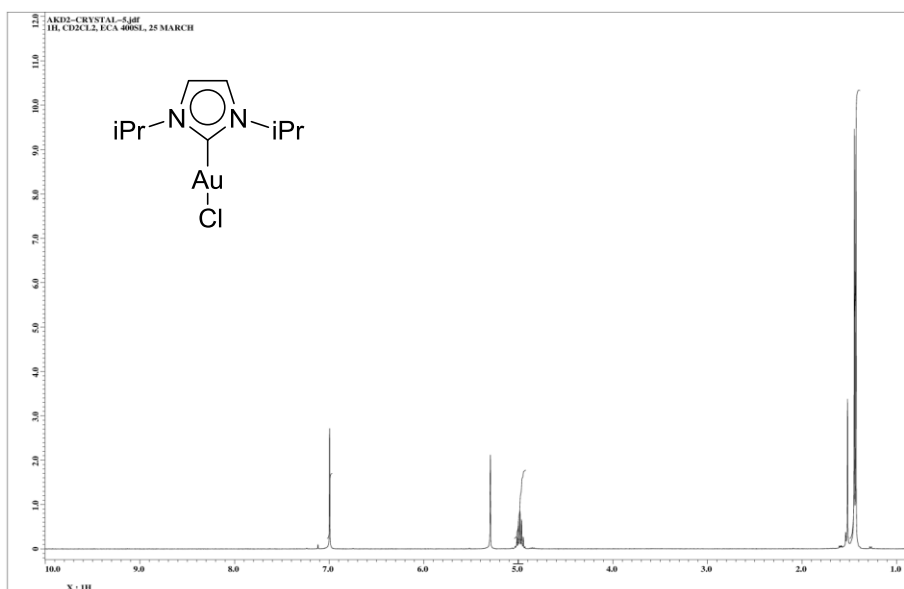
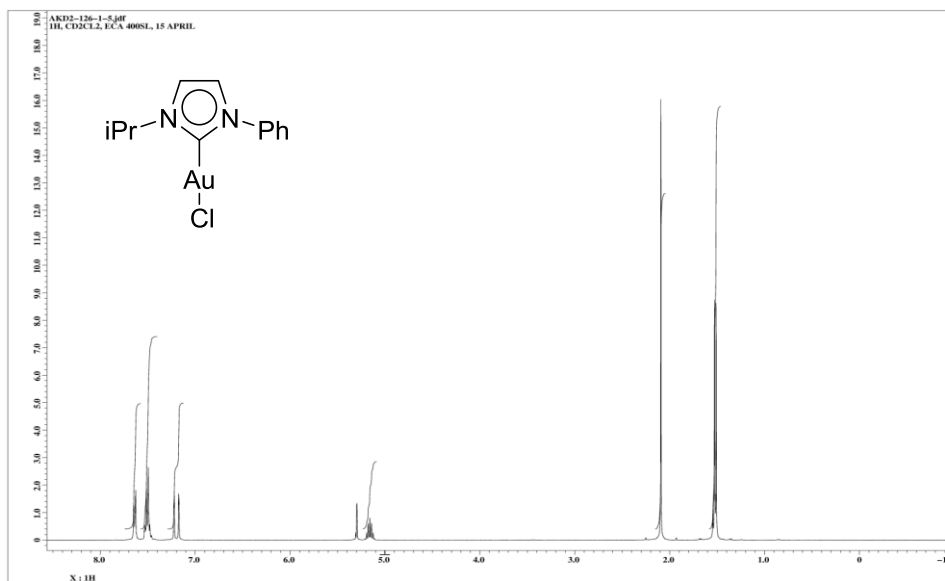


Chapter – 5









국문초록

전이금속을 촉매로 이용한 친환경 반응법 개발

전이금속 촉매를 이용하여 친환경 탄소 재료인 메탄올 혹은 이산화탄소를 활성화시켜 유기반응에 적용하는 연구를 하였다. 최근에 발표된 메탄올과 이산화탄소를 이용한 촉매 반응을 1장을 통하여 소개한다. 연소가스에 섞여 있는 이산화탄소를 이용하여 유용한 유기화합물을 합성하는 전략을 개발하였다 (2 장). 연소가스에는 이산화탄소 이외에 일산화탄소, 산소, 수분 등이 존재 하는데, 이 물질들은 일반적인 촉매 시스템을 파괴한다. 에탄올아민 수용액을 이용하여 그 문제를 해결하였다. 초를 태워 연소가스를 발생시킨 후 에탄올아민 수용액으로 연소가스의 이산화탄소를 선택적으로 포집한 후, 유기합성을 진행 하였다. 그리나드반응, 전이금속 촉매 반응 등의 다양한 유기반응에 적용하였으며 고품질의 이산화탄소(99.999%)를 이용하였을 때와 같은 효율로 생성물을 얻을 수 있다. 이산화탄소를 메탄올로 전환시킬 수 있는 방법을 연구 하였다 (3장). 현재까지 발표된 균일계 촉매를 이용한 이산화탄소로부터 메탄올 생성법은 효율은 매우 낮다. 따라서 이를 보완하기 위해 이산화탄소로부터 합성하기 쉬운 포밀 에스테르, 고리화 카보네이트의 환원 반응을 통한 메탄올 생성법이 주목 받고 있다. 하지만 이러한 카보닐 화합물은 케톤, 알데하이드와 같은

카보닐 화합물과 비교하여 친전자성이 떨어지기 때문에 안정성이 높아 환원시키기 위해 고압의 수소가 이용되고 있다. 효율적인 촉매시스템을 이용하여 고압의 수소를 사용하지 않고 2-프로판올을 수소 재료이자 용매로 사용하여 메탄올을 생성하는 반응법을 개발하였다. 유기합성분야에서는 독성이 매우 강한 포스진, 일산화탄소, 메틸 할라이드 등이 대표적인 탄소 재료로 사용되고 있다. 이러한 물질의 사용은 강산 등을 부산물로 생성하는 큰 단점이 있다. 메탄올은 전 세계적으로 매년 8천만 톤 이상이 생산될 정도로 풍부하고 저렴한 물질이어서 기존의 탄소재료를 대체할 물질로 주목 받고 있다. 하지만 메탄올은 용매로 쓰일 정도로 반응성이 매우 낮아 유기합성에 사용된 예가 많이 없다. 효율적인 촉매시스템을 이용하여 메탄올을 활성화한 후 탄소재료로 사용하여 요소작용기를 합성하는 반응 개발을 하였다 (4 장). C4 또는 C5 결합의 NHC은 특이한 성질 및 구조로 인해 (abnormal N-heterocyclic carbene, aNHC)라 불리며 일반적인 C2 결합의 NHC 보다 전자적 성질이 풍부하다. 따라서 aNHC는 촉매의 중심이 되는 전이 금속에 전자를 보다 잘 밀어주는 리간드 역할을 하는 것으로 알려져 있다. 먼저 NHC 전구체인 imidazolium salt 두종을 합성하고, 이 화합물로부터 은과의 금속교환반응을 이용하여 두 종의 aNHC 금 촉매를 합성하였다. 이 두 Au 화합물들은 NMR분석, X-ray 단결정 구조 분석과 DFT 계산을 통하여 전자밀도와구조 등이 상세히 분석되었다. aNHC 금 촉매를 페닐아세틸렌의 수화 반응에 적용하였으며,

일반적인 NHC 금 촉매와의 비교실험을 진행하였지만 기존의 시스템보다 더 좋은 효율을 보여주지 못하였다 (5 장).

주요어: 친환경 화학, 메탄올, 이산화탄소, 전이금속촉매, 탄소 재료

학번: 2012-20268